Republic of Iraq
Ministry of Higher Education
and Scientific Research
University of Babylon
College of Engineering
Department of Electrical Engineering

Single-Stage Single-Phase Transformer-less Multilevel Inverter for Photovoltaic Applications

A Thesis

Submitted to the department of Electrical Engineering, Faculty of Engineering, University of Babylon in Partial Fulfillment of the Requirements for the Degree of Master of Science (M.Sc.) in Electrical Engineering / Industrial Electronics

By

Israa Hussein Amwayshi Hasson

Supervised by

Assist. Prof. Dr. Tahani Hamodi Mazher AL-Mhana

2023 A.D. *1444 A.H.*

بِسْمِ اللَّهِ الرَّحْمَنِ الرَّحِيمِ

قالَ رَبِّ اشْرَحْ لِي صَدْرِي (25) وَيَسِّرْ لِي أَمْرِي (26) وَاحْلُلْ عُقْدَةً مِنْ لِسَانِي (27) يَفْقَهُوا قَوْلِي (28) وَاجْعَلْ لِي وَزِيرًا مِنْ أَهْلِي (29) هَارُونَ أَخِي (30) اشْدُدْ بِهِ أَزْرِي (31) وَأَشْرِكْهُ فِي أَمْرِي (32) كَيْ نُسَبِّحَكَ كَثِيرًا (33) وَنَذْكُرَكَ كَثِيرًا (34) إِنَّكَ كُنْتَ بِنَا بَصِيرًا (35)

صدق الله العلي العظيم

طه : (25-35)

Dedications

It wasn't easy, but I managed to finish it. I dedicate this work to my parents, who deserve all the appreciation for helping and supporting me in obtaining my master's degree. Thank you so much! Words can .hardly do justice to my gratitude and admiration

She has given me inspiration, encouragement and direction. You instilled in me the will to succeed in everything, the will to continue, and the confidence to believe in myself. I sincerely appreciate all your .good wishes and prayers for me, which have always given me courage

I also dedicate this work to my great fortune my brothers and sisters – .who believed in me and in my abilities to succeed

Last but not least, I dedicate my work to Imam Mahdi (may God hasten his arrival) and all scholars….

Israa Hussein

2023-2024

Acknowledgements

First of all, I would like to express my deepest gratitude to God for His grace and for granting me blessings throughout this journey and for ...facilitating my thesis despite all the difficulties

I also express my thanks and gratitude to my family for believing in my ambition and standing by my side to achieve it. This would not have been possible without my dear father, **Mr. Hussein Amwayshi Al-Fatlawi**, I thank you for your faith and encouragement to me …

I also express my thanks and gratitude to my supervisor, **Dr. Tahani Al-Mhana**, for accepting to supervise my thesis, in addition to her support and advice that made me learn a lot...

In addition to her patience and enthusiasm which helped me and gave me the confidence to continue what I set out to do

I also express my gratitude to so many people for their help and support, they are too many to list here, but no matter if your name appears here or not, your appreciation is always in my heart and will not change over time and my special thanks to my friends for their encouragement and care during this the work...

Israa Hussein

2023-2024

Abstract

Solar photovoltaic (PV) generation system is one of the preferred renewable energy sources which is able to produce electrical energy which is environmental friendly with no pollution and noise.

In grid connected PV system, a low frequency transformer is typically used to galvanically isolate the inverter from the utility grid and to step up the inverter voltage. A transformer PV system has disadvantages of increased system weight, size, cost and reduction in system efficiency. To overcome these downsides, a transformer-less single stage grid connected PV system is introduced with a multilevel inverter (MLI). MLI is employed to integrate the PV system with the utility grid. However, the leakage current due to the absence of galvanic isolation is one of the challenges in PV systems.

Three level neutral point clamped inverter is one of the attracting topology to be used in PV systems due to its ability to eliminate the leakage current with the availability of the neutral point. However, it suffers from shoot through problem which increase the total harmonic distortion.

This thesis investigates a single phase three level power electronic multilevel inverter based on Neutral Point Clampd (NPC) topology to be employed in a single stage grid connected PV system, which characterized with unity power factor and low current total harmonic distortion, low voltage stress on the semiconductor switch, no shoot through problem, high reliability and efficiency.

This work compares between the performance of two NPC- MLI circuit topologies (basic NPC and split inductor NPC circuits) under different level shifted carrier based pulse width modulation (LSCB-PWM) techniques and its suitability to be employed in a grid- connected transformer-less PV system.

A detailed investigation of an improved NPC topology is presented in this work to be employed in grid connected PV system. By examining the ISI-NPC (Improved Split Inductor Neutral Point Clamped) inverter behavior under different (LSCB-PWM), the thesis proposes the ISI-NPC inverter as an effective candidate to be employed in a transformer-less PV systems.

A Hysteresis Current Controller (HCC) is designed to track the inverter output current and force it to be in phase with volatge in order to achieve high power quality grid power and maintain unity power factor.

A conventional and advanced Maximum Power Point Tracking (MPPT) algorithms including Perturb and Observe (P&O) and Artificial Neural Network (ANN) are examined to ensure extracting the maximum power from the PV panel. A better performance is achieved under ANN approach.

The whole system is designed and simulated in this work. The results validate the ability of the ISI-NPC inverter under HCC control and artificial neural network to transfer PV maximum power through a unity power factor to the utility grid, high power quality, very low Total Harmonic Distortion (THD) of current with a 0.37% less semiconductor switches stress, and thus high reliability. Therefore, the thesis highlights that ISI-NPC is considered as an effective MLI to be employed in PV systems.

Table of contents

List of Tables

List of Figures

List of Abbreviations

Abbreviation	Definition
AC	Alternating Current
ANN	Artificial Neural Network
APOD	Alternate Phase Opposition Disposition
CHB	Cascade H-Bridge
CMC	Common-Mode Current
DC	Direct Current
EA	Evolutionary Algorithm
EMI	Electromagnetic Interference
FC	Fly Capacitor
FLC	Fuzzy Logic Controllers
GA	Genetic Algorithm
HC	Hill Climbing
HCC	Hysteresis Current Control
HF	High frequency
H-MCPWM	Hybrid Multicarrier Pulse Width Modulation
INC	Incremental Conductance
ISI-NPC	Improved Split Inductor Neutral Point Clamped
KCL	Kirchhoff Current Low
LS	Level Shifted

MLI	Multilevel Inverter
MPP	Maximum Power Point
MPPT	Maximum Power Point Tracking
NPC	Neutral Point Clamped
P&O	Perturb and Observe
PC	Parasitic Capacitance
PD	Phase Disposition
PLL	Phase Locked Loop
POD	Phase Opposition Disposition
PSO	Particle Swarm Optimization
PS-PWM	Phase Shift-Pulse Width Modulation
PV	Photo-Voltaic
RMS	Root-Mean-Square
SHE	Selective Harmonic Elimination
SI-NPC	Split Inductor- Neutral Point Clamped
SPWM	Sinusoidal Pulse Width Modulation
SVPWM	Space Vector Pulse Width Modulation
THD	Total Harmonic Distortion

List of Symbols

Item	Description	Unit
I_D	Diode current	Ampere, A
I_{Sc}	Short circuit current (at G=1000 W/m2 and T= 25°C)	Ampere, A
I_{max}	Short circuit current (ISc)	Ampere, A
I_{mp}	Maximum current at the maximum power point	Ampere, A
I_{ph}	Photovoltaic current generates from the PV cell due to falling the solar radiation on its surface	Ampere, A
I_{pv}	The output current of the PV cell	Ampere, A
I_{sh}	Shunt current	Ampere, A
I_{sat}	Saturation current of a diode	Ampere, A
K_1	Temperature coefficient current Degree	Celsius, °C
C	Capacitor	Farad, F
L	Inductor	Henry
Fs	Switching frequency	Hertz,
k	The Boltzmann's factor (1.381× 10−23)	J/K
R_{pv}	Photovoltaic resistance	Ohm, Ω
R_s	Series resistance	Ohm, Ω
Rsh	Shunt resistance	Ohm, Ω
T_{OFF}	Time when MOSFET at open state	Second, s
T_{ON}	Time when MOSFET at close state	Second, s
T_S	Switching time	Second, s
D	Duty cycle	Unitless
V_{in}	Input voltage to converter from PV panel source	Voltage, V
V_{mp}	PV cell voltage at maximum power point	Voltage, V
Voc	open circuit voltage of the cell	Voltage, V
$Vout$	Output voltage of converter	Voltage, V
V_{pv}	output voltage of the PV cell	Voltage, V
P_{pv}	Photovoltaic power	Watt, W

CHAPTER ONE

Introduction and Literature Review

CHAPTER ONE

Introduction and Literature Review

1.1 Introduction

Over the past 20 years, people have become more interested in renewable energy sources. This is in contrast to energy sources that rely on fossil fuels, which are expensive and keep running out. This interest comes as a result of the fact that renewable energy sources do not depend on fossil fuels. in addition to others, encouraged developing nations to make use of renewable energy resources for the generation of electricity in order to meet a significant number of day-to-day necessities upon which humans rely. The absence of pollution and noise, in addition to the relatively low costs of operation and maintenance, are some of the defining characteristics of renewable energy. Numerous forms of renewable energy resources, such as wave, tidal, wind, and solar energy, amongst others, have been modified in various ways. The photovoltaic system, which is the one that converts solar energy into electricity and is the most common type, is popular because solar energy is free and readily available in the majority of countries. Despite the high initial installation costs associated with PV systems, they have been widely adopted for a range of applications. PV systems are a major source of renewable energy. Some examples of these applications include large-scale power plants, solar home systems, water pumping stations, spacecraft, satellites, and reverse osmosis water for service plants [1]. A number of significant factors impact the amount of energy generated by the PV panel source. These factors include the amount of solar radiation, the temperature, the internal structure of the PV panel, and the load. Solar radiation and temperature are significant factors that play significant role in determining the performance and efficiency of PV panel. As a

result, it is essential to develop strategies that can keep the maximum amount of PV generation in place regardless of the conditions.

The number of cells contained within each panel, as well as the area of each cell and the type of semiconductor material, are all components of the PV panel's internal structure. In order to draw power from the photovoltaic panel, the load must first be connected to the panel's terminals [2].
A transformer-less PV inverter has been used in grid-connected PV systems to increase system efficiency overall while lowering the cost, size, and weight of the conversion stage. Galvanic isolation between the grid and the PV system would be lost if there were no transformer, though. This could result in potentially hazardous situations in the case of ground faults [3]. Furthermore, Leakage currents could occur due to the capacitance between the PV array and the ground, commonly referred to as "common-mode currents," to pass through it. Additionally, without a transformer, the inverter might deliver direct current (DC) into the grid, which would load every transformer in the distribution network to capacity. [3].

The utilization of a grid-connected transformerless multilevel inverter (MLI) is considered as one of the important configuration to interface the PV system and utility grid.
An array of power semiconductors and capacitor voltage sources are included in multilevel inverters. These components work together to generate the voltage waveforms when the inverter is turned on. The commutation of the switches makes it possible to add the voltages of capacitors, which results in a high output voltage. Three types of multilevel inverters are commonly used in various applications includes: Diode-clamped inverter, Flying capacitor inverter, and Cascade H-bridge inverter [4]. The PV system must be operated at an MPP, or maximum power point, in order to create the greatest amount of power that it is capable of

producing. The maximum power point can be tracked by analysing the voltage and current of the PV system to identify the greatest region that fits inside the current-voltage (I-V) characteristic curve. Therefore, users are interested in designing MPP tracking (MPPT) methods to control the amount of generating power from the PV system and to ensure high efficiency under all environmental conditions and loads. This is because MPPT tracking allows researchers to control the amount of power that can be generated from the PV system [3]. Photovoltaic systems could be connected using either an on-grid, off-grid and hybrid connection of PV system connection, depending on the user's preferences. Because it is connected to the main utility grid, and does not require the use of batteries, the on-grid photovoltaic system is currently the most popular type of solar power system. Therefore, it is not appropriate for use in remote areas where there is no access to electricity because of this. The off-grid PV system is not dependent on the conventional electrical distribution network in any way. As a result, it requires battery storage to guarantee that there will be sufficient power for connecting loads. This PV system is quite pricey because it needs to be equipped with several batteries [4].

1.2 Literature Review

Z.Pan, et al, 2004 [5], a topology for multilevel converters using clamping diodes less frequently, a five-level converter is used as the basis for discussion of the suggested topology and its switching pattern. N-level converters can be added to the topology with ease. The proposed topology can greatly lower the quantity of clamping diodes and the multilevel converter's system cost when compared to the conventional architecture. A topology for a multilevel converter that uses fewer clamping diodes. Multilevel converter cells with several levels are combined in the innovative topology. The suggested topology, which utilizes a five-level converter,

The proposed topology can greatly lower the quantity of clamping diodes and the multilevel converter's system cost when compared to the conventional architecture.

X. Guo, et al 2012 [6], for three-level neutral-point-clamped inverters in three-phase transformer less solar systems, modulation technique is one of the most crucial considerations. How to maintain consistent common-mode voltages to lessen the effects of modulation is a difficulty. In **[6]** suggested to use single-carrier modulation. The common-mode voltages may be maintained constant without the use of complicated space-vector modulation or multicarrier pulse width modulation because of its extremely straight forward construction.

S. Ozdemir, et al, 2014 [7], have presented an MPPT technique based on combining several conventional MPPT methods**,** including modified incremental conductance method, variable step size method, and constant voltage method. The maximum power point can be tracked by grid-connected three-level NPC inverter that is currently under development without the need for a separate power electronic converter.

J. Ferdous, et al, 2014 [8], instead of using a traditional NPC inverter, a split Inductor based Neutral point clamped (SINPC) inverter, which completely reduces the fluctuating common mode voltage at the enhanced modulation technique. Additionally, the split inductor design of the proposed inverter produces little system leakage current.

F. Faraji, et al, 2017 [9], have reviewed a various topologies of single phase single stage grid-connected three-level neutral point clamped (3L-NPC) inverters for photovoltaic system. They are also presented a model to represent the leakage current in the NPC topology. They look at over 45 types of single-stage,

single-phase 3L topologies with a particular focus on the 3L-NPC voltage source inverter (VSI) family.

S. Dhara et al, 2018 [10], have introduced a novel single phase T-type PV inverter configuration controlled by level-shifted sinusoidal pulse width modulation (LS-SPWM) to achieve better Dc utilization. This topology is capable of exhibiting a conventional output voltage with five levels while all the switching frequency transitions that take place between the neutral point of the load and the source terminals can be avoided. This is a prerequisite for the use of PV inverters in any given application.

A. Sinha, et al, 2018 [11], a review for various topologies of grid connected MLI has been introduced include, cascaded converter, neutral point clamped (NPC) and flying capacitor (FC) . Several control and modulation strategies have been also described to highlight converter performance and its complexity.

V. senthil, and A.kokila, 2018 [12], have demonstrated a solar cell system with boost converter to achieve higher overall output. A diode-clamped multilevel inverter is employed to generate three distinct levels of output,. In the NPC multilevel inverter, a comparison is made between the efficiency of various control methods, such as SPWM and SVPWM

A. Zarein, et al, 2019 [13], a multilevel transformer less single-phase inverter has been presented in. It is made up of one H-bridge, one bidirectional switch, and one damper circuit to cut down on ground leakage current. Based on the number of components in the power circuit, a comparison is made between the

configuration of the proposed inverter and that of the transformer-less single-phase inverters.

X.Jiang, et al, 2019 [14], a comparative analyses of three distinct three-phase, three-level inverter topologies are demonstrated , A multi-carrier sinusoidal pulse width modulation (SPWM) technology is adopted to realize the closed-loop control model of the grid-connected photovoltaic system. To compare the waveforms of the outputs of multilevel inverters, the amount of total harmonic distortion (THD) in the output voltage is illustrated.

K. Chenchireddy, et al, 2019 [15], a sinusoidal pulse width modulation technique was presented to control single-phase four-level NPCs. This technique balances the neutral point when a dynamic load is connected or any AC loads. Adopting this approach is also helps in reducing the switching loss and harmonics.

B. Chokkalingam, et al, 2019 [16], have examined the effect of using Multi-Carrier Pulse Width Modulation (MCPWM) schemes on the behavior of five-level T-type NPC MLI. Various PWM strategies have been compared based on voltage profiles, conduction losses, and total harmonic distortion (THD). In addition, the switch counts, clamping diode counts, main diode counts, and capacitor counts of a typical NPC are compared to those of a 3L T-type NPC MLI.

I. Harshith, et al, 2019 [17], a hybrid multicarrier pulse width modulation technique was proposed for transformer-less solar seven-level inverter systems to ensure minimal leakage current , this method is characterized as simple to install and employing fewer carriers**.** A transformer less cascaded multilevel inverter is used to interface the PV system with the hybrid multicarrier pulse width

modulation (H-MCPWM). By adopting this approach, the amount of current loss due to leakage is reduced.

F. Bovolini, et al, 2020 [18], have introduced a five-level transformer less for PV generation systems. In order to reduce the risk of leakage currents, the topology connects the negative terminal of each PV module to the potential of the neutral grid, which is typical of inverters that share a common ground. In addition to that, this converter makes use of a flying capacitor leg in conjunction with a half bridge cell, which ultimately results in the generation of a multilevel PWM voltage that contains less harmonic content.

H. Tian, et al, 2020 [19], the balancing of DC-link capacitors is an important issues which needs to be taken into consideration in order to allow the ANPC topology to work properly. have introduced a balancing circuit to clamp the DC voltages by combining the signal injection technique with the phase-shifted PWM techniques.

R. Palanisamy, et al, 2020 [20], a space vector pulse width modulation for neutral point clamped multilevel inverter systems is presented in [20]. When the NPC topology is utilized, a reduction in the common mode voltage is achieved. Monitoring the voltage vectors and controlling the output voltage are two of the system's primary objectives, respectively. The total harmonic distortion (THD) of the output is one of the components that the efficient SVPWM technique helps to reduce.

A. Kumar, et al, 2020 [21], a model for a (PV) system with a one hundred kilowatts (kW) rating are presented in MATLAB/SIMULINK environment. In this work, the performance of a (PV) system that includes a power

electronic converter and a stand-alone alternating current (AC) load is analyses and presented under varying environmental conditions. Incremental conductance (IC) algorithm is used for maximum power point tracking (MPPT) in order to get the most of the PV system power under a variety of lighting conditions and panel temperatures.

B. Karami, et al, 2020 [22], have introduced a new grid- connected photovoltaic (PV) systems with 5-level single-phase transformer less PV inverter. This inverter is able to directly link the grid neutral point to the negative terminal of the PV which is helping in eliminating the leakage current.

P. Madasamy, et al,2021 [23], The shoot-through issue that occurs on the bridge legs which affects certain MLI topologies such as the NPC-MLI which is used frequently in medium/ high voltage power systems. This issue is another big concern in grid-connected transformer-less PV system which needs to be taken in consideration as it affect the system reliability .

H.S. Maaroof, et al, 2021 [24], Two split-inductor have been added to the TRL three level- NPC inverter to overcome the shoot-through problem and improve the reliability of grid-connected-PV inverter with no need to set dead-time between the switches located at the same converter leg **.**

1.3 Problem Statement

According to the above literature review, the thesis will try to deals with the common issues and challenges in designing a single-stage grid-connected TRL-PV Inverter. These issues are:

1. Shoot-through problem.
2. DC- link capacitor voltage balance.

3. Current total harmonic distortion (THD).
4. Voltage stress across the semiconductor device.
5. Maximum power point tracking for PV panel.

The thesis deals with each problem by proposing a multilevel inverter for single stage PV system.

1.4 Thesis Contribution

The thesis contributions can be summarized as follows:

1- Comparison between NPC & SI- NPC for PV system under PD & POD in terms of all DC and AC current and voltage waveforms in addition to the current total harmonic distortion.
2- Investigate the effectiveness of adopting hysteresis current controller with ISI-NPC inverter.
3- Examine the operation of ISI-NPC inverter to interface PV system.
    I. Examine the performance of grid connected ISI-NPC inverter under P&O MPPT.
    II. Examine the performance of grid connected ISI-NPC inverter with artificial neural network MPPT.
    III. Study the effect of the irradiation and temperature variation on the constant and variable behavior of PV system.
4- Capacitor voltage balancing approach for grid-connected inverters for PV applications.
5- Evaluate the ability of ISI-NPC to transfer the maximum PV output power to the grid.

1.5 Thesis Objectives

The main goal of this thesis is:

1- The thesis provided HCC and MPPT controllers design for single phase 3-level improved split inductor multilevel inverter (ISI-MLI) transformer-less PV power system design.
2- This work attempts to present some of methods in the photovoltaic system that is more effective, simpler in implementation, and less expensive.
3- The thesis presented MPPT algorithms to regulate the input voltage of the inverter.
4- The suggested method will provide a small amount of harmonics, reduce the total harmonic distortion in the current, and eliminate shoot-through.

The main objective of this thesis can be summarized as :

1- Study PV panel characteristics under constant and variable temperature and irradiation.
2- Design the 3-level ISI-NPC MLI.
3- Design Hysteresis Current Controller.
4- Design MPPT based on P&O and ANN algorithms
5- Test the whole system performance.

MATLAB/SIMULINK 2021a was utilized to design the transformer-less grid connected PV system.

1.6. Thesis Layout

In terms of size, efficiency, and simplicity, this thesis proposes a system that relies on a transformer-less multilevel inverter of single phase, three-level Improved Split Inductor Neutral Point Clamped (ISI-NPC) based on a Hysteresis Current Control of HCC and PLL. There are two different types of MPPT

algorithms: P&O and ANN adopted in this work. This thesis has the following six chapters:

Chapter one includes Introduction, literature review, thesis objectives, a problem statement, and thesis contribution .

Chapter two discusses the theoretical background of transformer-less PV systems.

Chapter three introduces the design of a single stage transformer-less PV grid-connected system.

Chapter four demonstrates the results for the proposed system with two parts :

Part one : Multilevel inverter under DC source (results in comparison between the original NPC and ISI-NPC with PD and POD PWM. And also a comparison in the case of linking the ISI-NPC inverter with constant and variable HCC PWM based on DC source)

Part two : Multilevel inverter under PV system (results for the proposed system and results in comparison between the PV system based on P&O and ANN algorithms at constant and variable temperature and irradiance).

Chapter five includes conclusions and future work that could add development to the PV power systems.

CHAPTER TWO

Theoretical Background of Transformer-less PV system

CHAPTER TWO

Theoretical Background of Transformer-less PV system

2.1. Introduction

The photovoltaic (PV) power system has received much attention recently because it is sustainable and free of pollutants [25]. A photovoltaic array and power converter make up the majority of it. The photovoltaic (PV) is an essential component that generates sun electricity. One of the most critical characteristics that distinguish grid-connected PV power systems is the presence or absence of a transformer. The traditional PV inverter connects the transformer between the PV array and the grid to provide electrical isolation. Most solar power systems use this configuration. However, the entire structure is large, making it difficult to move and expensive and inefficient. Therefore, a non-isolated inverter system has been proposed as a transformer-less inverter solution. These inverters have a small footprint and little energy waste because they do not include a transformer. They are inexpensive, higher efficiency and lightweight compared to the transformer [26]. The non-isolated inverters have a structure in their design. This structure changes the DC output of photovoltaic cells into an AC output.

There are many benefits, such as a simple structure, low costs, little loss, and easy deployment [27]. However, this structure has more stringent requirements for photovoltaic energy conversion on the DC input side and corresponding challenges in terms of energy conversion and circuit design efficiency. It will also bring about other issues, such as leakage current. Considering the two-stage isolated inverter, this circuit structure usually has a boost circuit in the front stage of the inverter. It is often used as the boost circuit for the two-stage isolated inverter. This type of circuit can output the voltage of the photovoltaic array, boost the voltage through

the circuit structure and modulation method, and then convert it to the ac voltage required by the load. The energy conversion efficiency can be improved with this type of circuit. Constructing this kind of circuit allows it to realize the decoupling of the front stage from the backstage. The control of the entire circuit is simple, the volume is low, and there is very little interference. Non-isolated inverters have drawbacks, such as parasitic capacitance leakage current, which can cause personal safety threats, grid harmonics, and other issues [28]. However, adopting some approaches can suppress or eliminate the leakage current.

This chapter discusses the primary components of an associated single-phase transformer-less multilevel inverter as well as other benefits of a PV system.

2.2 PV system configurations

Inverter topologies for grid-connected photovoltaic systems can be divided into two categories: those that use a transformer and those that do not. Figure (2.1) depicts the inverter's initial step-up of its DC input voltage and subsequent ac output voltage for the grid interface. This transformer can either be high frequency (HF) on the DC side or low frequency on the AC side, depending on which side it is connected to [29], the transformer also provides the Galvanic separation between PV modules and the grid. Thus, it eliminates the possibility of DC and leakage current being introduced into the grid. On the other hand, line frequency transformers are bulky, expensive, and power inefficient because of the power loss that occurs in the windings [29].

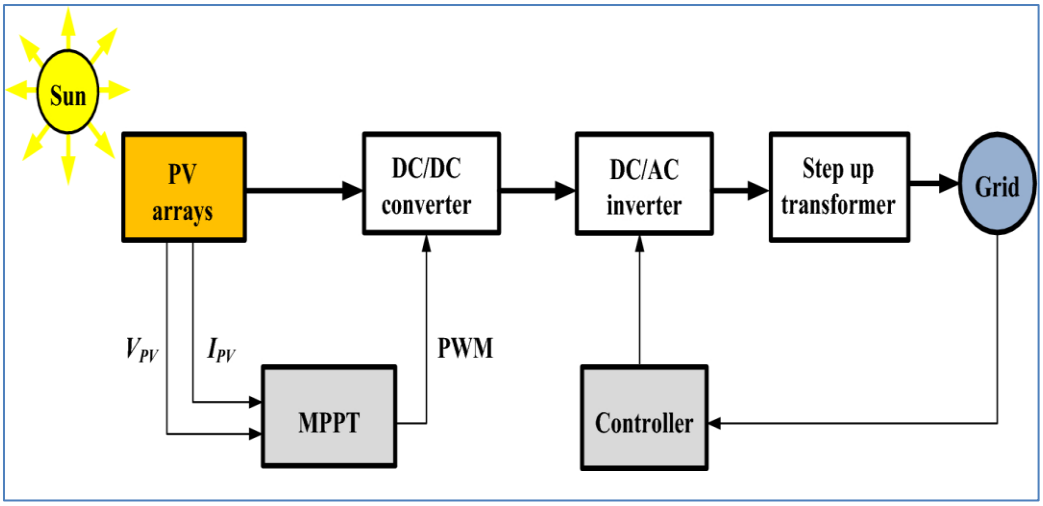

Figure (2.1) Two-stages grid connected PV system [30]

As a result, transformer-less inverter topologies have been developed specifically for PV applications to avoid these problems, as illustrated in Figure (2.2). The system's efficiency may improve by 1%–2% due to eliminating the first stage (i.e. DC-DC converter) [30]. They are also less expensive, in addition to being less bulky and lighter in weight. However, they suffer from excessive leakage current. Without galvanic isolation, leakage current can construct a direct path from the PV module to the grid. When a high-frequency potential is applied across the parasitic capacitor that forms between the metallic frame of the module and PV cells, it simultaneously produces a large leakage current. This occurs because the parasitic capacitor is located between the PV cells. Leakage current is responsible for increased system losses, electromagnetic interference (EMI), and the grid current's total harmonic distortion (THD). Additionally, it harms the personal safety of individuals[31]. In order to meet the demands of the grid regulatory authorities and improve efficiency by using multilevel inverters, various methods have been adopted to reduce leakage current and total harmonic distortion.

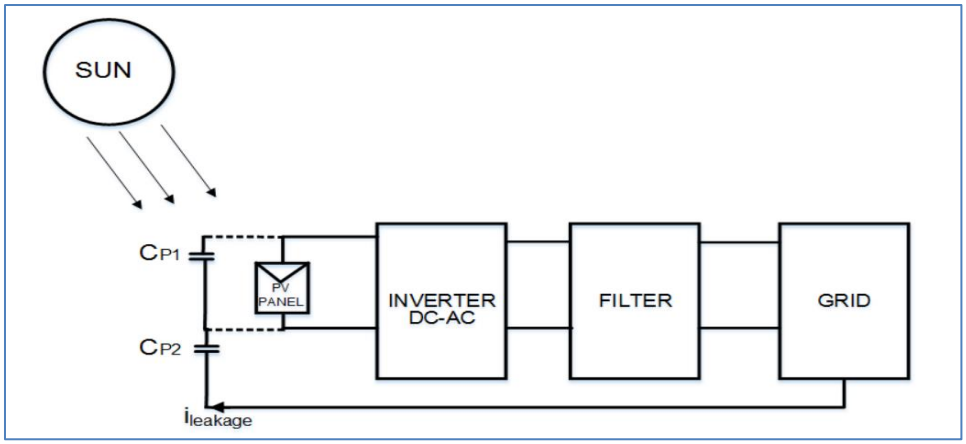

Figure (2.2) Single-stage transformer-less grid connected PV system[31]

2.3 Photovoltaic system

Photovoltaic (PV) turns sunlight into a form of electricity that can be used. Because the sun is their primary light source, these devices are called solar cells [32]. Solar energy is widely regarded as one of the most advantageous forms of renewable energy because it does not add to the overall pollution in the surrounding environment, It is sustainable and uses little in exchange for money. PV modules are now substantially less expensive than they were previously due to an increase in industry production capacity. As a result, lowering the cost of the grid-connected inverter increases the appeal of power provided by photovoltaic cells (PV). When two different types of materials come into contact with one another, an electric field is created that is quite close to the cell's top surface (the P-N junction). When sunlight strikes the surface of a photovoltaic (PV) cell, it generates an electric field. When the cell is connected to an external electrical load, the electrical field imparts momentum and direction to the light-stimulated electrons, resulting in a current flow [33]. Solar photovoltaic technology allows for the generation of electricity that is not only ecologically friendly, but also dependable and quiet.

The fact that photovoltaic (PV) technology does not require the use of any moving parts is among its most significant advantages, Because of this, the hardware has an exceptionally long lifespan, a low rate of wear and tear, and needs only a small amount of maintenance overall [33]. PV panels are now a part of everyday life, supplying loads at remote locations, powering watches and small calculators and last but not least, connecting to the public grid to supply the future's environmentally friendly energy [34]. PV panels are no longer just used for applications in space, they are now a part of everyday life. There are primarily two categories of photovoltaic systems: grid-connected PV systems and stand-alone PV systems. Both of these categories can be used to generate electricity. Although there have been significant improvements in PV system installation over the past decades, there are still obstacles to solar technologies. These obstacles directly cause solar technologies' failure to compete with fossil fuels and other energy types on the market. As a result, solar technologies still need help to break into the energy market. A few issues with solar power need to be addressed, including the high cost of installation, the unreliability of solar energy production, and the inefficiency of its energy conversion [35]. Novel technologies that can deliver higher conversion efficiencies at lower manufacturing costs are urgently needed to speed up the incorporation of solar technology into the energy market [36]. In the context of solar-powered devices, PV cells are typically used to facilitate the transformation of solar energy into usable forms of electrical energy. The elements of a solar energy conversion system are represented by the (PV) cells, power converters, and a control device for changing the output of the PV cells , To increase the effectiveness with which renewable energy is transformed into usable electricity. Numerous control strategies, systems for power tracking, and power converter topologies have been developed. Efforts to increase the efficiency of power grid operations are driving an increase in research into the integration of

renewable energy sources [37]. Due to their importance in the power conversion process and the regulation of output power, power converters and their controls are receiving increased focus.

2.3.1 PV characteristics

Although the PV system has low efficiency and a high installation cost compared to other systems that rely on fossil fuels, it is the most reliable and essential renewable resource for power generation [34]. This is because the sun is abundant and will continue to shine for a long time. PV cells are the individual components that make up the photovoltaic panel. These photovoltaic cells are connected in series or/and parallel to create the PV panel (module), and a number of these modules are connected in series and parallel to create the PV array. The amount of power that can be taken from a PV source depends on the amount of sunlight (radiation) and the temperature Figure (2.3).

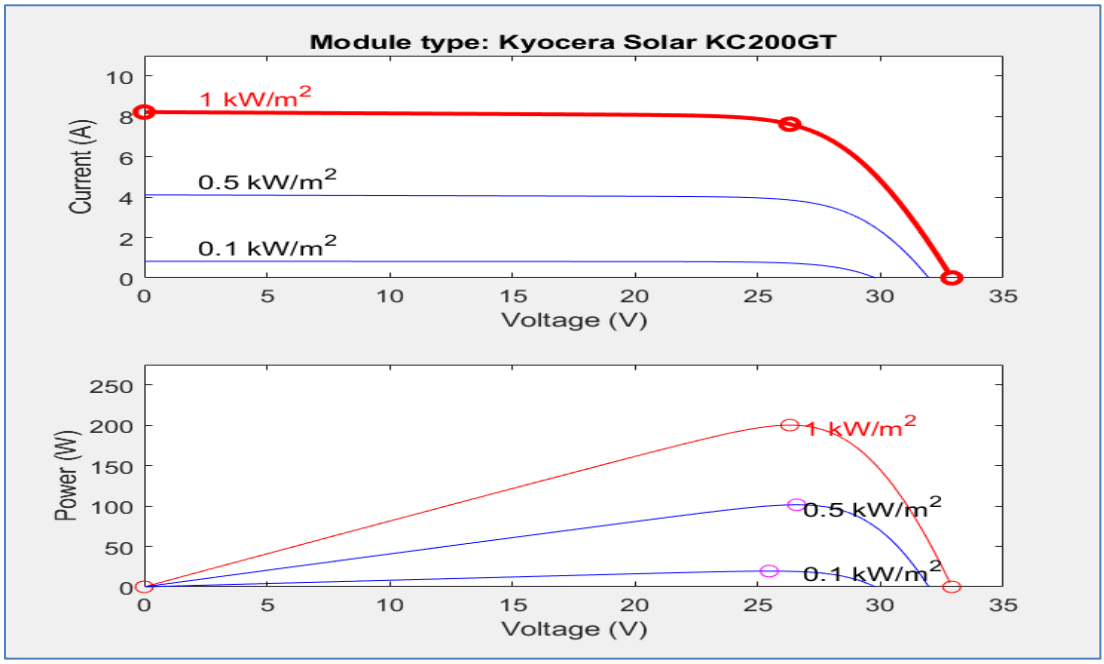

Figure (2.3) I-V and P-V curve of PV panel

2.3.2 Modeling circuit of the PV cell

As can be seen in figure (2.4), which depicts the PV cell equivalent circuit, it is possible to represent the photovoltaic cell, which is the smallest unit of a solar panel. This cell is also known as the PV cell. It is a parallel arrangement of a DC source (I_{ph}) and a diode with a DC current (I_D). The amount of solar radiation that strikes a photovoltaic cell causes positive and negative ions to become mobile and generate a direct current (I_D). The magnitude of this current is directly proportional to the amount of solar radiation that strikes the PV cell. The photovoltaic cell is made up of two resistances: a very high shunt resistance (R_{sh}), which has a parallel connection to a diode, and a minimal series resistance (R_S), which has a series connection to the load [34].

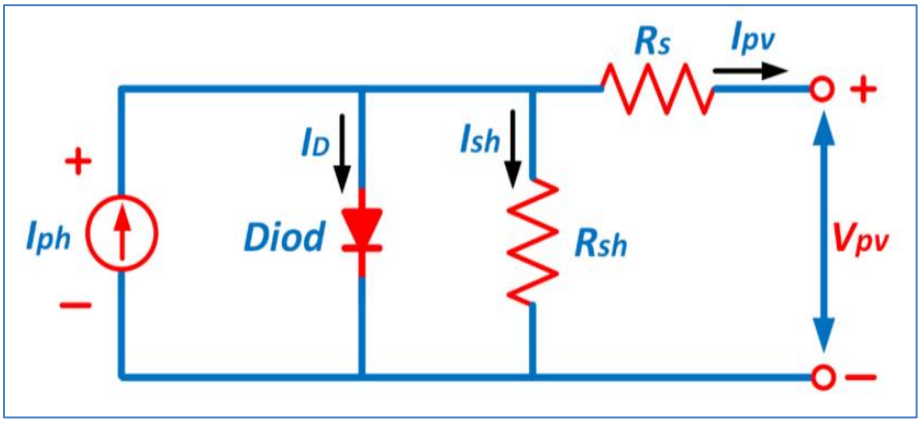

Figure (2.4) The PV cell equivalent circuit. [34]

Figure (2.4) depicts a practical illustration of a single solar cell. The resistance in the series of a PN junction cell, denoted by R_S, is opposed by the resistance in the shunt, denoted by R_{sh}, which is inversely proportional to the amount of current lost to the ground in this circuit. The series resistor that connects a solar cell's individual junctions significantly impacts its I-V characteristic. In a solar cell equivalent circuit, where : I_{pv} the output terminal current, is calculated

using KCL, I_D and I_{sh} are referred to as the diode current and the shunt leakage current, respectively, in a solar cell equivalent circuit.

The PV cell output current (I_{pv}) can be represented by the following equation [34]:

$$I_{ph} = I_{pv} - [I_D + I_{sh}] \quad (2.1)$$

It is clear from the equation (2.1) that the current (I_{pv}) consists of the following currents i.e. I_{sh} and I_D

The current (I_{sh}) which represents the current passing through the shunt resistor (R_{sh}), can be given as:

$$I_{sh} = \frac{[V_{pv} + R_s I_{pv}]}{R_{sh}} \quad (2.2)$$

The current (I_D) which represents the current passing through a diode, is explained in the equation (2.3) as follows:

$$I_D = I_{sat}\left[e^{\frac{Q[Vpv+lpvR_S]}{nKT}} - 1\right] \quad (2.3)$$

where:

n: Idealist factor ($1< n < 2$).

k: Boltzmann's factor (1.381×10^{-23}J/K).

I_{sat}: Saturation current of a diode (A).

Q: The Charge of an electron of value (1.602×10^{-19}) C.

T: The Temperature of a solar module in (°C).

The PV current (I_{ph}) represents the current generated by PV cells as a result of solar radiation dropping off their surface. The operating temperature (Top) and solar radiation (G), two meteorological parameters, have the following effects on this current's value:

$$I_{ph} = \frac{G}{G_{ref}}\left[I_{SC} - K_I\left(T_{ref} - T_{op}\right)\right] \quad (2.4)$$

where:

G: Refers to solar radiation (W/m^2).

K_1: Temperature coefficient current

Gref: Reference solar radiation (1000 W/m^2)

Isc: Short circuit current (at 1000 W/m^2 and 25°C)

Tref: Reference temperature (°C).

The equation (2.1) can be rewritten as equation (2.5), depending on the previous equations (2.2) and (2.3) [32], [34].

$$I_{pv} = I_{ph} - \frac{\left[V_{pv} + R_s I_{pv}\right]}{R_{sh}} - I_{sat}\left[e^{\frac{Q[Vpv + IpvR_S]}{nKT}} - 1\right] \quad (2.5)$$

2.4 Maximum Power Point tracking (MPPT)

In recent years, several significant advancements have been made in the quest to improve the capacity of photovoltaic energy to satisfy the ever-increasing demand for energy on a global scale. However, the high starting cost of photovoltaic (PV) materials makes it challenging to deploy photovoltaic (PV) systems in an efficient manner and to make use of them. This makes it challenging

to use PV systems [35]. Associated with the PV module is a low conversion efficiency, another factor that impedes the development of photovoltaic (PV) systems. Therefore, researchers are focusing their efforts on incorporating power converters with the capability of maximum power point tracking (MPPT) into PV systems to guarantee the most efficient energy harvesting possible from the environment around them. The MPP's stability may be compromised due to shifts in the weather, which is determined by the conditions of the atmosphere (temperature and irradiation). the MPP has to be monitored around the clock and in any weather to ensure that the photovoltaic panels produce the maximum amount of power possible, given the resources at their disposal. This fact must be kept in mind, as it depends on the PV parameters and weather conditions [36]. It is common practice to use MPPT controllers to monitor and follow the MPP in photovoltaic (PV) systems to boost their overall efficiency. The importance of maximum power point tracking controllers as a crucial part of a PV system that needs to be optimized has increased. Because each of these controllers uses a different set of algorithms, there is a significant variation in the tracking speed of each of them, as well as their performance, level of efficiency, and level of complexity. helpful for PV system tracking with MPPT or for tracking the MPP for a single MPP under uniform irradiation. Both of these tracking methods require the MPP. According to the evidence presented in the research that has been published, MPPT algorithms, each of which has its unique set of restrictions, specifications, and applications. These methods are classified according to the various forms that MPPT can take, such as sensors, tracking methods, and modern, which serve as the basis for this classification. These basic categories are then further subdivided into sub-categories based on specific criteria, operating principles, or application techniques [37]. The following is a general classification of the three basic types that can be found among them:

• Traditional MPPT methods.
• Advanced MPPT methods (soft computing).
• MPPT hybrid methods.

2.4.1 Conventional MPPT Methods

The primary advantages of the conventional MPPT are that they are straight forward, making it easy to put them into practice. When the irradiance is constant, these methods can only accurately track a single MPP. Conventional MPPT methods are Perturb and Observe (P&O), Incremental Conductance (INC), Parasitic Capacitance (PC), and Hill Climbing (HC) [37]. These methods have several drawbacks, one of which is that they are unable to function appropriately in Partial Shading Conditions (PSCs) because they are unable to easily observe the global maximum point (GMPP) in PSCs. They also have poor tracking accuracy and large oscillation. Therefore, they typically exhibit inefficient levels of performance [38].

2.4.1.1 Perturb and Observe MPPT algorithm

The "perturb and observe" method has received a lot of attention because of how straight forward it is. In this approach, a perturbation in the duty cycle of the converter causes a disturbance in the system current, which in turn causes a disturbance in the voltage produced by the PV system. The P&O algorithm is a frequently preferred MPPT method in PV applications due to its advantages, such as its simple structure, easy applicability, and few parameters, as shown in Fig. (2.5). [39] The P-V characteristics of the PV panel serve as the foundation for the primary operational principle that underpins the P&O algorithm. Through the use of sensors, the working current and voltage of the PV panel can be measured at any given moment. The value of the generated power is calculated from the measured

values of current and voltage. The duty period rate is controlled by D, resulting in MPPT, and the running voltage is gradually adjusted so that the power difference (ΔP) and voltage difference (ΔV) may be monitored.

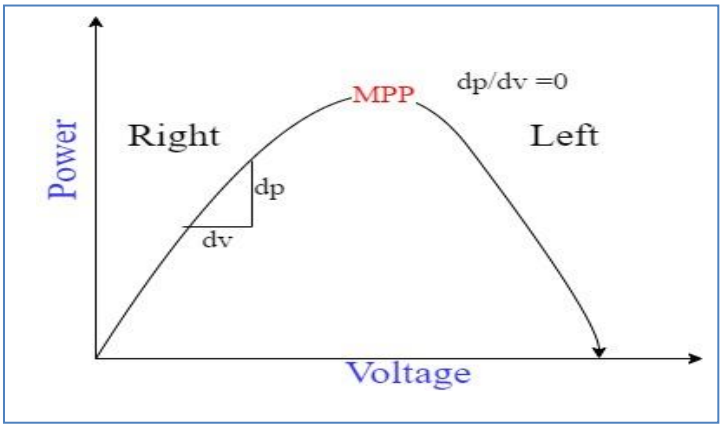

Figure (2.5). Characteristic of the PV panel power curve

It is self-evident that if the left-side power source needs to increase the voltage, the right-side power source will have to decrease it. Consequently, in order to reach the MPP, the next duty cycle should be held constant when the power level rises, and the duty cycle should be inverted when the power level lowers. This iteration's purpose is to repeat itself until the system reaches the MPP. There are two major drawbacks to this approach: first, it is difficult to determine the magnitude of the oscillation, and second, it is difficult to determine the convergence rate of the tracking MPP. The MPP is able to keep up with big perturbations more quickly than other methods, but this speed comes at the cost of a greater oscillation amplitude. [40] The convergence rate and the amount of oscillation around the MPP are both reduced when there is only a little disturbance. Therefore, there is a decrease in, the quantity of regular oscillations around the MPP. Various P&O iterations have been created in an effort to solve this issue.

$$\left.\begin{aligned} P &= V.I \\ \frac{dP}{dV} = 0 &= I.1 + V\frac{dI}{dV} \\ \frac{dP}{dV} = 0 &= \frac{I}{V} + \frac{dI}{dV} \end{aligned}\right\} \qquad (3.5)\ [40]$$

If $\frac{dP}{dV} > 0$ Right Increase ΔD

If $\frac{dP}{dV} < 0$ Left Decrease ΔD

If $\frac{dP}{dV} = 0$ MPP ΔD =0

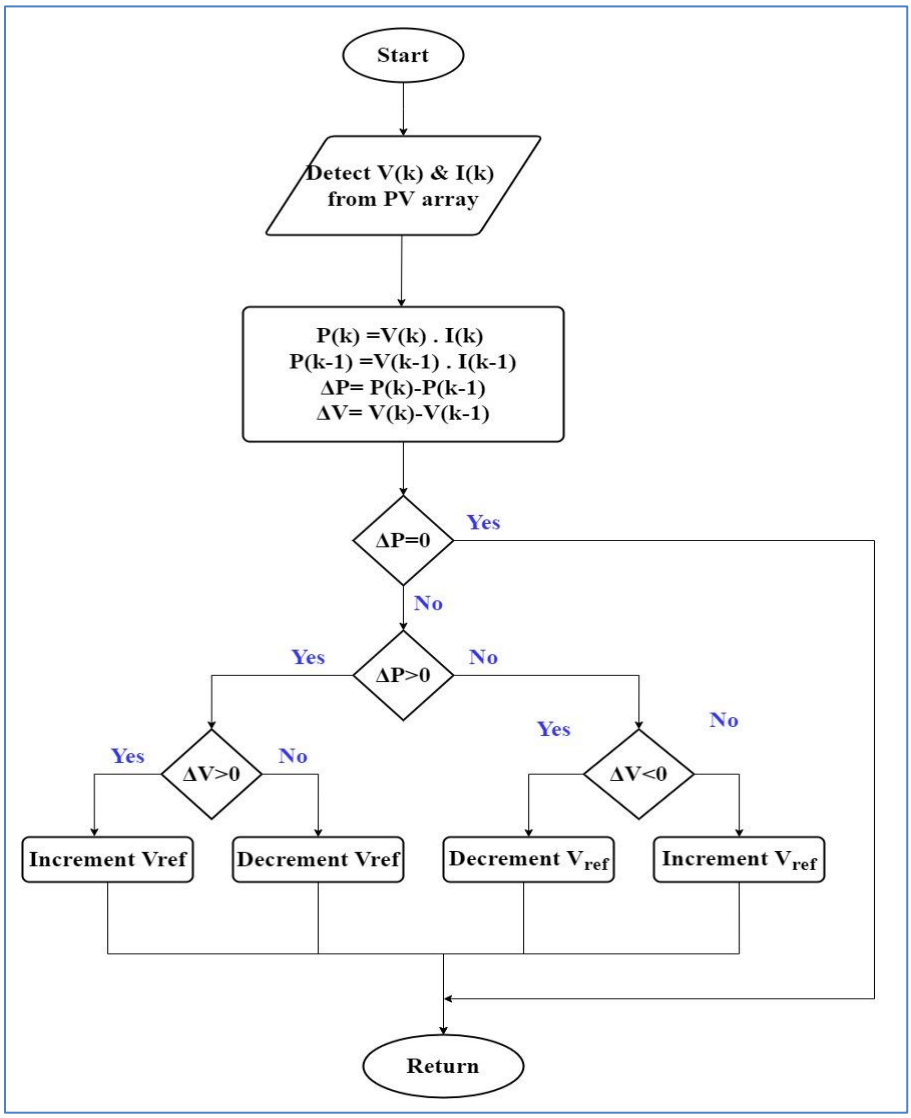

Figure (2.6). P&O MPPT algorithm proposed

2.4.2 Advanced MPPT Methods

In response to the numerous short comings of the traditional MPPT methods, such as their low efficiency and slow tracking speed in shaded settings, advanced approaches were created [40]. The more advanced methods will be able to bring the level of perturbation closer to MPP. The MPPT methods based on soft computing are more challenging to implement than those based on conventional techniques. However, due to their dependability, robustness, and adaptability, they are the methodes of choice for PSCs. These techniques have proven to be highly effective in a wide range of applications, especially when subjected to conditions of complete or only partial shading from sun irradiance [41]. These techniques rely heavily on the foundations of artificial intelligence in addition to various evolutionary algorithms (EA). As a direct consequence of this, the genetic algorithm (GA), artificial neural networks (ANN), fuzzy logic controllers (FLC), and particle swarm optimization (PSO) are some of the most frequently utilized advanced techniques. The ability of these algorithms to solve nonlinear problems and the flexibility with which they can do so is their primary strength point [43]. They can locate the multipeak GMPPT or optimal solution with a degree of accuracy proportionate to the problem's difficulty.

2.4.2.1 Artificial Neural Network (ANN) algorithm

ANN is an information processing technology inspired by the human brain's ability to learn. [41] It generally consists of 5 sections which are described below;

Inputs: Data sent to be collected in the neuron nucleus are called inputs.

Weights: Multiplying the inputs by the weights and then sending them through the original link modifies the impact of the inputs on the output.

Joining Function (NET): The function that calculates the net input of a cell. The sum of inputs multiplied by their weights gives the net input function.

Activation Function : It is the part where the NET obtained in the combining function is sent to form the total cell output. When choosing the activation function, the processing speed should be ensured to be easily differentiable.

Outputs : The value obtained as a result of the activation function expresses the output of the current neuron. Not only the values of the output are used as a result of ANN, but also they can be sent back to the network structure for further learning.

In order to make an accurate prediction of the voltage (V) or output power (P) at any given time, MPPT controllers make use of ANN. To figure out the load cycle, the calculated value is put up against the instantaneous values that have been gathered. The temperature (T) and the gravitational acceleration (G) will both serve as examples of independent variables that will be used as **input variables** to the first layer of the network. Additional variables that are part of the panel, such as V and I, may be included as input. The processing of these information requests will be handled by the ten **hidden layers** [42]. The final performance will be determined by a number of factors, including the activation function and training algorithm of your choice as well as the number of neurons in the hidden layers. It is recommended that a significant quantity of data be amassed for processing in order to further improve ANN's accuracy as shown in Figure (2.7).

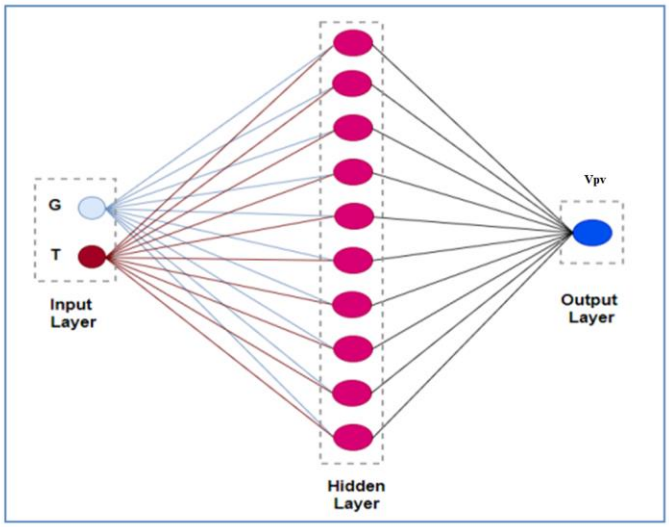

Figure (2.7) ANN structure [42]

2.4.3 Hybrid MPPT Methods

Concerns with traditional and cutting-edge methods have prompted the suggestion that hybrid MPPT approaches might be the way to go. Hybrid approaches are characterized by their ability to boost overall efficiency and keep working well even when subjected to partial shading. They are developed by combining different techniques in varying proportions, such as soft computing and traditional algorithms [41]. Various methods are often mixed and matched in different proportions to create them. A hybrid system is produced when two or more soft computing algorithms are combined. Hybrid tracking techniques have the potential to improve performance over that of single-algorithm approaches significantly.

2.5 Multilevel Inverter

It is common practice to describe the use of DC/DC converters as the initial step in incorporating renewable energy sources into the power grid. The highest priority now is meeting the process's high-efficiency standards. This is

because renewable energy sources, such as wind and PV, have inherent voltage fluctuations associated with their output. Dual-output or two-level inverters are widely used in utility and light manufacturing [43]. In addition to the high voltage stress they experience when in use, this is principally caused by a reduction in the efficiency with which these devices work. Therefore, multilevel inverters are typically used in grid-connected Figure (2.8), large-scale renewable energy installations due to their high switching frequencies, high efficiencies, low switching losses, ability to operate at high voltages, low electromagnetic interference (EMI) output, and low switching losses. Multilevel inverters (MLI) are receiving more attention from researchers. In addition, MLI inverters' switching losses and EMI emissions are pretty low (low THD output).

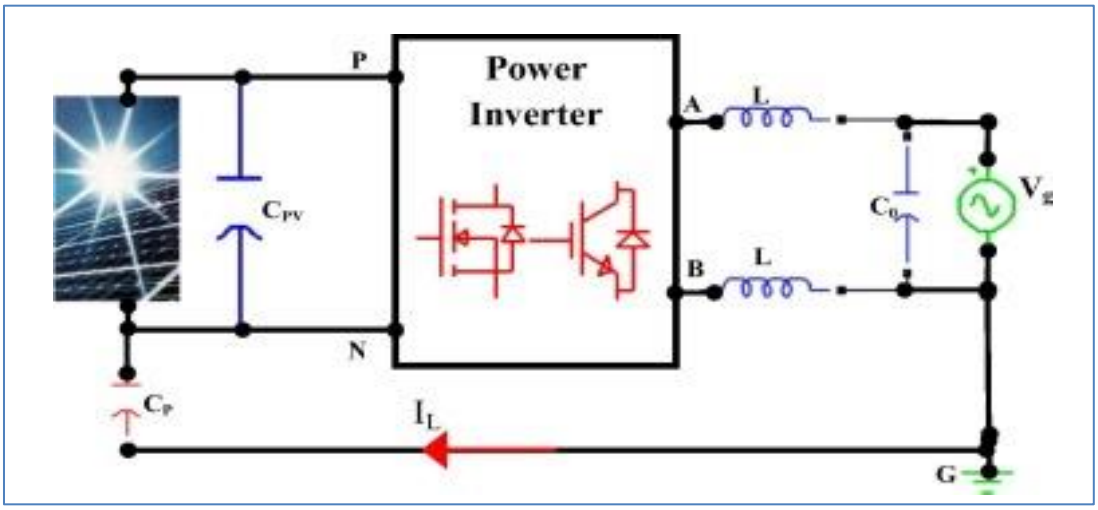

Figure (2.8) PV system transformer-less. [30]

2.5.1 Advantages of Multilevel Inverters [44]

1. A lower switching frequency: the reason for the lower switching frequency is that more switches are used to provide scaled output levels.
2. Low output voltage dv/dt: to get a lower output voltage dv/dt, the output levels are spread out over a large number of semiconductors. This lowers the voltage stress on each switch.
3. Structure: the use of a modular design makes it possible to increase both the number of input sources and output power.
4. An increase in output power without a corresponding increase in topology's switch ratings
5. Total Harmonic Distortion (THD): The signal has a lower THD because it is more sinusoidal, which results in a lower total harmonic distortion.
6. Lower switching and conduction losses contributed to the overall reduction in losses.
7. Utilize state redundancy and an efficient control strategy to create a fault-tolerant operation.

2.5.2 Disadvantages of Multilevel Inverter [43][44]

1. One of the problems is that there needs to be a larger number of power semiconductor switches.
2. Lower voltage rated switches are able to be utilized in multilevel inverters. However, each switch is equipped with its own gate driving circuit. Thus, the overall system may become more expensive and complicated.

2.5.3 Types of Multilevel Inverters (MLI)

There are three main types of the multilevel inverter used as shown in Figure (2.9), the staircase voltage waveform is generated by picking a voltage level from among several possible options presented by the load's proper connection to a variety of DC voltage sources. [44].

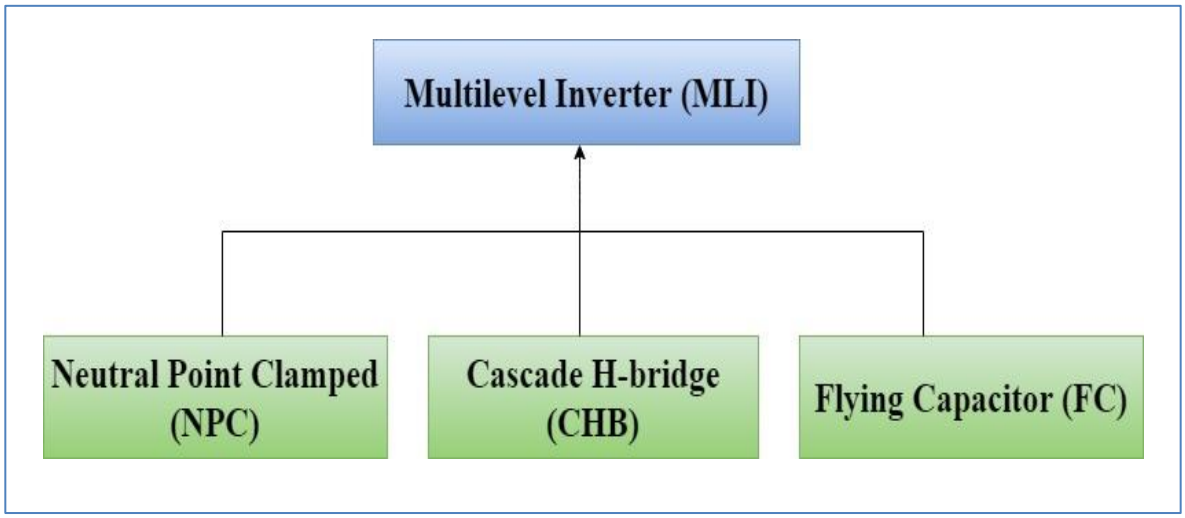

Figure (2.9) Classifications of Multilevel Inverters [44]

2.5.3.1 Three Level Neutral Point Clamped (NPC) Inverter

Neutral-point-clamped (NPC) (also referred to as diode-clamped inverter), were the first multilevel topologies that were practically applicable. Clamping diodes are utilized in multilevel inverters that are controlled by diode clamping. It reduces the voltage stress that power electronic devices are subjected to Nabae, Takashi, and Akagiin [45] were the ones who initially put forward the idea in 1981. An m-level diode clamped inverter needs :

2(m-1) Switching devices , (m-1) series dc supplies or capacitors and (m-1)(m-2) Clamping diodes.

The voltage across both diodes and the switch is denoted by the symbol V_{dc}. The illustration in the Figure (2.10) depicts a diode-clamped inverter with three levels [46].

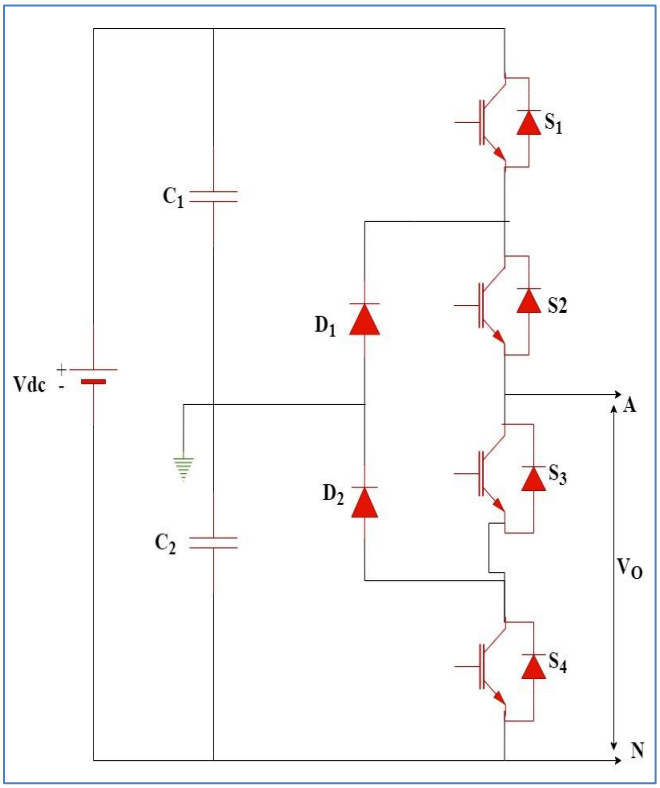

Figure (2.10) 3-level NPC MLI [46]

I. Advantages of Neutral Point Clamped Inverter: [45][46]

1.It is an excellent choice for use in various industrial applications

2. It has a high efficiency at the fundamental frequency

3. Capacitors can be precharged as a group if desired.

4. The method of control is straightforward.

5. It decreases the required number of DC sources

6. It is Suitable for use in error-tolerant applications.

II. Disadvantages of Neutral Point Clamped Inverter [46]:

1. The number of clamping diodes as voltage level increases.

2. If control and monitoring are not done with enough accuracy, the DC level will go down .

2.5.3.2 Cascaded H-bridge Inverter (CH-B) :

Constructing a cascaded H-bridge multilevel inverter is possible by connecting two full-bridge inverters in series. Each bridge is powered by its independent DC supply as shown in Figure (2.11) such as solar panels or batteries. By utilizing these decentralized DC sources, the H-bridge multilevel inverter can generate voltage with a nearly sinusoidal waveform [47], The output voltage of an m-level H-bridge multilevel inverter is calculated by adding the voltages generated by each inverter. Compared to diode-clamped and flying capacitor inverters, it has a more straightforward design, lower total harmonic distortion (THD), and fewer components on each level. However, it needs isolated DC voltage sources, which is only sometimes possible and increases the implementation cost [48]

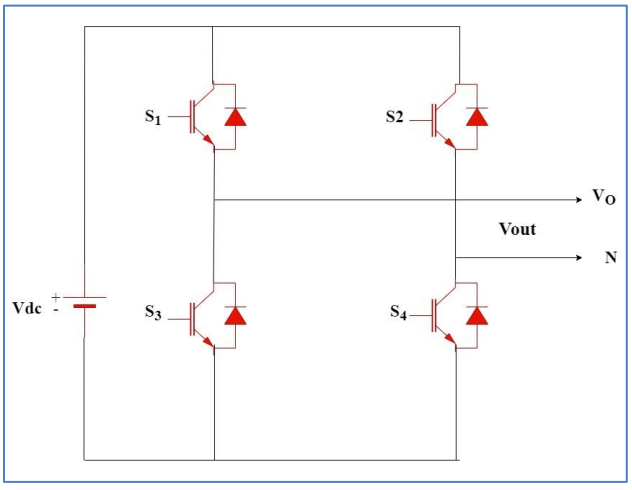

Figure (2.11) 3-level cascade H-bridge MLI [48]

2.5.3.3 Flying Capacitor Inverter (FC):

While the DC-MLI and FC-MLI share similar topologies, the FC-MLI uses floating capacitors instead of clamping diodes. An FC-MLI's output waveform will exhibit voltage steps of varying magnitudes depending on the voltage variation in nearby capacitors. This holds whether or not the capacitors have been charged. For the "m"-level inverter, the FC-MLI topology comprises (m–1) DC link capacitors. The three-tiered FCMLI topology is depicted in a simplified in Figure (2.12). A DC supply with two capacitors and four unidirectional power switches makes up this topology. [49] These parts, respectively, produce voltages of $V_{dc}/2$, 0 volts, and $-V_{dc}/2$. In order to get a voltage with a positive polarity from the output, switches S_1 and S_2 must be activated. To achieve this, turn on both switches. For the output voltage to be in a negative direction, both S_3 and S_4 must be activated. For this purpose, turn on both of those toggles. It takes the simultaneous activation of switches S_1 and S_3 or S_2 and S_4 to generate the 0 output voltage levels. FC-MLI voltage synthesis is more flexible than DC-MLI voltage synthesis. Compare this to the DC-MLI's voltage synthesis. Voltage balancing can be achieved at more than five levels by selecting the proper switching combination [46]. This is a must-have feature when the level count exceeds five. Gaining command over-reactive and active powers is a major advantage of this topology. However, it is more expensive and time-consuming to assemble than alternative methods because of the numerous capacitors it requires. If real power is transmitted, switching frequency losses become very noticeable [50].

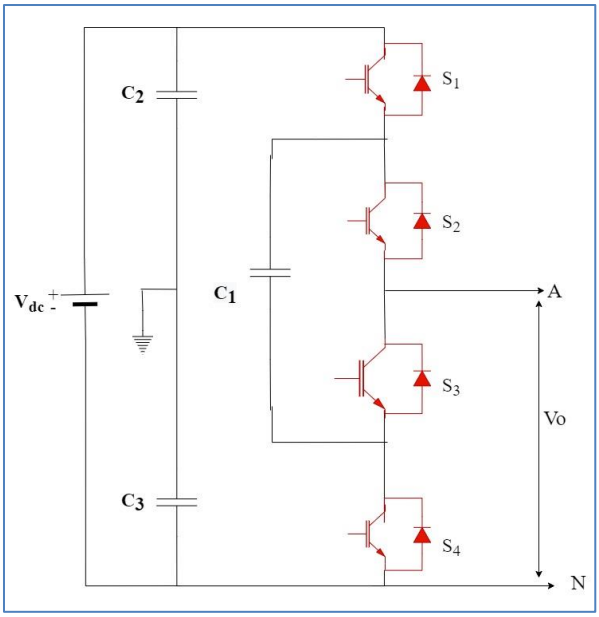

Figure (2.12) 3-level Flying Capacitor MLI [49]

2.6 Modulation Techniques

By alternately turning on and off the power electronic switches of an inverter in the correct order, modulation creates a virtually sinusoidal waveform. This procedure is known as modulation. The modulation techniques can be broken down into the categories shown in Figure (2.13) according to the switching frequency [51], Only one of the two possible commutations of power semiconductor switches takes place during each cycle of output voltage in fundamental switching frequency techniques. The most well-known application of the fundamental switching frequency technique is known as Space Vector Control (SVC).

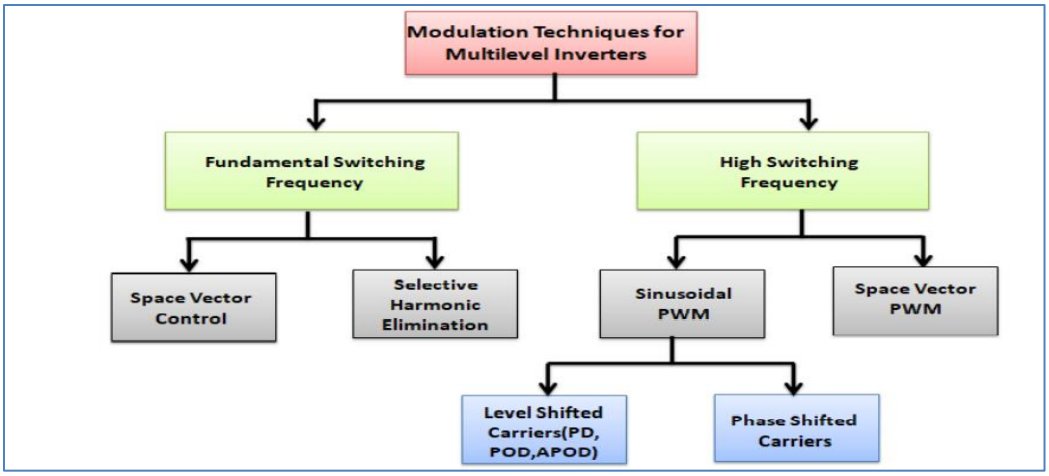

Figure (2.13) A generalized categorization of the modulation techniques used for multilevel inverters [51]

The number of power electronic switches triggered and commutated within one cycle of actual voltage is exceptionally high in high switching frequency techniques SPWM, which stands for sinusoidal pulse width modulation.

2.6.1 Space Vector PWM

In 1987, Holtz et al. came up with the idea of space vector PWM, in 1988, Van der Broeak et al. [52] made some adjustments to the concept. The main goal of the SVPWM technique is to approximate the voltage space vector trajectory by sequentially switching different power electronic components. During this time, the continuously rotating reference vector being sampled is subjected to a sampling frequency. It is presumed that the reference vector will not change during this period. The switching periods for each switching state must also be calculated using this method . The SVPWM principle can be used with a variety of multilevel inverters and output voltages that are greater. Compared to the SPWM technique, the voltage utilization ratio achieved by SVPWM is 15% greater [53][54]. Because of this, the converters can be used where high voltage and high power are needed.

2.6.2 Selective Harmonic Elimination PWM

In 1973, Richard and Husmukh were the ones who first proposed the idea of selective harmonic elimination as a principle. The output of the square wave is chopped multiple times using this technique [55] , This technique is efficient in removing lower-order harmonics, and as a result, it can produce an output waveform of higher quality [56].

2.6.3 Sinusoidal Pulse Width Modulation

Creating pulse width modulated (PWM) output using a sine wave as the modulating signal is known as sinusoidal pulse width modulation (PWM). In this instance, as illustrated in Figure (2.14), the modulating wave (a reference sinusoidal wave) and the carrier wave are compared to determine the PWM signal off and on periods (a high-frequency triangular wave). The carrier wave is triangular and high-frequency, while the modulating wave is a reference sinusoidal wave. Sinusoidal pulse width modulation (often shortened to "SPWM") is commonly used in many business and manufacturing applications. [57] The wave's frequency of modulating signal determines the voltage frequency. The modulation index and the output voltage's root mean square are determined by the peak amplitude of the modulating wave (RMS). Adjustment the modulation index to modify the output voltage's root-mean-square (RMS) value [58]. The SPWM categories into :

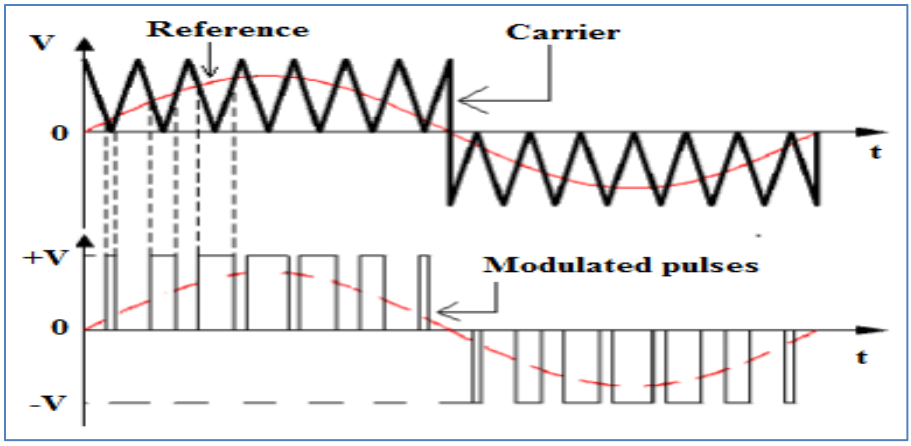

Figure (2.14) Sinusoidal pulse width modulation [57]

- Phase Shifted Pulse Width Modulation (PSPWM)
- Level Shifted Pulse Width Modulation (LSPWM) which include :-

1. Phase Disposition (PD).
2. Phase Opposition Disposition (POD).
3. Alternate Phase Opposition Disposition (APOD).

2.6.3.1 Phase Shifted Pulse Width Modulation (PSPWM)

Additionally, this method is well-known for its ability to evenly distribute power to each H-bridge cell contained within an inverter. It is essential that all of the carrier signals have the same amplitude and frequency when performing phase-shifted modulation [58]. On the other hand, the number of carrier waves necessary for m-level inverter is m-1, that should be displaced by $\frac{360^{\circ}}{m-1}$ with respect to each other. For creating the gate pulses necessary for the inverter circuit, triangular carrier signals that are compared to a sinusoidal reference wave are frequently used [59], Figure (2.15) .

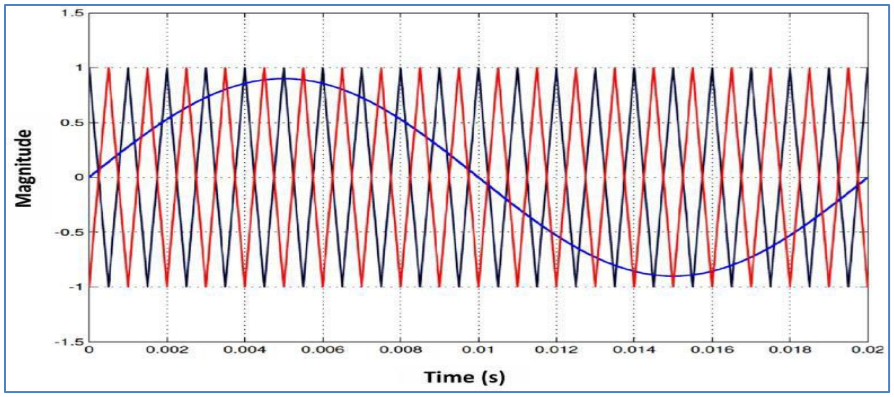

Figure (2.15). Carrier waves in PSPWM [59]

2.6.3.2 Level Shifted Pulse Width Modulation

The amount of carrier signals needed for an m-level inverter while utilizing LSPWM is m-1. The signals must be identical in terms of frequency and amplitude. Every carrier signal has its phase shifted. A comparison is made between the modulating signal and the carrier signals, a pulse is generated when the modulating signal's amplitude is greater than the carrier signal's [60] [61]. The several kinds of LSPWM methods are listed below.

I. Phase Disposition

All of the two carriers are in phase when using the PD technique, as shown in Figure (2.12) [60].

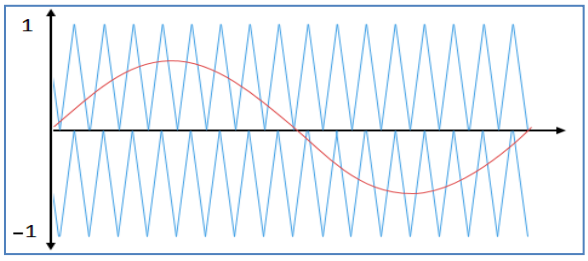

Figure (2.16). Signals used as the reference and carrier in the PD Modulation method

In PD-PWM all the carriers are in the same phase. For 3-level NPC and SI-NPC , two carriers are needed with one reference voltage (Vref). By comparing the carrier signals with the reference, the output signals are used to drive switches S1–S4 ,This section only examines the operation of the inverter during the positive half-cycle. Due to the fact that the opposite half cycle is the same. The converter's output voltage is set to +Vdc/2 when the reference is greater than both carrier waveforms. The output voltage of the converter will be zero if the reference is higher than the lower carrier waveform but lower than the upper carrier waveform. When the reference is smaller than both carrier waveforms, a negative output voltage (-Vdc/2) is produced [60].

Mode 1 [P]: By comparing carrier 1 (high frequency sawtooth signal) with a reference signal (the sine wave with 50 Hz), S1, S3, are controlled whereas switches S2 and S4, are controlled when carrier 2 and Vref are compared.

Mode 2 [O]: when the reference signal is lower than carrier1, S1 is off and S3 is on. Switches S2 and S4 stay in a continuous state because the reference signal in this mode is larger than carrier 2, which prevents them from switching for the whole of the positive half cycle.

Mode 3: Switches S3 are on, S2 is being turned off, and S1 and S4 are both off.

II. Phase Opposition Disposition

According to the POD approach, the carriers above the zero reference point are 180 degrees out of phase with the carriers below the zero reference point [61], as shown in Figure (2.13)

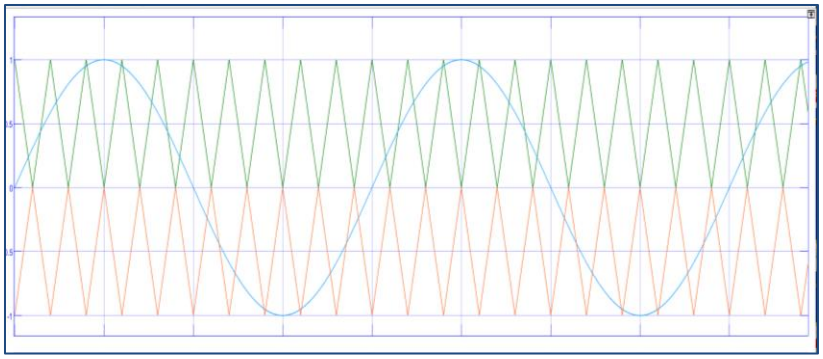

Figure (2.17). In the POD modulation method, reference and carrier signals both exist.

III. Alternate Phase Opposition Disposition (APOD)

It is worth mentioning that in 3-level inverter the POD is similar to APOD. [61] .

2.6.4 Hysteresis Current Control (HCC)

The output of hysteresis band system is said to have "hysteresis" if it is allowed to oscillate freely within a specific error band called the "hysteresis band." The nodes of the triangular wave shown in Figure (2.18) are the source of the switching instants here. Hysteresis-band can be used independently of knowledge of the inverter load. So long as the inverter's output voltage is not maxed out, the inverter's output will continuously track the reference band if the reference signal is known. "Saturation" occurs when the inverter's output voltage reaches its maximum. [62] In this technology, the frequency at which power devices turn on and off varies according to the size and rhythm of the reference signal. Therefore, the switching losses associated with this approach may be more significant than those of alternative approaches.

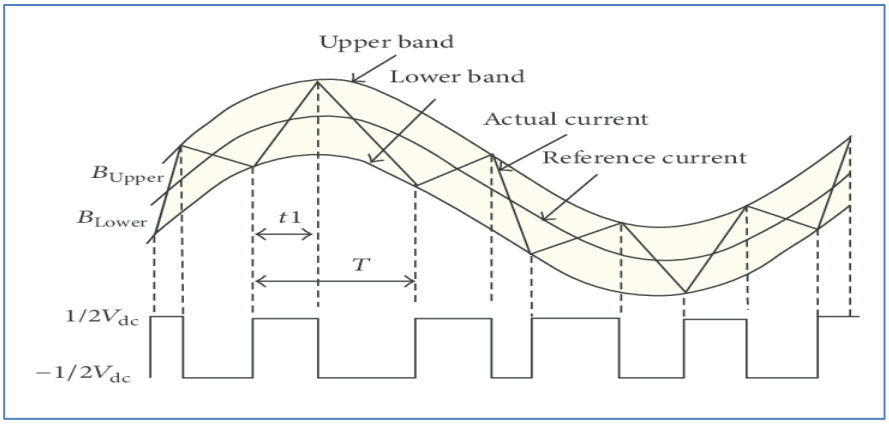

Figure (2.18) Hysteresis band [62]

The Hysteresis Band is in control. The features of HCC method that uses instantaneous feedback current control the actual current continuously tracks the command current within a given hysteresis band. If the inverter has a unity power factor, and the current through the inductor, iL_{12} (the total current I_T), is synchronized with the grid voltage. This is necessary because a PV grid-connected inverter needs to keep the grid voltage and current at a unity power factor. However, the current through the inductor must be consistently lowered to zero before the grid voltage drops below zero if the device is to operate safely. It is possible to precisely track the inductor current with the help of hysteresis current control. As can be seen in Figure (2.19), the inductor current should be zero before the grid voltage does (i.e inductor current should be zero at time xπ). Ideally, the grid voltage should cross zero before the inductor current reaches zero. The following expression can be used to determine x, a period of time required to turn off high-frequency switching signals:

$$\frac{\int_{x\pi}^{\pi}[V_g \cdot sin(\omega t)+V_D(ON)+V_S(ON)]}{L} \geq I_{ref} \cdot sin(x\pi) + \frac{h}{2} \qquad (3.3)$$

When they are both "on," these voltages are represented by their respective symbols, V_D (on) and V_S (on). The high-frequency driving signal's continuity is represented by the symbol x, and the inductor current ripple, also known as the bandwidth of the current hysteresis, is represented by the symbol h. An efficient ways to implement hysteresis current control is through Hysteresis Band Real-Time Regulation, as it offers great performance, a simple realization circuit, high stability, and an inherent capability to limit current. This can be done by adjusting the hysteresis band.

$$h = \frac{V_g(V_{pv}-2\cdot V_g)}{V_{pv}\cdot L\cdot f_s} \qquad (3.4)\ [62]$$

where f_s stands for the expected switching frequency . In addition, anti-islanding system may re-evaluate the amount of time it takes. The signals used for high-frequency switching are disabled. When the frequency of the measured voltage is rising in islanding mode, reaching the over-frequency limit requires decreasing time x via positive feedback. When the limit is reached, (i.e by increasing the gap of the current reference).

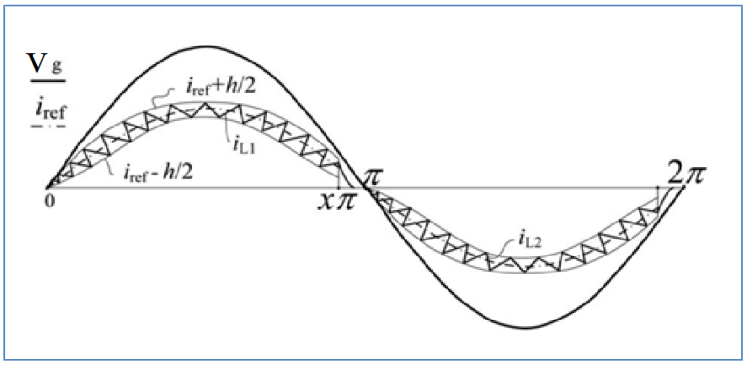

Figure (2.19). Phase control of inductor current i_{L12} .

Implementing a hysteresis-current controller often entails the use of a closed-loop control system. A error signal called error (e) controls the inverter's switches. Symbolized by Iactual, the inverter's error is the disparity between the actual current and the reference current, Iref. as shown in figure (2.20). Whenever the error rate rises over a predetermined limit, transistors are switched limit the current they receive. As the error grows, the current must rise since it has nowhere else to go. The hysteresis band refers to the range of the error signal, which determines how much ripple there is in the inverter's output current. The two bounds that deal with deviations from the reference signal are known as the lower hysteresis limit and the upper hysteresis limit, respectively. These boundaries are also known as the lower and upper hysteresis limits. The actual current remains within these limits regardless of changes a reference current.

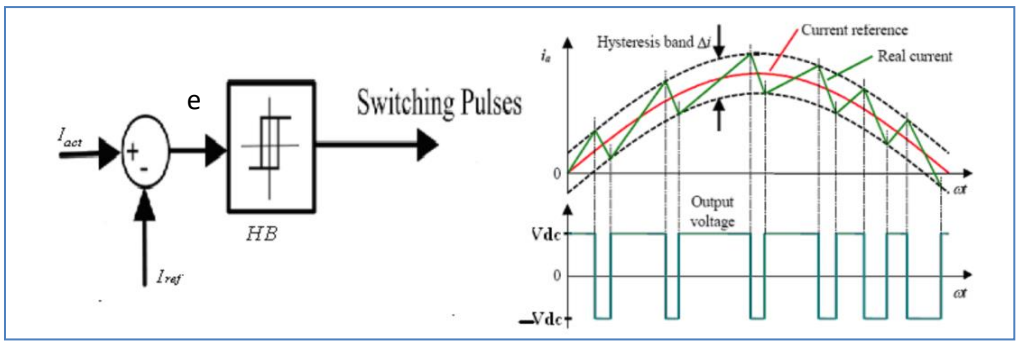

Figure (2.20) Hysteresis PWM Current Control and Switching logic.[62]

2.7 Phase- locked Loop

It is necessary to have a grid synchronization mechanism in place in order to ensure that the correct amount of current is injected into the electrical system. To achieve that, one must be familiar with the phase and frequency of the voltage that is derived from the power grid. When the PLL is used to estimate the phase of a

current injection into the grid, Phase and phase angle of the reference output current are equal. The formula for determining this phase angle is as follows:

$$i_{ref}^{*} = i_{f}^{*} \times sin(\varphi_{PLL}) \quad (3.6)\ [63]$$

where i_f * is the amplitude of the reference current's fundamental component, which is equal to:

$$i_{f}^{*} = I^{*} + I_{DC} \quad (3.7)$$

where I_{DC} is the current reference provided by the DC link regulation, and I * is the PV current reference provided by the MPPT algorithm [63].

2.8 Capacitors balance Voltage Control,

The DC-link voltage should be distributed equally between the DC capacitors to ensure the effective operation of the converter.The current reference will be adjusted by the controller-imposed increment or decrement. [64]A PI controller controls the voltage across the capacitors to control the DC-link voltages, and to prevent the attenuation between them .The standard voltage is given by the following expressions:

$$V_{DC} * = V_{C1} + V_{C2} \quad (3.8)$$

2.9 Design of PI control

PI control is used to regulate the output voltage and power of converter , The parts of PI control are integral gain and proportional gain. Proportional gain, Kp is effective to reduce the step up time but it is not exact solution to eliminate the steady state error. The integral controller Ki, is effective to eliminate steady state error [65].

CHAPTER THREE

Design of Single-Stage Transformer-less PV system

CHAPTER THREE

Design of Single-Stage Transformer-less PV system

3.1 Introduction

In chapter two, both the two-stage and the single-stage photovoltaic systems are discussed. The two-stage system is made up of an inverter and a DC to DC convert. An inverter is used to manage the voltage on the ac side, the DC/DC converter is used to control the voltage on the DC side. This chapter investigates the employment of single-stage grid-connected photovoltaic system rather than using a two-stage system, It is represented by a multilevel inverter that operates without transformers (transformer-less) which has three levels, a controller MPPT that relies on specific algorithms to determine the voltage entering the inverter, and uses a HCC controller that has the advantages of simplicity and accuracy in tracking. In this system, the voltage entering the inverter is determined through MPPT controller, In addition, PLL was utilized to ensure that the output voltage was synchronized with the voltage of the electrical power grid.

In this chapter, the proposed methods included the improvements in (V, I, P, THD) that were applied to the PV system in all of its parts. There will be a comparison of two systems, both of which are composed of the same parts with the exception of the MPPT algorithm. In one of the two systems, the P&O algorithm is used, and in the other system, ANN algorithm will be used. This will result in improvements to (V, I, P, current THD, and efficiency).

3.2 System configuration for the Proposed transformer-less grid connected PV system.

Referring to Figure (3.1) which represents the scheme of the single stage grid-connected photovoltaic system proposed in this thesis, the following points are discussed:

1. Design of the PV system
2. Three-level Improved Split Inductor Neutral Point Clamped ISI-NPC multilevel inverter
3. Proposed Controller

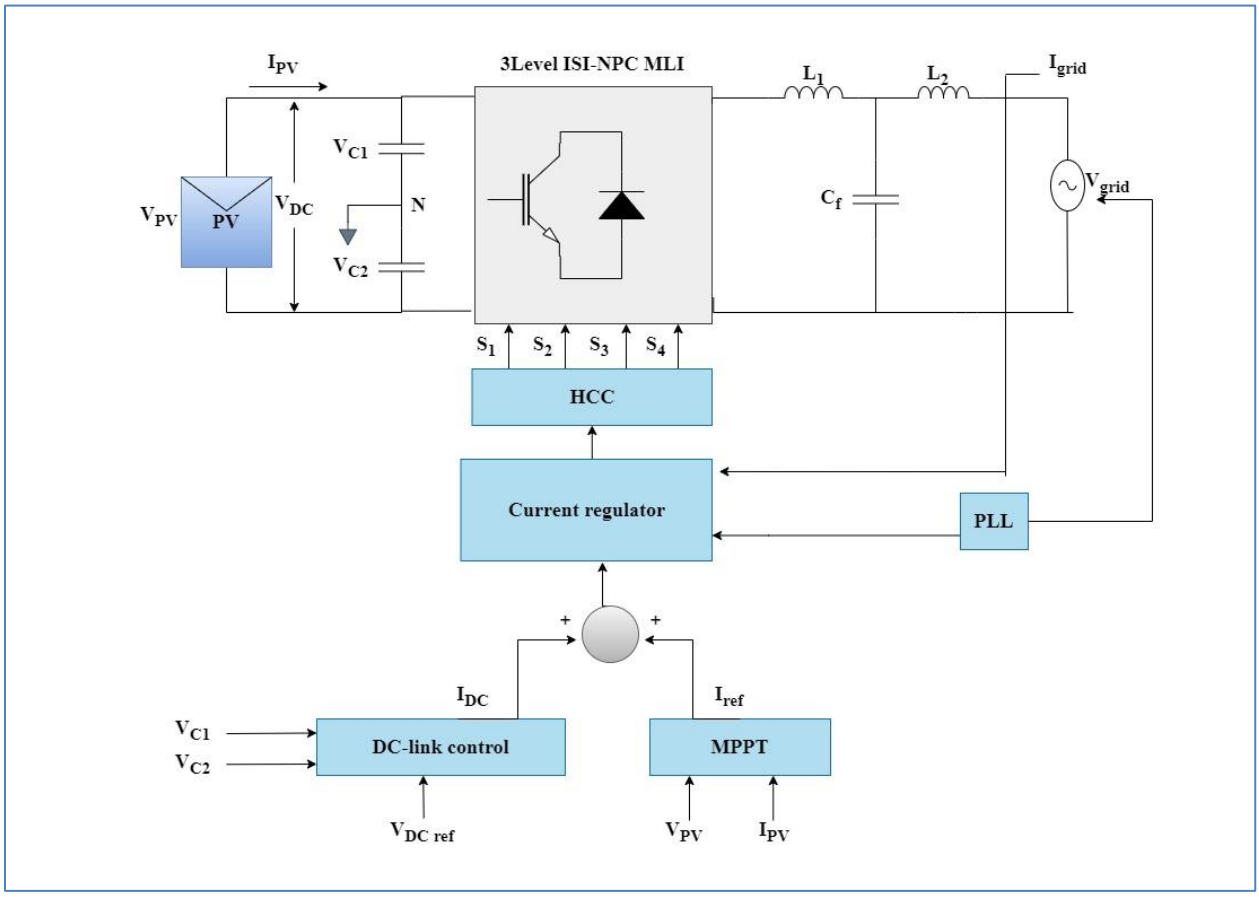

Figure (3.1) Proposed of Single stage grid connected photovoltaic system.

3.2.1 Design of the PV system

The photovoltaic source used in this thesis is the Kyocera solar KC200GT module type it consists of a string formed by thirty modules connected in a series. Each module has the specification listed in Table (3.1)

Table (3.1). Specification of Module

$V_{OC}(V)$	32.9	$I_{SC}(A)$	8.21
$V_{mp}(V)$	26.3	$I_{mp}(A)$	7.61
$P_{mp}(W)$	200.143	*No. of Cell*	54
Temperature (°C)	25	*Irradiance (W/m$^{2)}$*	[1000]
Temperature coefficient of $V_{oc}(\%/°C)$	-0.355	*Temperature coefficient of* $I_{SC}(\%/°C)$	0.06

3.2.2 Three-level Improved Split Inductor Neutral Point Clamped ISI-NPC multilevel inverter

The schematic representation of the three-level ISI-NPC inverter is demonstrated in Figure (3.2). In advance of the analysis, the following hypotheses are presented: All inductors and capacitors are perfect ($C_1 = C_2$, $L_1 = L_2 = L$), semiconductors devices (diodes and IGBT switches) are ideal, and the diode between two inductors is used to prevents the passage of reverse current, the inverter runs at a unity power factor (the voltage at output or grid (Vg) is in phase with the grid current (I_g) [68]. A shoot-through in a multilevel inverter is an undesirable condition in which two or more switches in the inverter are conducting simultaneously, allowing current to flow directly from the input to the output without passing through the inverter's storage elements. This can cause problems

such as increased power loss, increased switching losses, and increased electromagnetic interference (EMI). It can also result in an increase in the switching frequency of the inverter, which can lead to additional problems such as increased switching losses and reduced efficiency. To prevent shoot-throughs, it is important to design the control logic for the inverter carefully and to use appropriate protection measures such as snubber circuits and diodes.

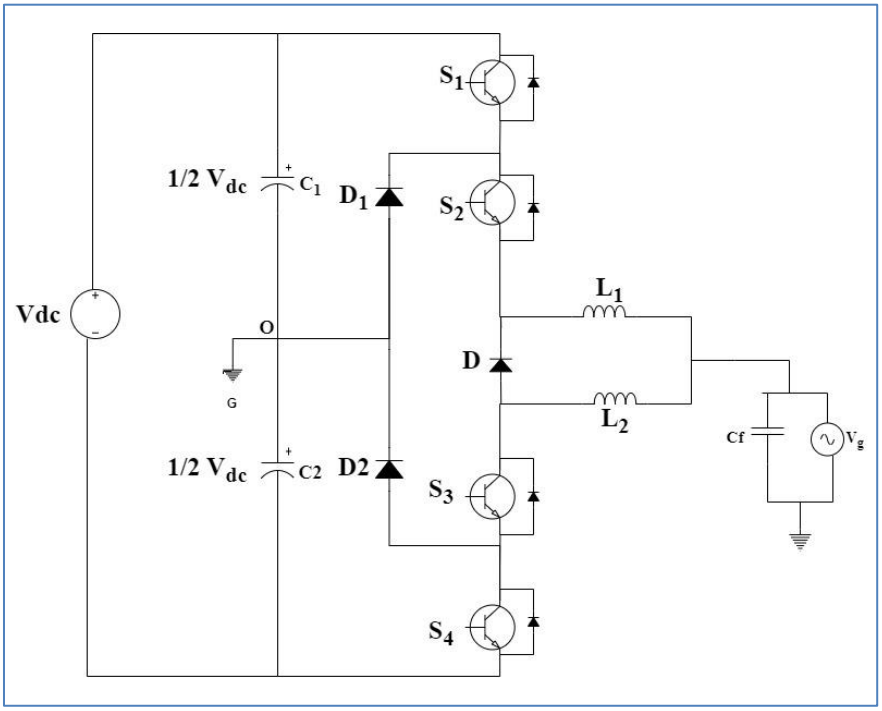

Figure (3.2). Three-level Improved SI-NPC [66]

In this converter, the mid-point shared between two DC link capacitors and the clamping diodes. Two clamping diodes are employed D_1&D_2 to acquire the zero voltage level via mid-point. It also has a four semiconductor switches S_1, S_2, S_3, S_4 as shown in Figure (3.2). The upper switches S_1 and S_2 are operating in a complementary manner with the lower switches $S_3$and S_4. Split inductors (L_1 and L_2) are used to avoid the shoot through. Table (3.2) presents the design values of the three level Improved Split Inductor Neutral Point Clamped Multilevel inverter .

Table (3.2) Three level Improved Split Inductor Neutral Point Clamped Multilevel inverter components [66]

Components	Units	Value
Input voltage (Vin)	Volt	800
Capacitors (C_1=C_2)	µF	2000
Capacitor initial voltage (V_{C1} =V_{C2})	Volt	400
Inductors (L_1=L_2)	mH	4
Grid Voltage (Vg)	Volt	240

In this converter, three levels of the output voltage can be achieved: Vdc/2, 0 and -Vdc/2. Table (3.3) shows the switching state of the converter where S_1 and S_2 must remain on to obtain Vdc/2, while S_3 and S_4 must be on for - Vdc/2. Turning on either S1 and S4 or S2 and S3 will result in the same value of zero voltage level.

Table.(3.3) Switching states for a single-phase 3L (ISI-NPC) [66]

Switching -state	S_1	S_2	S_3	S_4	Output Voltage
P	ON	ON	OFF	OFF	$\frac{1}{2}Vdc$
$(\pm\mathbf{0})$	OFF	ON	ON	OFF	0
N	OFF	OFF	ON	ON	$\frac{-1}{2}V_{\mathrm{dc}}$

There are three modes of operation for 3L ISI-NPC inverter as described below:

Mode 1 [P]: Comparing reference signal with carrier1 drives switches S1 and S3, and comparing reference signal with carrier2 drives switches S2 and S4. In the mode1 figure (3.3-a) the reference signal is greater than carrier1, hence, switch S1

is ON and its complemental switch S3 is OFF. The reference signal is greater than carrier2 across the positive half cycle, thus, S2 is ON and its complemental switch S4 is OFF. The output voltage of the bridge leg is the voltage of capacitor C1, (1 /2)V_{DC} .The output current io is positive and the current of inductor L1 (iL1) increases at this duration. In this mode, ibias=- iL2 and the voltage of L1 is

$$L_1 \frac{di_{L1}}{dt} = \frac{1}{2} V_{DC} - Vg \qquad (3.1)$$

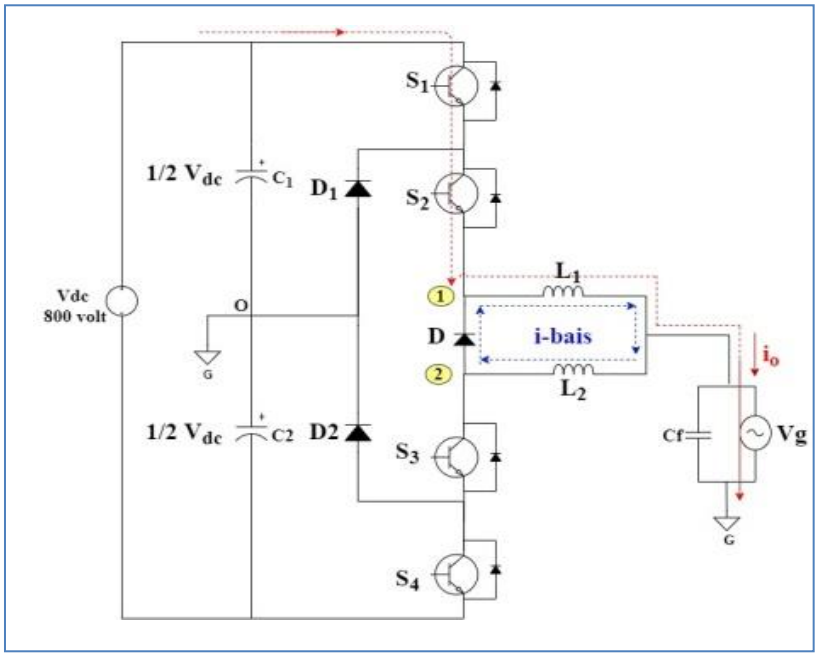

Figure (3.3) The Various Efforts of Operation: (a) mode1 [66]

Mode 2 [O]: Figure (3.3-b) illustrates that the switch S_1 is turned off while the switch S_3, which is its complement, is turned on and S_2 ON. A positive output current ($i_o > 0$) turns D_1 ON, connecting terminal (1) to the mid-point (O) by way of the connection between D_1 and S_2. Figure (3.3-b) shows that there is no voltage at the output of the bridge leg . During this time period, the current through inductor L_1 is in the freewheeling stage, which results in i_{L1} falling [66]. When operating in this mode, $i_{bias} = -i_{L2}$, and the voltage on L_1 is:

$$L_1 \frac{di_{L1}}{dt} = 0 - Vg \qquad (3.2)$$

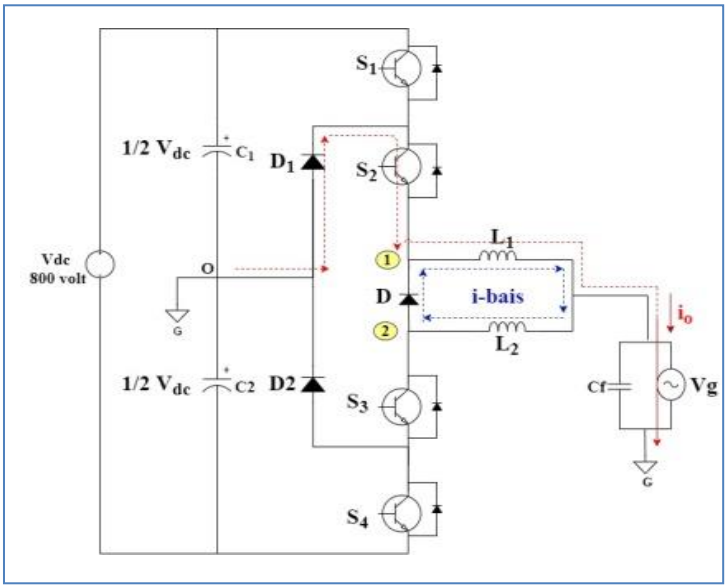

Figure (3.3) The Various Efforts of Operation: (b) mode 2. [66]

Mode 3: Figure (3.3-c) shows that switches (S_1 & S_4) are turned off, while switch S_3 is on and switch S_2 is currently being turned off. In this scenario, there is an abrupt drop in the voltage of V_1. Because of the induction potential of V_2, the parasitic body diode of S_4 will become active once its voltage drops below 1/2 V_{DC}, and the body diodes of S_3 and S_4 all contribute to a linear reduction in the current at the circuit's conclusion. The value of capacitor C_2 stores the voltage of the negative half of the bridge; hence, its output is (-1/2) VDC . In this mode, i_{bias} = - iL2.

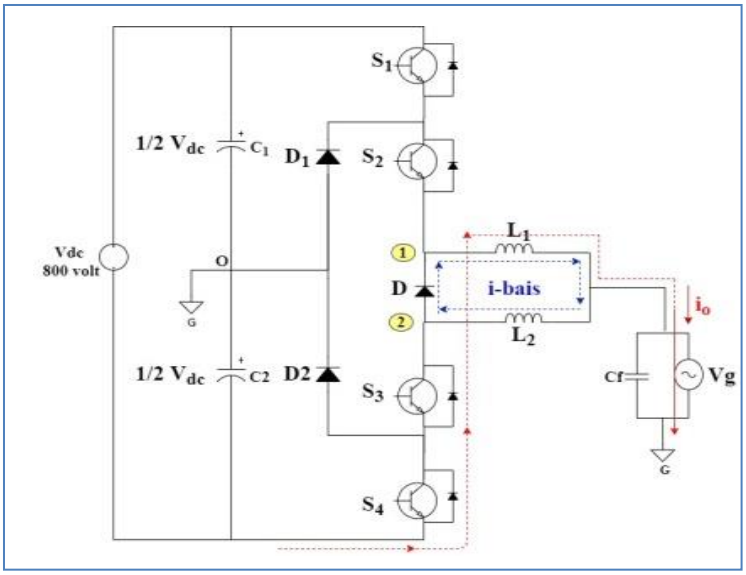

Figure (3.3) The Various Efforts of Operation: (c) mode 3.[66]

3.3 Proposed Controller

The MPPT takes in a current and a voltage and compares them with the V_{PV} to make sure there is no error; then it enters the PI to correct the error, and the resulting current is Ipv_{ref}, then the voltages V_{C1} and V_{C2} are collected and compared the voltage reference of 800V; and finally the PI controller is used to produce I_{ref} current, which is the output of Figure (3.4) The input current and a reference current, Ipv_{ref}, are added to create I_{Tmax}, and synchronization is maintained by releasing V_g, initiating the phase lock loop, and releasing theta. When entering HCC with all switches turned on, I_{Tmax} amplitude, 7.61 A total current, and a 0.2 percent error rate are recorded.

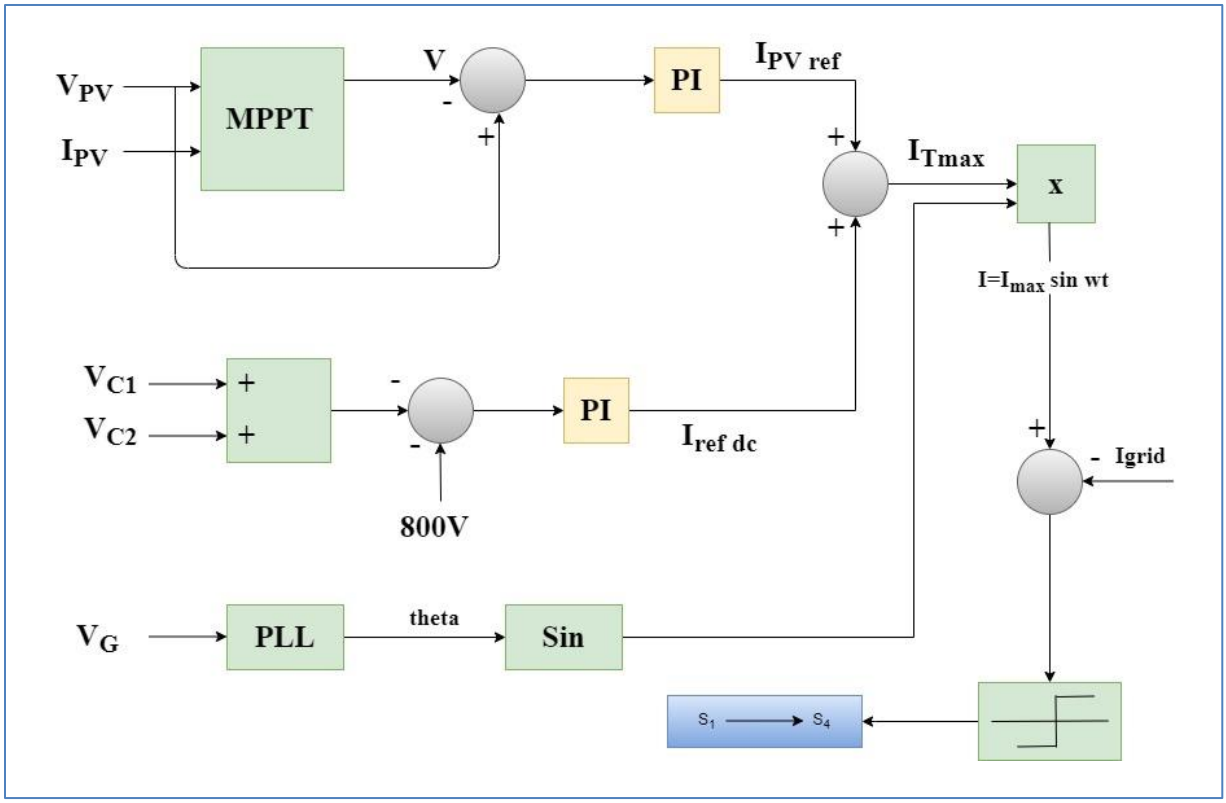

Figure .(3.4) The Simulink model of the proposed voltage balancing controller.

CHAPTER FOUR

Simulation Result of Three Level Single-Stage Transformer-less Multilevel Inverter

CHAPTER FOUR

Simulation Result of Three Level Single-Stage Transformer-less Multilevel Inverter

Part One : Multilevel Inverter (MLI) with DC source

4.1 Introduction

Three-level neutral point clamped (NPC) inverter has drawn much attention for employment in single stage transformer-less PV systems due to its ability to eliminate the leakage current. However, the shoot through problem (short circuit fault) in the NPC converter is an issue which needs to be solved by setting a dead-time which increase the current THD. Therefore, SI-NPC inverter is introduced to avoid the shoot through problem. However, it suffers from high switches overvoltage and a deviation in DC capacitor voltages. [67].

Therefore, this thesis adopts the 3L-ISI NPCI to be employed in a single phase TRL-PV system. An investigation is carried out to evaluate the effectiveness of employing 3L-ISI-NPCI in such system. This can be achieved by examining the behavior of the ISI-NPCI under different carrier-based PWM. In addition, the constant and variable behavior of the 3L-ISI NPCI under hysteresis current is examined for grid connected PV system. In this thesis, the hysteresis current control is adopted as a current control technique to track the inductor current reference when integrating the 3L-ISI NPCI with grid connected PV system.

This chapter firstly investigates the basic existing topologies of the NPC inverter and the SI-NPC under different CB-PWM to understand their behavior in TRL-PV system.

Secondly, a detailed investigation for the performance of the ISI-NPC inverter which utilizing a diode to interface the split- inductor to improve the efficiency and reliability. However, limited researches have been introduced for employment the ISI-NPC inverter in transformer-less PV system.

To understand the converters behavior, the system is designed and modeled in MATLAB/ SIMULINK environment with different NPC topologies. The simulation is carried-out for the system when employing a conventional NPC and SI-NPC under PD and POD-PWM to be used as a base to compare how much improvements can be achieved if the 3L-ISI-NPC is employed instead. The simulation results shows that the 3L-ISI-NPCI can be considered as a better candidate for TRL-PV system in terms of THD and semiconductor over voltage with no shoot through problem with a reduction in inductor values.

In addition, this thesis examines for the first time, the effect of applying the Hysteresis current control HCC-PWM on the operation of ISI-NPCI for transformer-less photovoltaic system. The results show that, using HCC-PWM improves voltage and current waveforms, and reducing the current total harmonic distortions in comparison with other PWM approaches.

It is worth mentioning that this chapter examines the performance of the TRL PV system when fed from ideal DC source, while the next chapter will evaluate the system performance operating with PV panels and its MPPT.

4.2 Design of 3-level single phase NPC and SI-NPC Multilevel Inverter Based on PD PWM & POD PWM Techniques.

I. Result of 3-level NPC and SI-NPC under PD PWM

The single-phase 3L-NPC and 3L-SI-NPC are designed and modelled using MATLAB/ SIMULINK. The simulation circuit parameters are based on [67], As shown in table (4.1). The simulation is carried out using PD-PWM Figure (4.1) and POD-PWM Figure (4.2) approaches with a carrier switching frequency of 20 KHZ and reference 50 HZ.

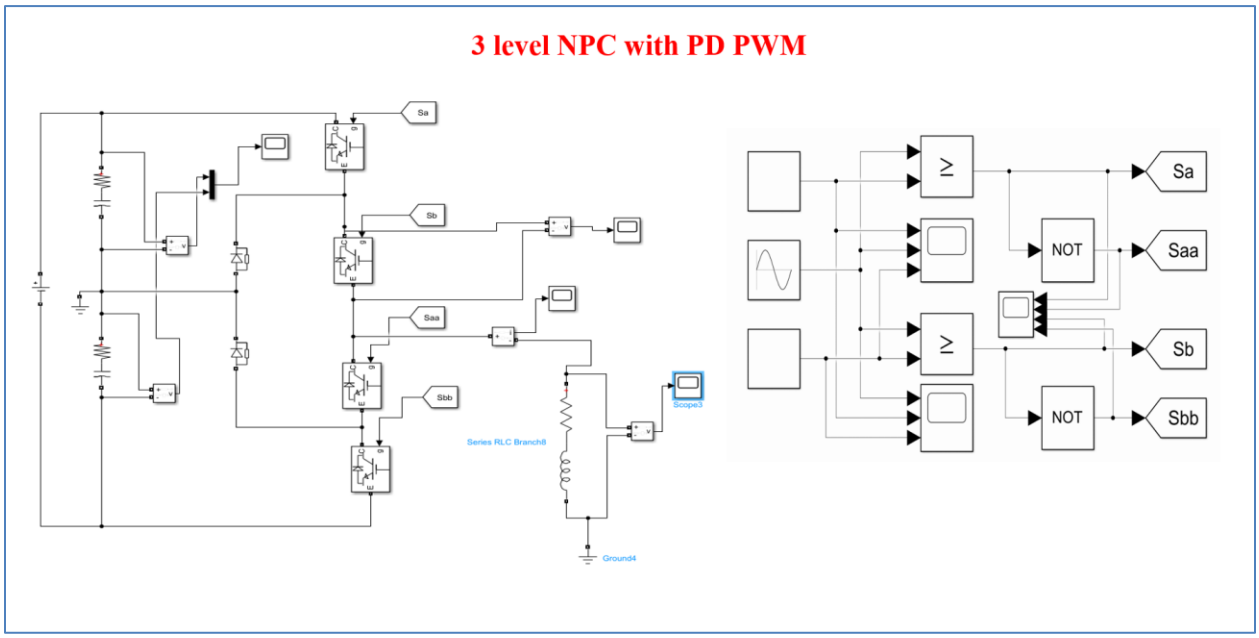

Figure (4.1) Simulink model of 3 level NPC under PD PWM

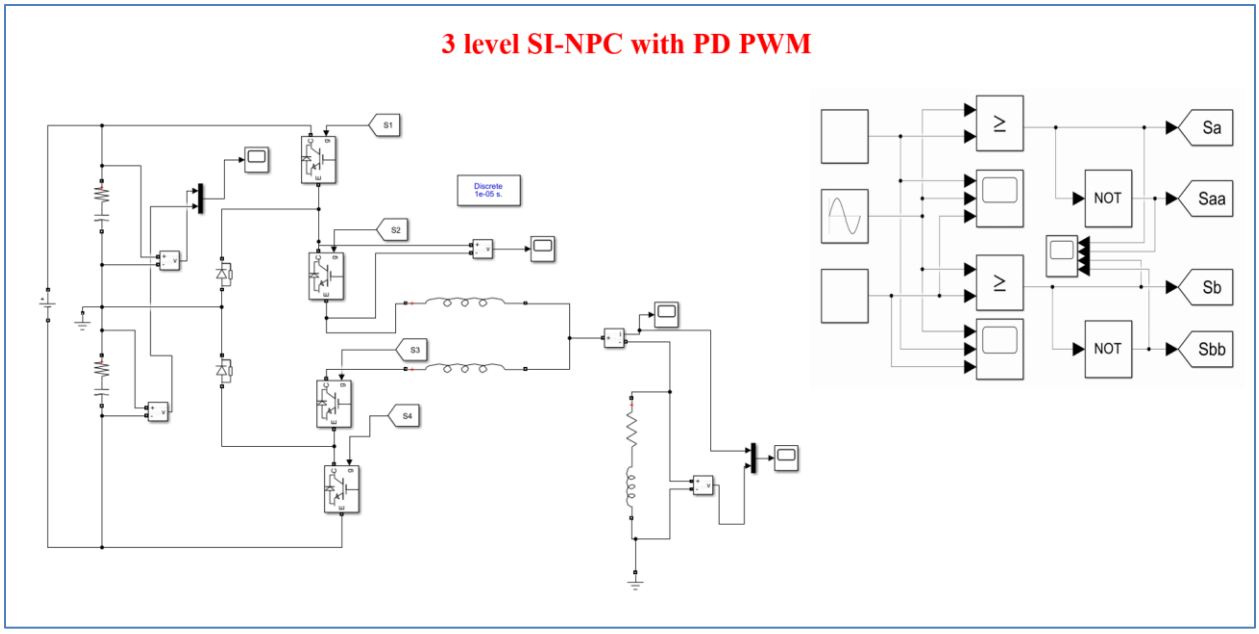

Figure (4.2) Simulink model of 3 level SI-NPC under PD PWM

Table.(4.1) Circuit parameters [67]

Parameters	Values	Units
Output filter inductor $L_1 = L_2$	4	mH
dc-link capacitors C_1=C_2 (NPC)	3300	µF
C_1= C_2 (for 3L-SI-NPC)	235	µF
Input voltage	800	volt
Load resisteanc	30	Ω
Inductor (L) (NPC)	25	mH

Figures (4.3) and (4.4) demonstrate the output voltage of the both inverters where there is an over voltage appears on the SI-NPC output voltage waveforms.

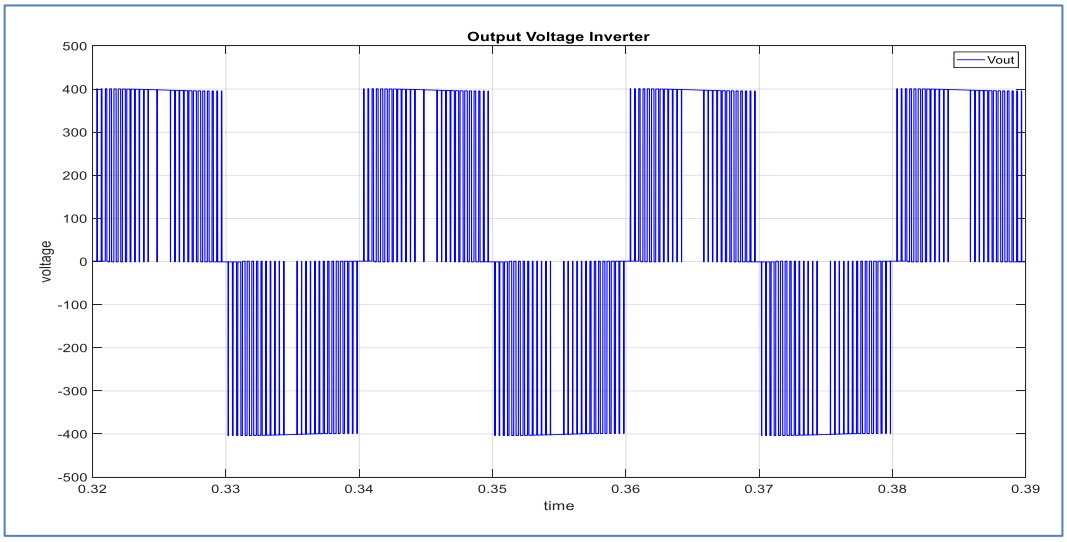

Figure (4.3) the 3L- NPC inverter's output voltage

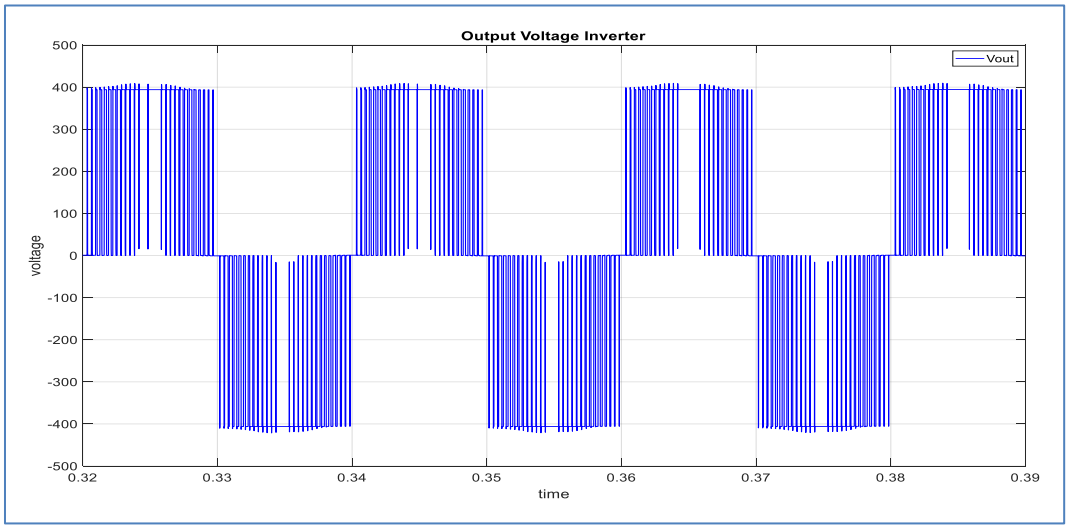

Figure (4.4) The output voltage of the 3L-SI-NPC inverter

Figure (4.5), illustrates that the NPC produces output current much lower than the SI-NPC with a peak-to-peak value of less than 10A. While SI-NPC can develop an output current of 24 A (peak to peak) as shown in Figure 4.5.

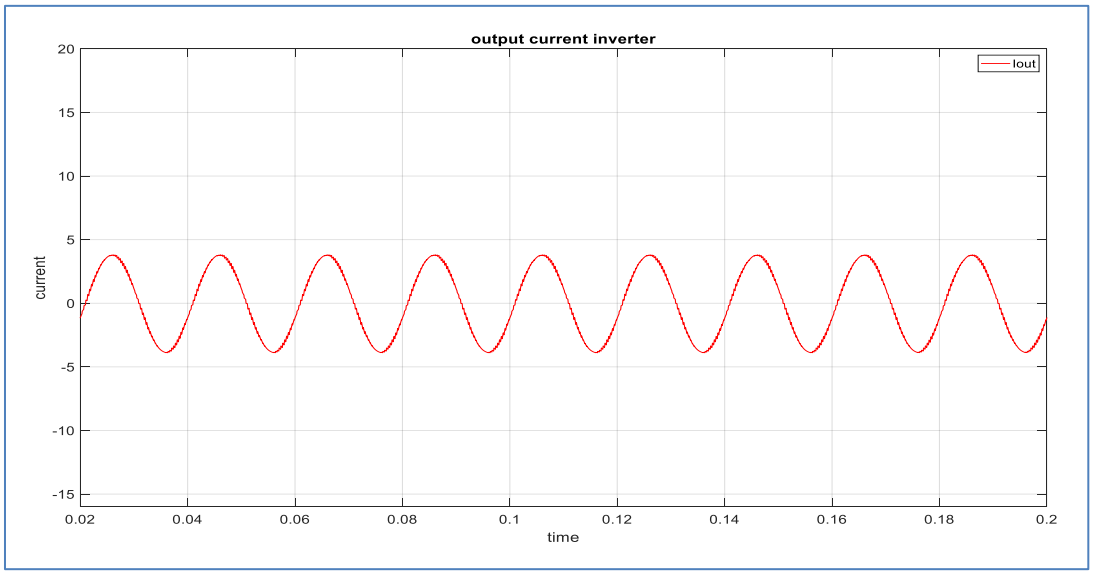

Figure (4.5) Output Current waveform of a 3-L-NPC inverter

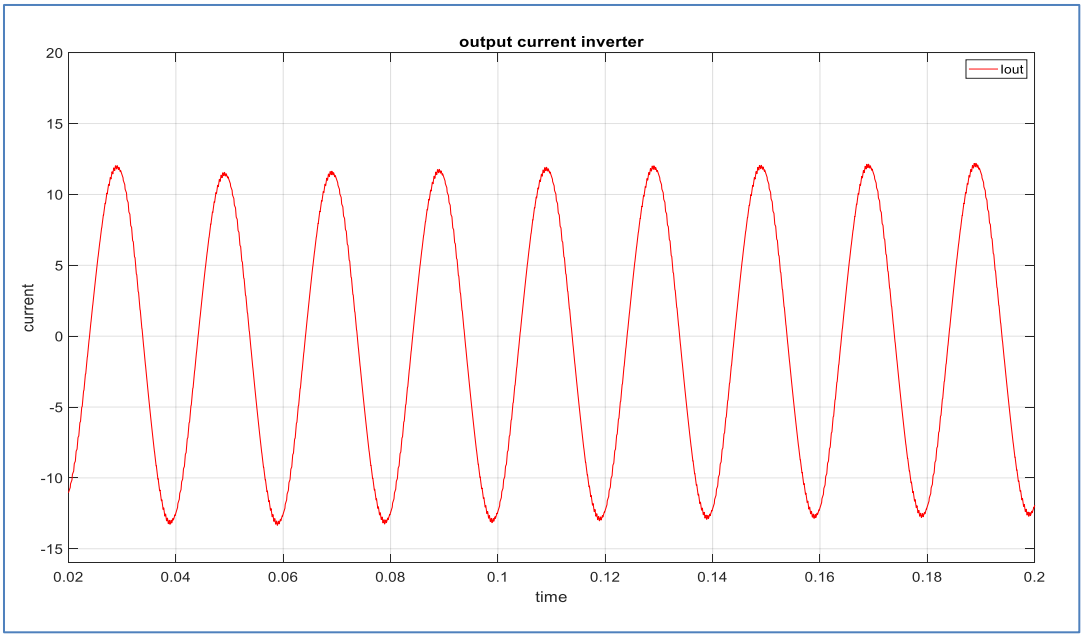

Figure (4.6) Current output of a 3-L-SI-NPC inverter

Similarly, the DC-link capacitors currents are much higher when using SI-NPC in comparison with NPC as shown in Figures (4.7) & (4.8) respectively.

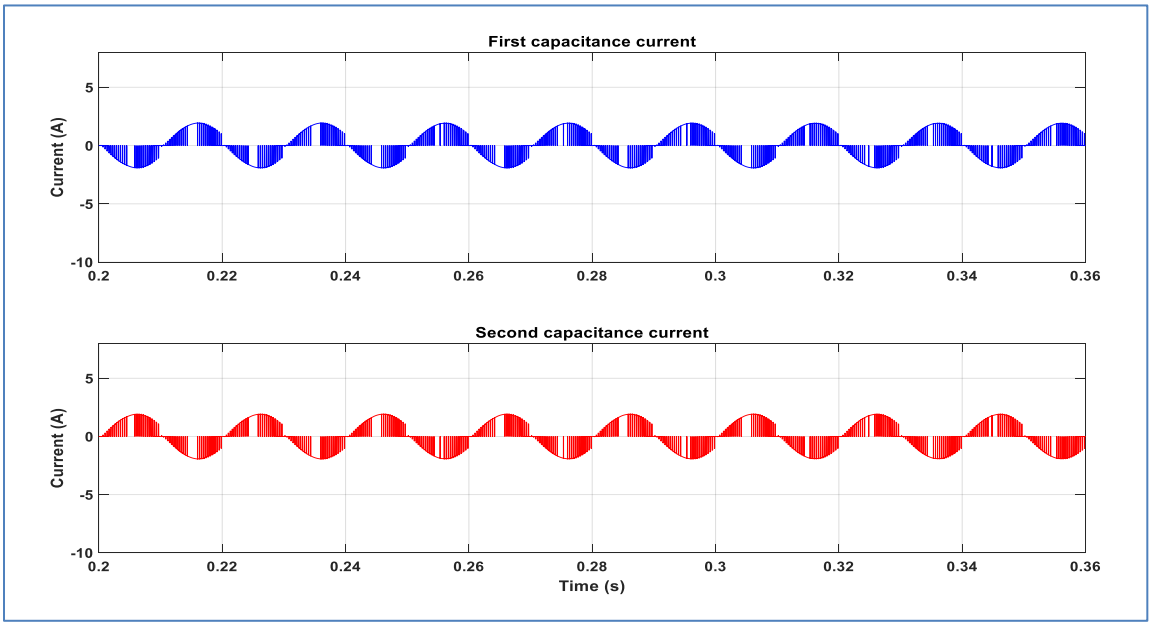

Figure (4.7) Output current of C_1 and C_2 of 3 level NPC multilevel inverter

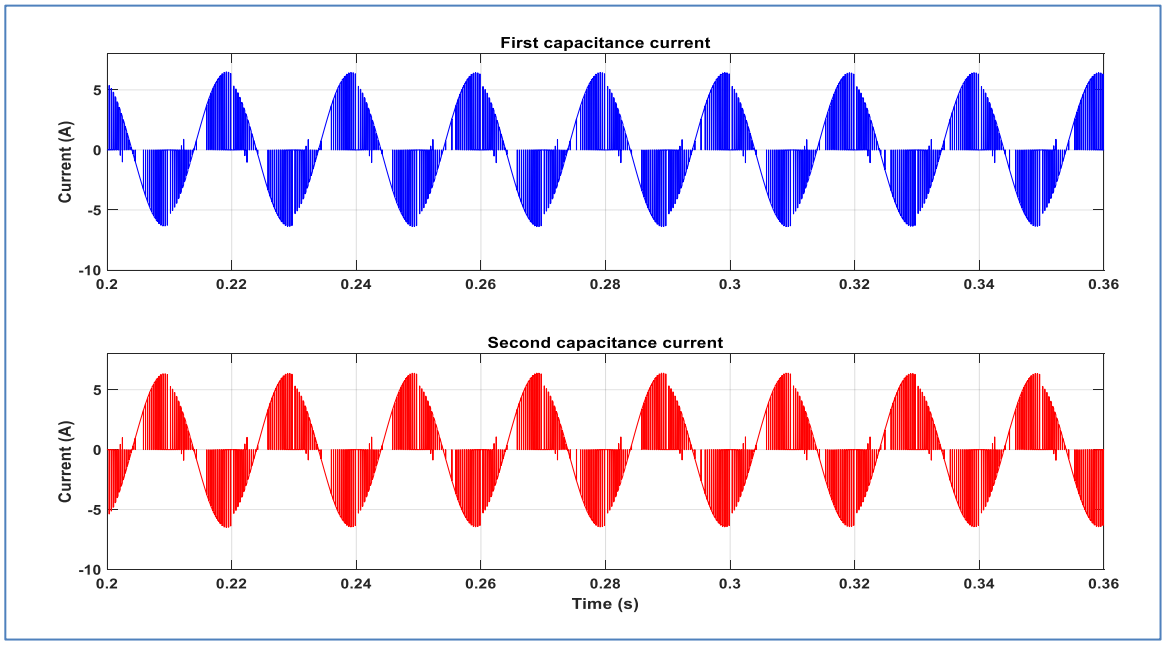

Figure (4.8) Output current of C_1 and C_2 of 3 level SI-NPC multilevel inverter

Figures (4.9) & (4.10) , illustrate the DC link capacitor voltages in both NPC topologies.

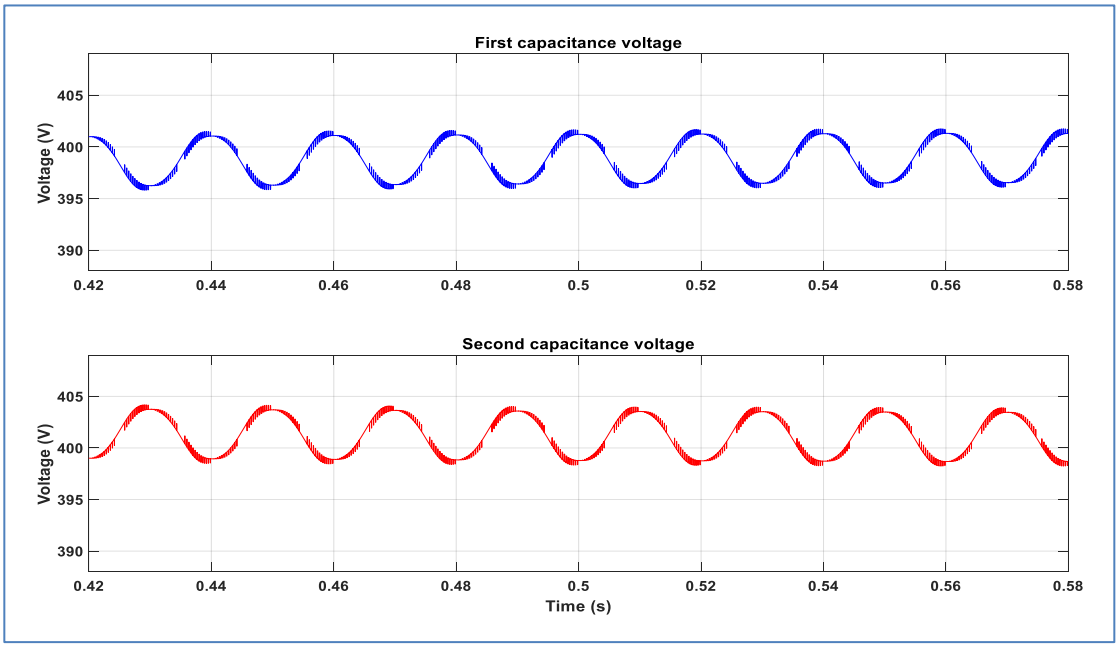

Figure (4.9) Output voltage of C_1 and C_2 of 3 level NPC multilevel inverter

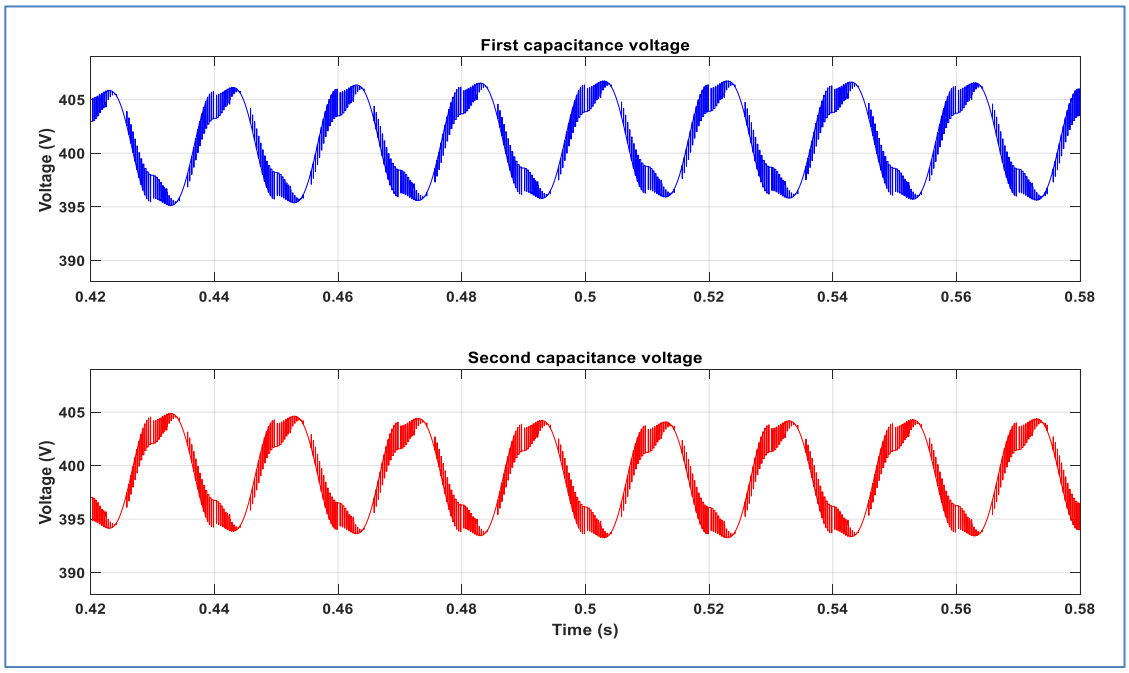

Figure (4.10) Output voltage of C_1 and C_2 capacitance of 3 level SI-NPC multilevel inverter

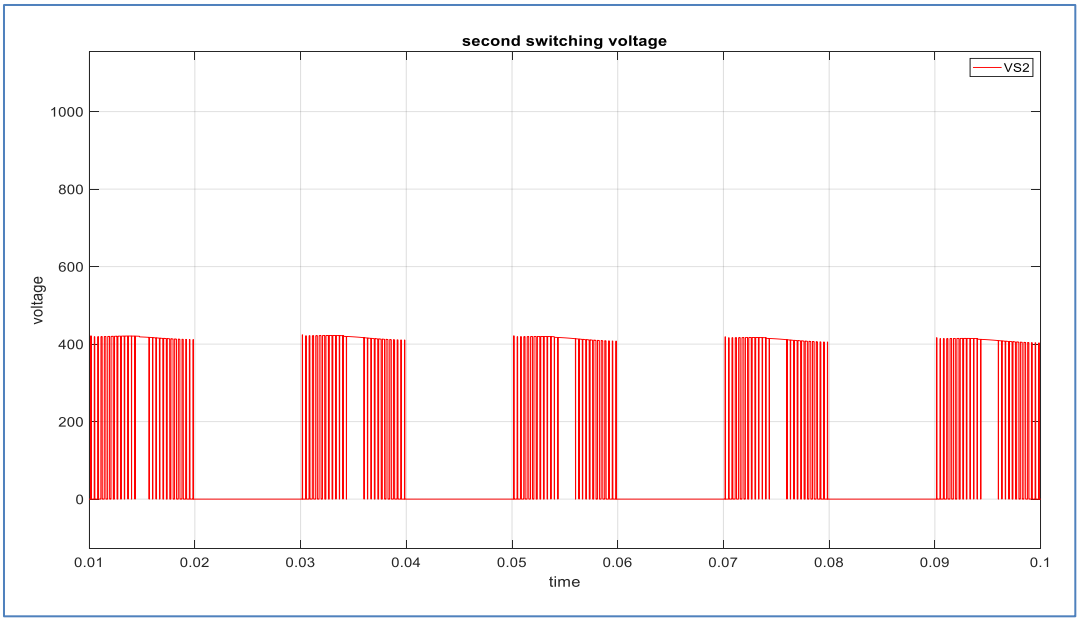

Figure (4.11) output of second switching voltage of 3L-NPC inverter

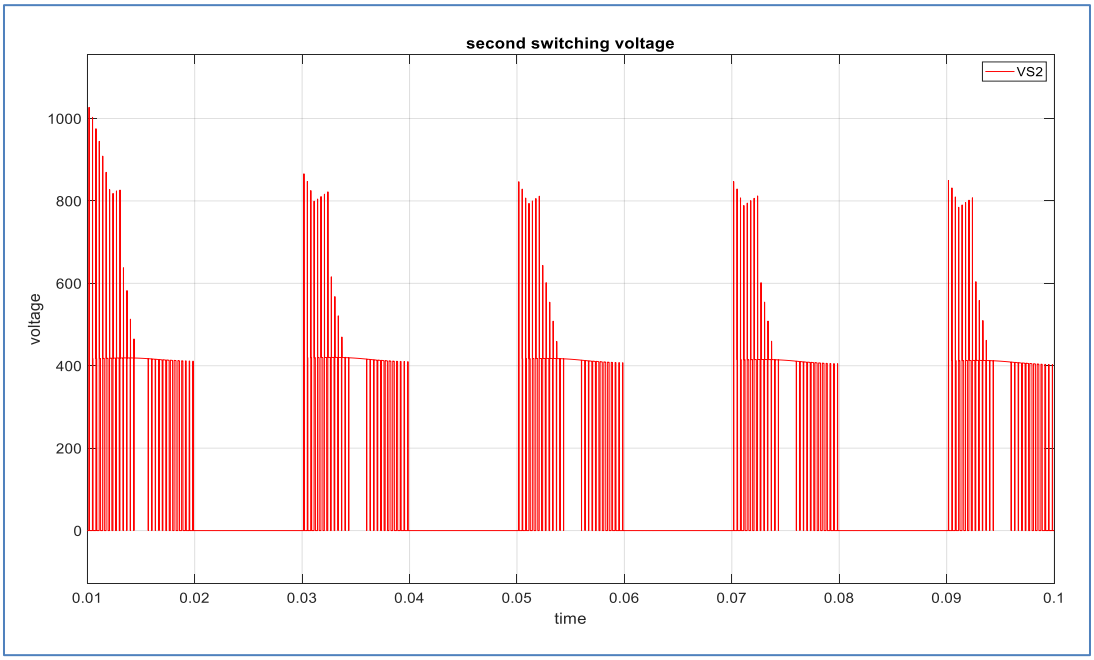

Figure (4.12) output of second switching voltage of 3L-SI-NPC inverter

From the figures shown above, it is clear that the SI-NPC Figure (4.12) topology suffers from over voltage switching in the second switch with a smaller amount, almost non-existent, compared to the NPC Figure (4.11) , where it is very high, up to 1000 Vpeak.

An FFT analysis is carried out for harmonic analysis of the current of both inverters , by comparing Figures (4.13) with (4.14), it is using NPC and SI-NPC with percentage current THD of 2.37% and 2.47% respectively.

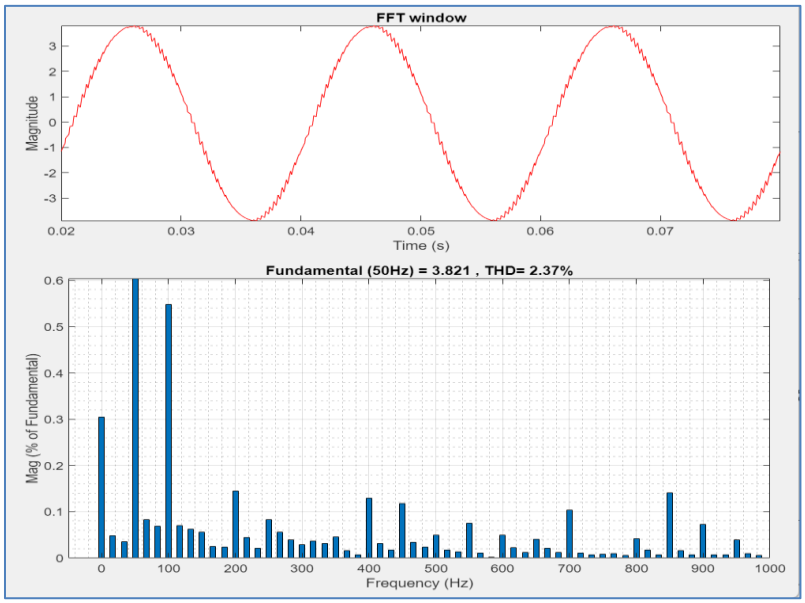

Figure (4.13) THD current of a 3L- NPC inverter using FFT analysis

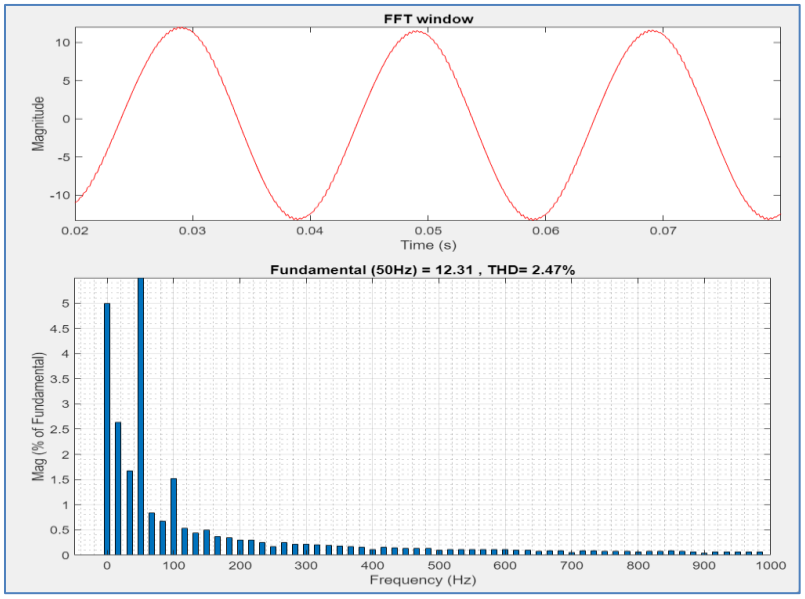

Figure (4.14) THD current of a 3L-SI-NPC inverter using FFT analysis

II. Result of 3-level NPC and SI-NPC under POD PWM

In this section, system is simulated when applying POD-PWM techniques to both inverter's topologies with the same circuit parameters shown in Table (4.1).

Figures (4.15) and (4.16) show the NPC and SI-NPC output voltages under POD-PWM.

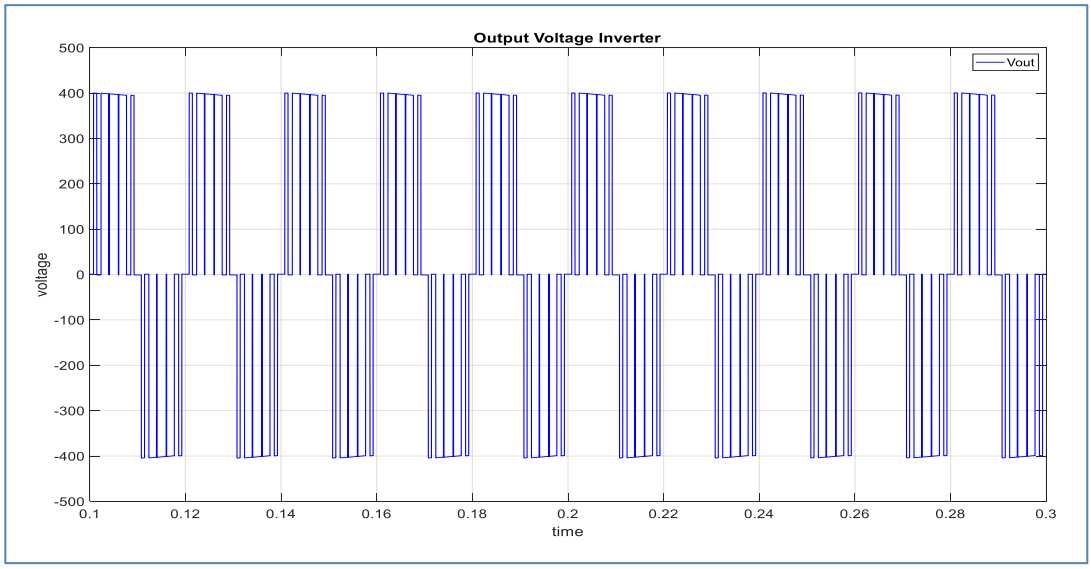

Figure (4.15) Output voltage of a 3L-NPC inverter.

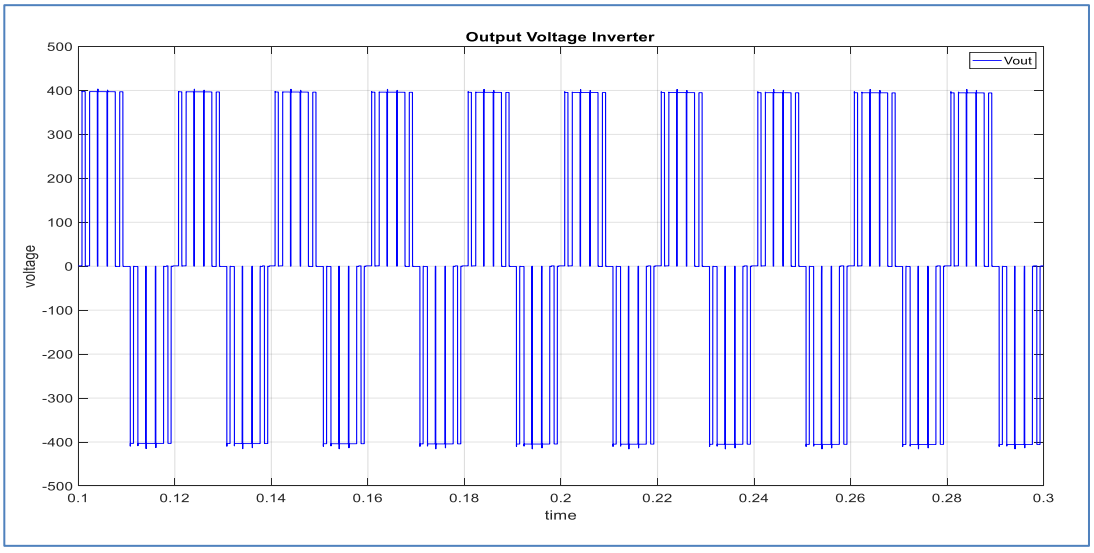

Figure (4.16) A 3L- SI-NPC inverter's output voltage

Also, the output current in SI-NPC is almost double the output current in NPC as shown in Figures. (4.17) and (4.18) illustrates the DC-link capacitor voltages in both topologies.

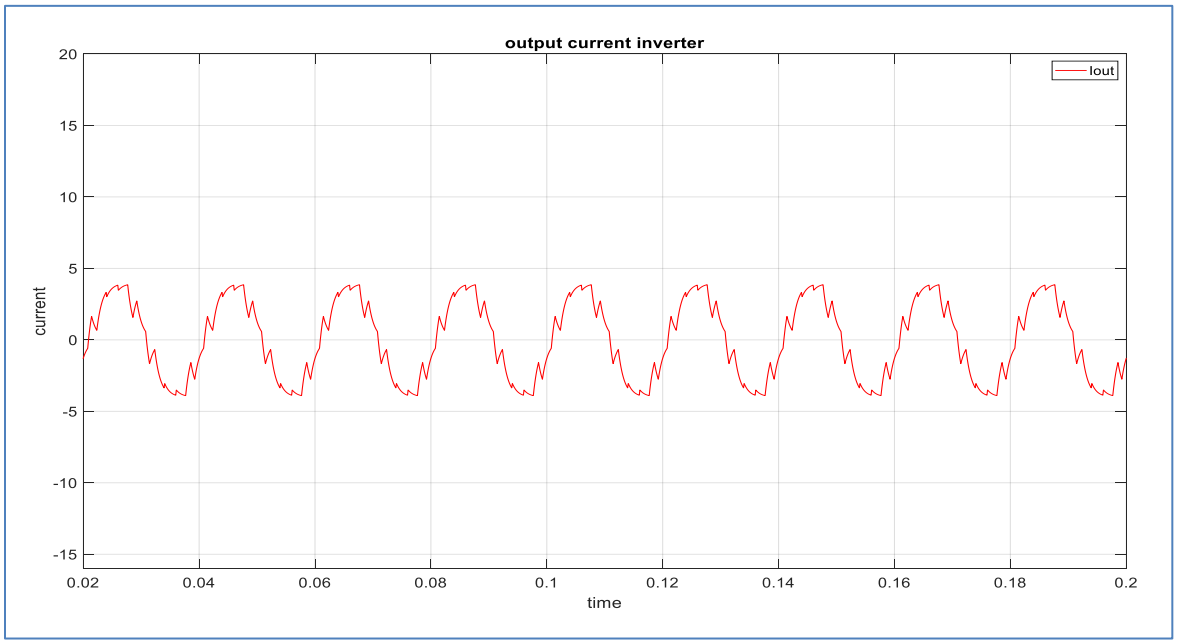

Figure (4.17) Output current of a 3L-NPC inverter.

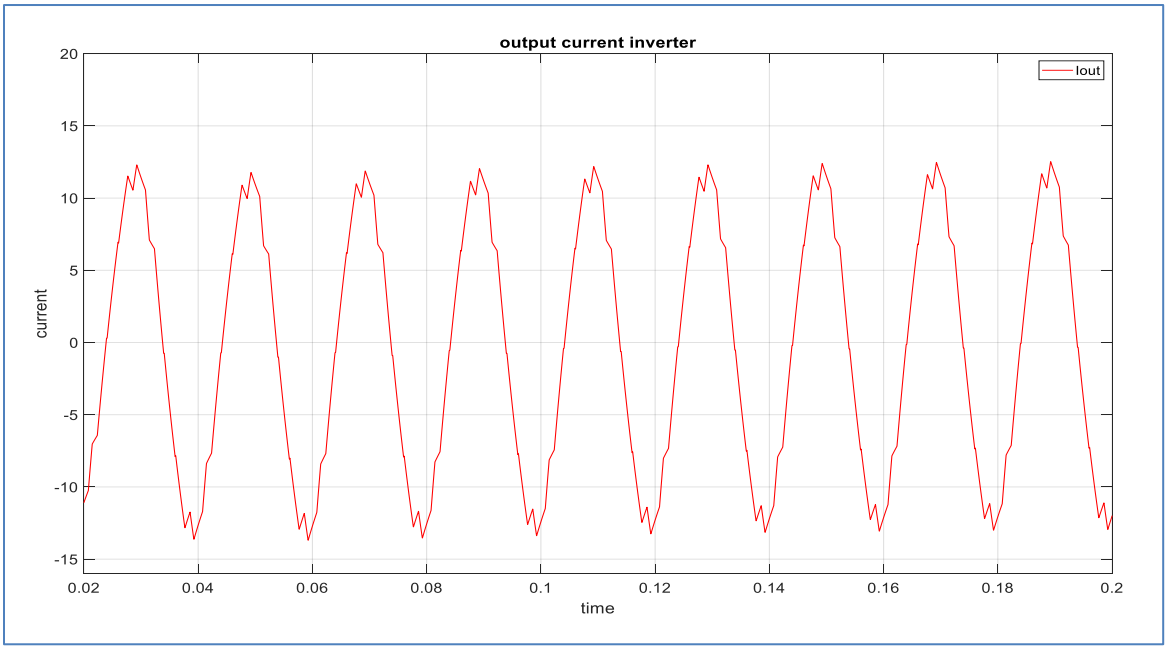

Figure (4.18) Output current for a 3L-SI-NPC inverter

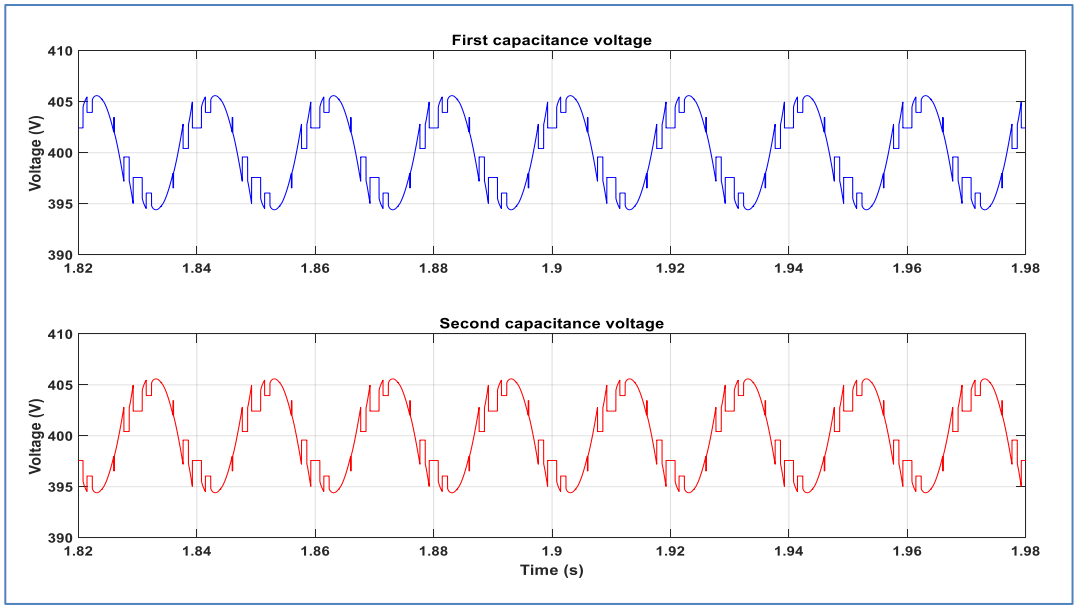

Figure (4.19) Vc_1 and Vc_2 of 3L- NPC inverter.

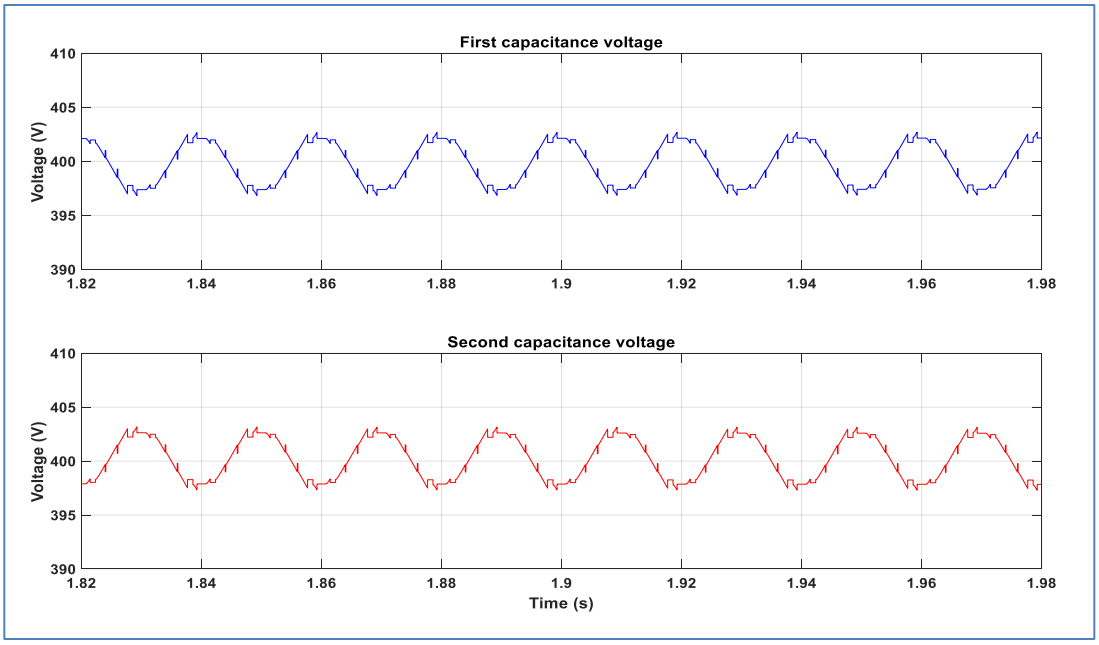

Figure (4.20) Vc_1 and Vc_2 of 3 L-SI-NPC inverter.

Similarly, the DC link capacitor currents is much higher in SI-NPC in comparison with NPC topology as shown in Figures. (4.21) and (4.22).

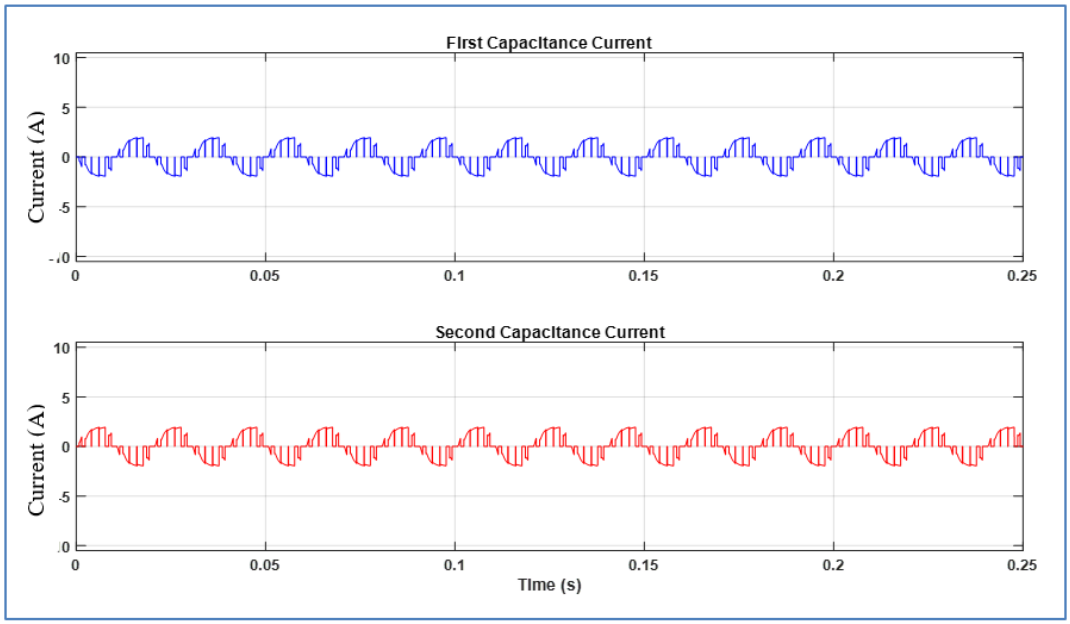

Figure (4.21) Ic_1 and Ic_2 of 3L-NPC inverter.

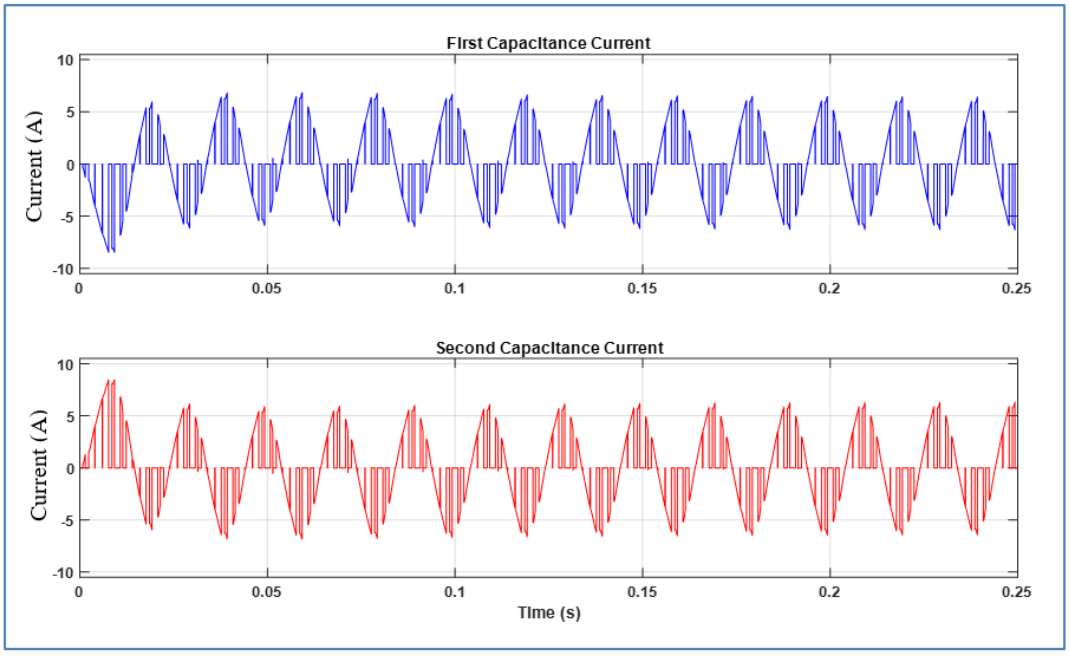

Figure (4.22) Ic_1 and Ic_2 of 3L-SI-NPC inverter.

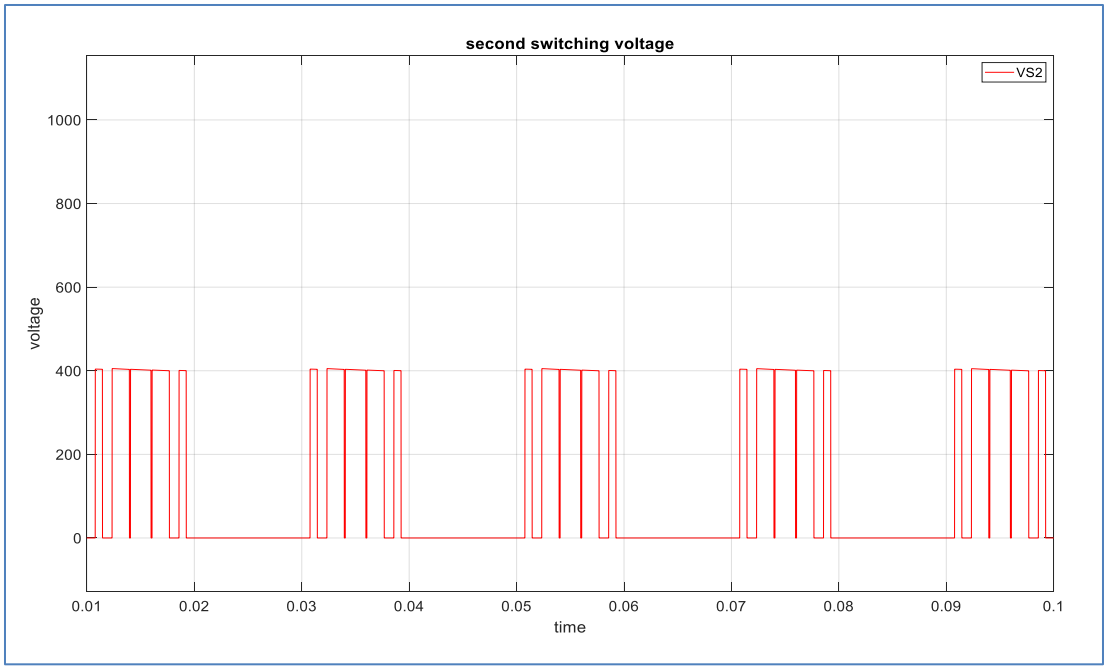

Figure (4.23) output of second switching voltage of 3L-NPC inverter

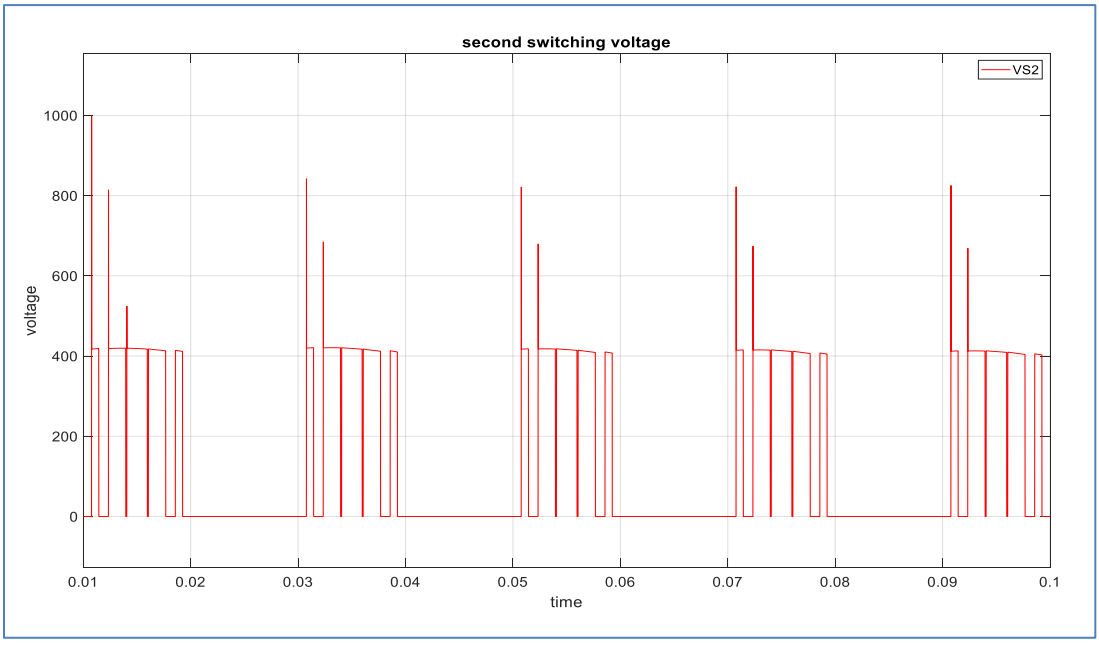

Figure (4.24) output of second switching voltage of 3L-SI-NPC inverter

When using the POD PWM, the overvoltage switching value is same when using the PD PWM, as it was shown previously. note from Fig.(4.23) and (4.24) that the overvoltage switching value was high in the SI-NPC inverter.

By using FFT analysis, Figure (4.25) shows that using SI-NPC topology can reduce the current THD from (14.71%) to (5.43%) as shown in Figures (4.25) and (4.26) respectively.

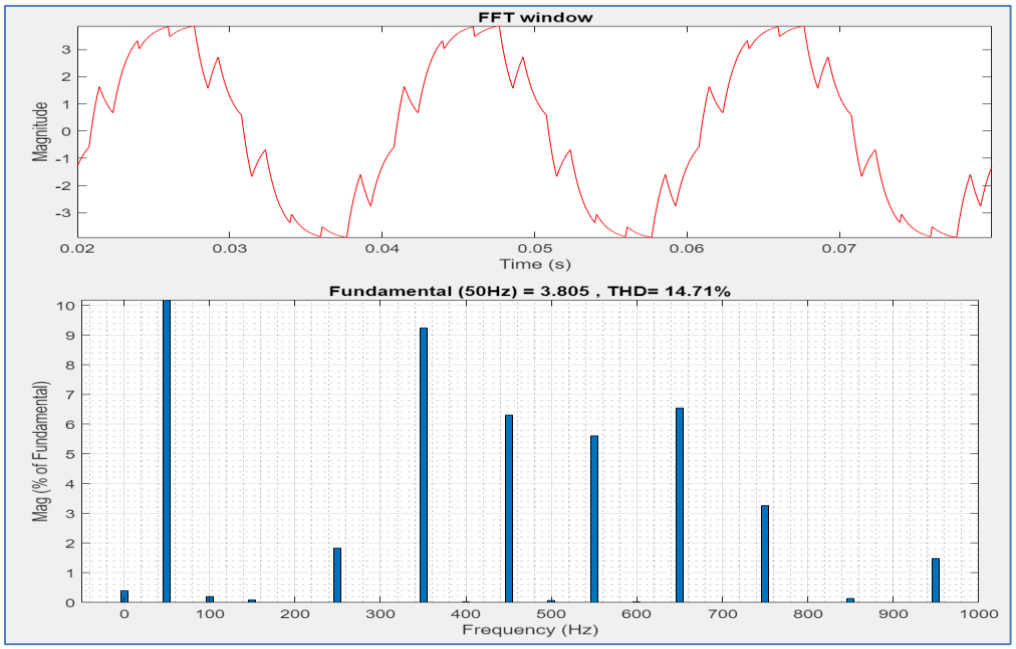

Figure (4.25) FFT analysis of THD current of a 3L-NPC inverter

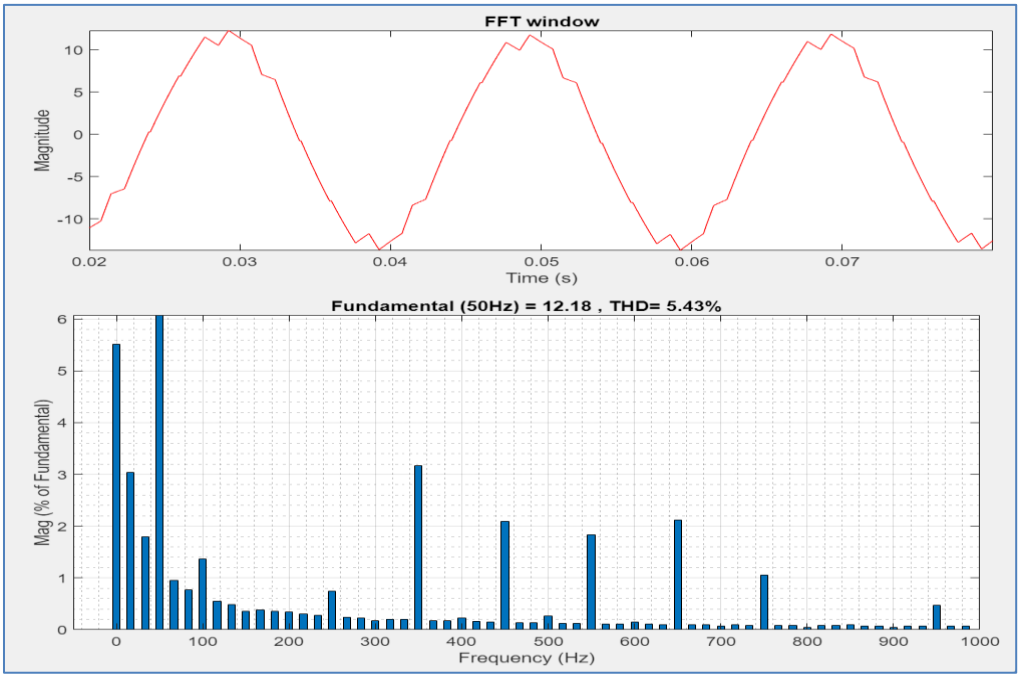

Figure (4.26) THD current of a 3L-SI-NPC inverter using FFT analysis

A summary for the comparison in terms of voltages, current and THD is presented in table (4.2). This table shows that adding a split inductor improves the NPC performance under PD-PWM by reducing the current THD to almost 1% and boost the output current supplied to the load, however the semiconductor switches can be exposed to a higher over voltages. The table is also shows that POD-PWM cannot be considered as a suitable PWM for such MLI due to high harmonic levels. It is worth mentioning that there is a slight deviation in the capacitor voltages Vc_1 &Vc_2 as in shown in table 4.2.

Table (4.2) Comparison between NPC & SI-NPC under PO & POD PWM .

Under PD PWM			**Under POD PWM**	
Measurement	**NPC**	**SI-NPC**	**NPC**	**SI-NPC**
$V_{out\ (rms)}$	327.1 V	330.8 V	328.7 V	330.7 V
$I_{out\ (rms)}$	2.893 A	8.796 A	2.916 A	8.699 A
V_{C1}	399.4 V	398.9 V	399.6 V	399.2 V
V_{C2}	400.6 V	401.1 V	400.4 V	400.9 V
$I_{C1\ (rms)}$	1.349 A	3.126 A	1.34 A	2.924 A
$I_{C2\ (rms)}$	1.349 A	3.126 A	1.34 A	2.924 A
THD (I_o)	2.37 %	2.47 %	14.71 %	5.43 %

4.3 Three level Improved Split Neutral Point Clamped (ISI-NPC) Inverter under PD & POD PWM

In this section, a 3L-ISI-NPCI model is simulated under PD and POD-PWM The circuit parameters are listed in Table (4.3).

Table.(4.3) Circuit parameters [66]

Parameters	Values	Units
Split inductor $L_1 = L_2$	0.2	mH
Fundamental frequency	50	Hz
dc-link capacitors $C_1=C_2$	2000	µF
Input voltage	800	volt
Load resisteanc	10	Ω
Filter Inductor (L)	0.1	H

Figures (4.27) and (4.28) illustrate the currents in the first and second DC-capacitors under PD and POD respectively.

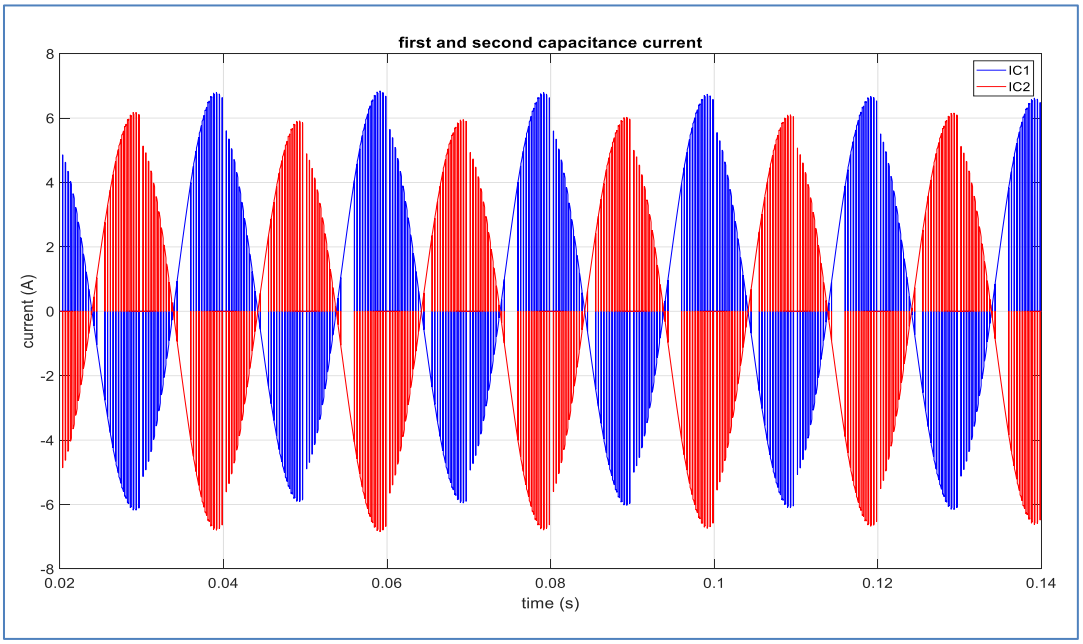

Figure (4.27) Ic_1 and Ic_2 of 3 level ISI-NPC Inverter under PD PWM

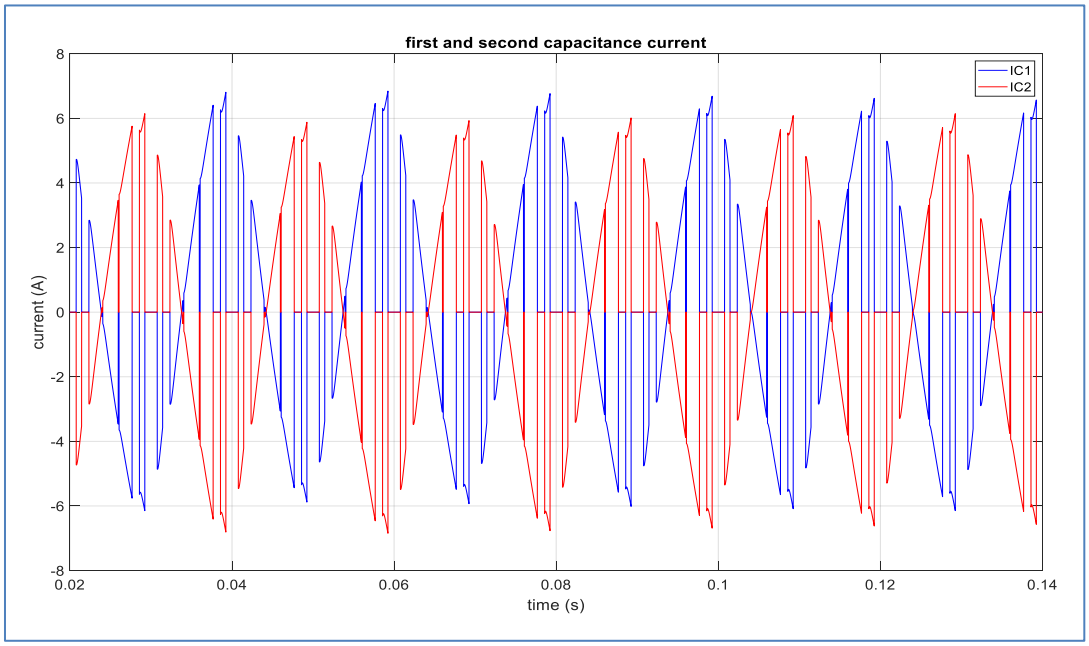

Figure (4.28) Ic_1 and Ic_2 of 3 level ISI-NPC Inverter under POD PWM

The capacitors voltage waveforms under both modulation approaches are shown in figures (4.29) and (4.30).

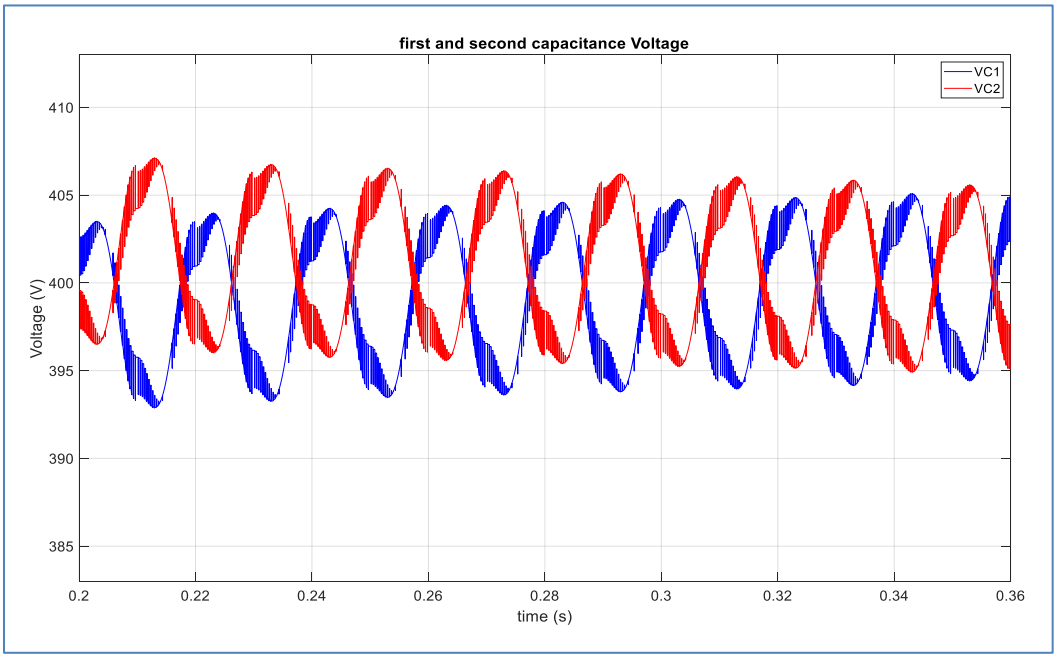

Figure (4.29) Vc_1 and Vc_2 of 3 level ISI-NPC Inverter under PD PWM

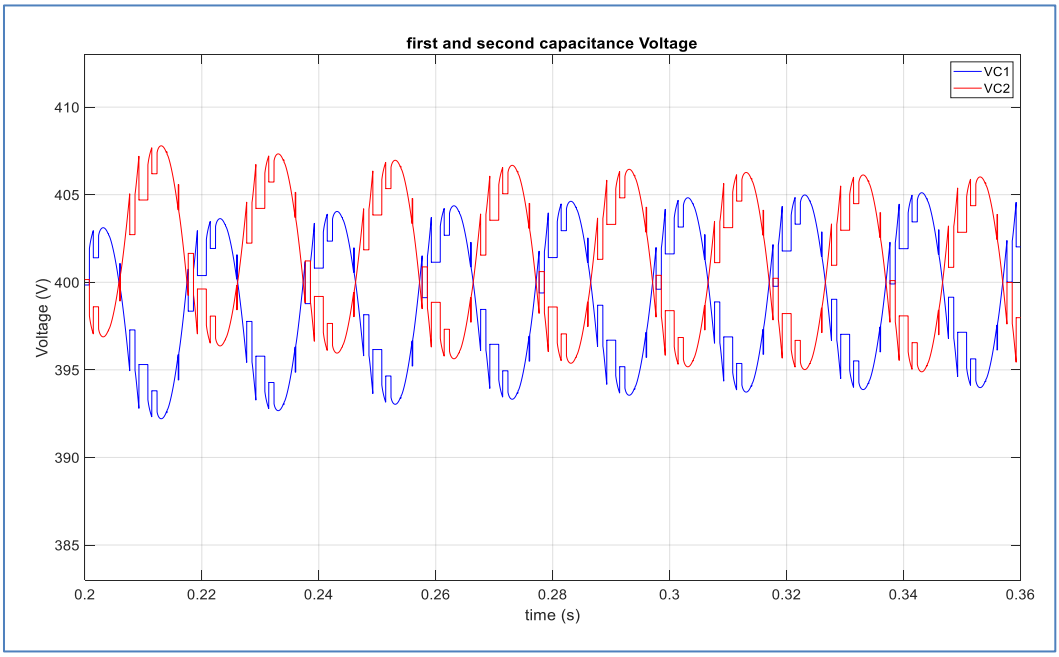

Figure (4.30) Vc_1 and Vc_2 of 3 level ISI-NPC Inverter under POD PWM

A low distorted inductor currents I_{L1}, I_{L2} and output current waveforms can be achieved under PD-PWM approach in comparison with POD-PWM as shown in Figures (4.31) and (4.32).

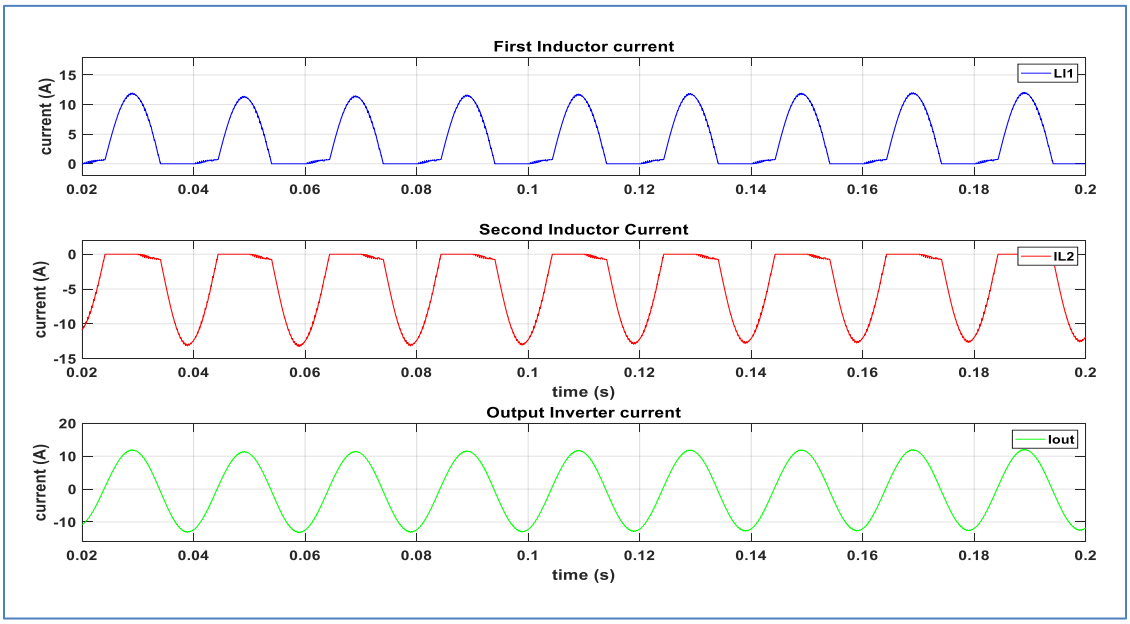

Figure (4.31) I_{L1}, I_{L2} and I_{out} of 3 level ISI-NPC Inverter under PD PWM

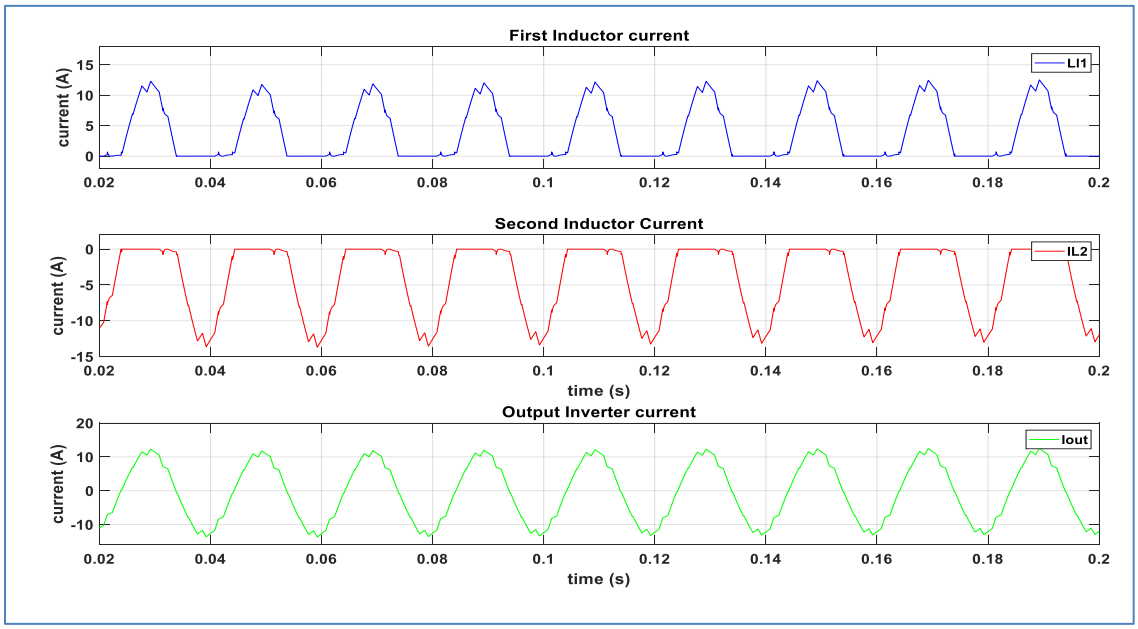

Figure (4.32) I_{L1}, I_{L2} and I_{out} of 3 level ISI-NPC Inverter under POD PWM

The three level output voltage waveforms are shown in Figures. (4.33) and (4.34)

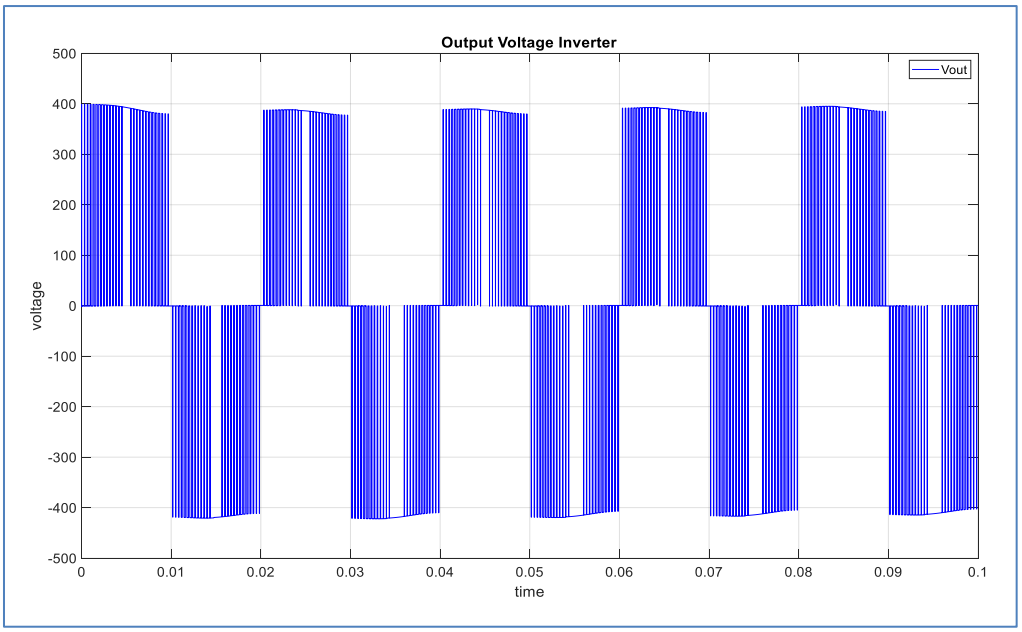

Figure (4.33) V_{out} of 3 level ISI-NPC Inverter under PD PWM

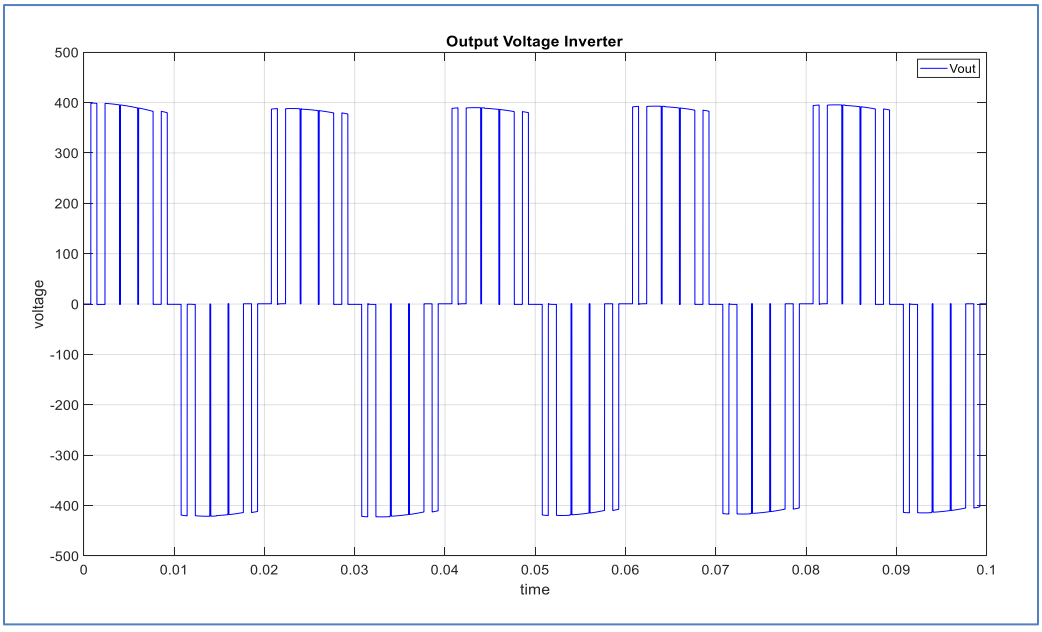

Figure (4.34) V_{out} of 3 level ISI-NPC Inverter under POD PWM

When using the PD PWM with the ISI-NPC , do not notice the presence of overvoltage switching in the second switch, and this is a very good feature as shown in Figures (4.35), and its presence in a very diminished quantity when using the POD PWM shown in Figures (4.36) .

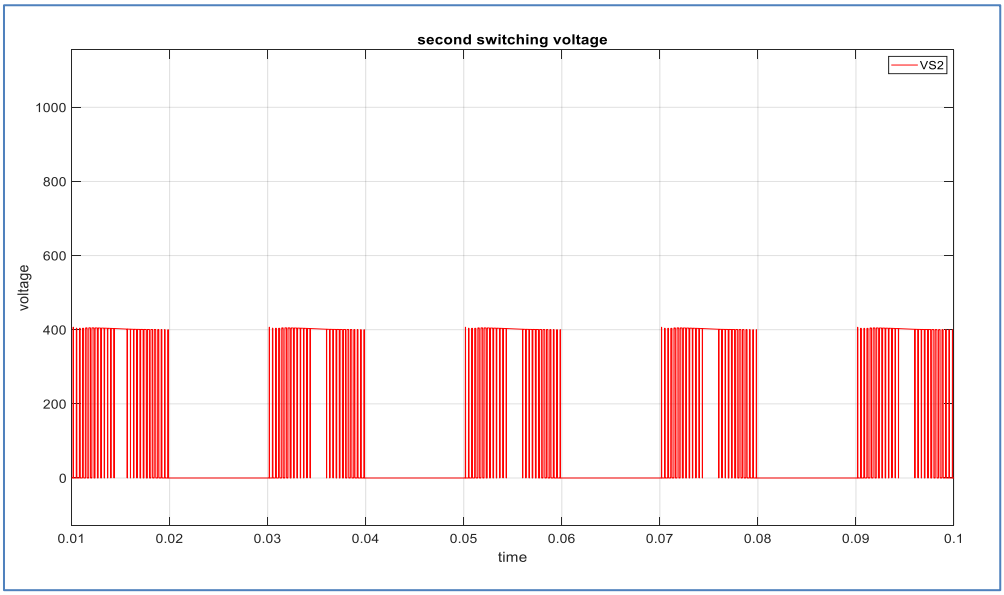

Figure (4.35) output of second switching voltage of 3L-ISI-NPC inverter

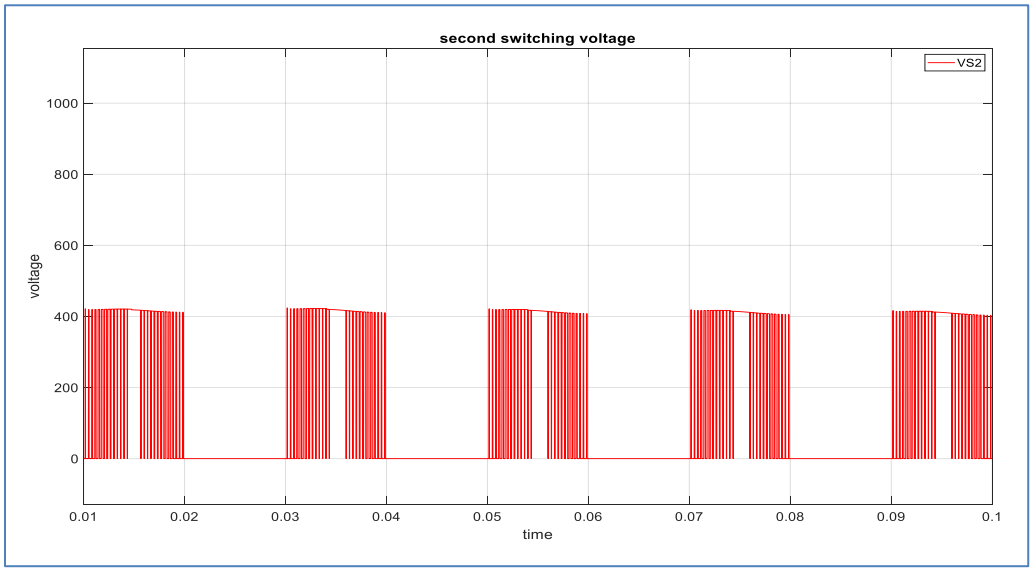

Figure (4.36) output of second switching voltage of 3L-ISI-NPC inverter

By carrying out the FFT analysis for harmonic components, Figures (4.37) and (4.38) show that the THD is highly reduced when applying the PD-PWM, therefore, it will be considered as the PWM approach in this work.

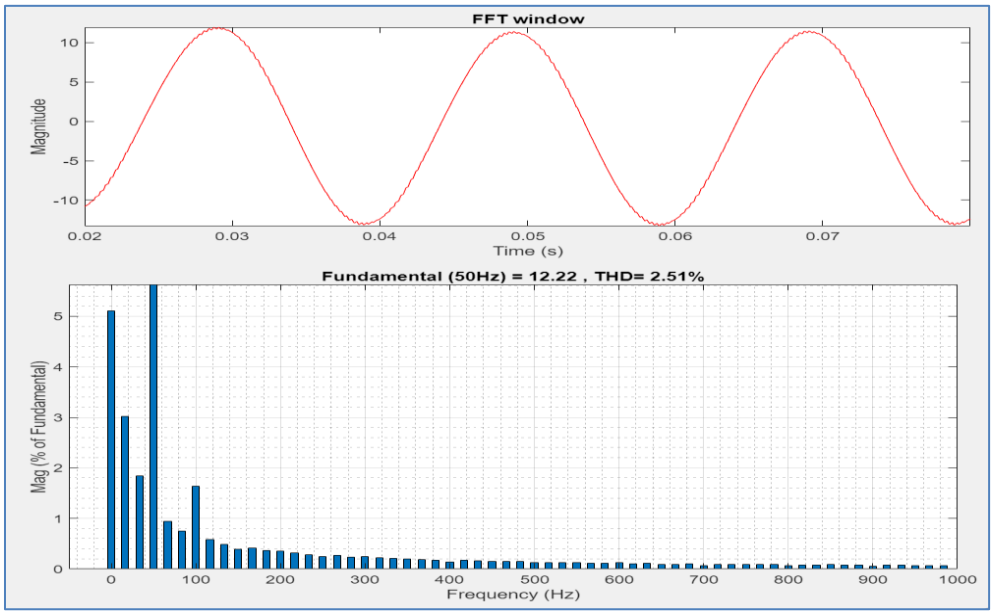

Figure (4.37) FFT analysis of output current inverter THD under PD PWM

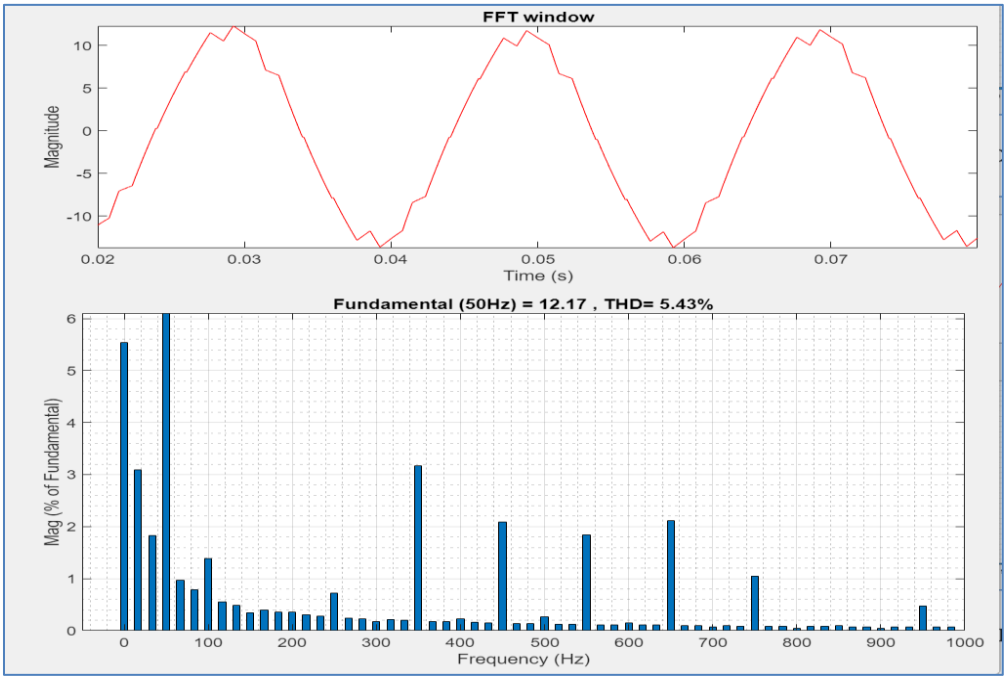

Figure (4.38) FFT analysis of output current inverter THD under POD PWM

A summary for the comparison in terms of voltages, current and THD is presented in Table (4.4), This table shows the ISI-NPC performance under PD & POD PWM.

Table (4.4) Comparison between ISI-NPC Inverter under PD & POD PWM .

Measurement	**ISI-NPC under PD PWM**	**ISI-NPC under POD PWM**
$V_{out\ (rms)}$	327.3 V	330.9 V
$I_{out\ (rms)}$	8.625 A	8.693 A
V_{C1}	400.6 V	399.2 V
V_{C2}	399.4 V	400.9 V
$I_{C1\ (rms)}$	3.045 A	3.107 A
$I_{C2\ (rms)}$	3.045 A	3.107 A
THD (I_o)	2.51 %	5.43 %

A three-level improved split-inductor NPC inverter (3L-ISI NPCI) is simulated to overcome the existing single phase NPC topology's problems. Therefore, this thesis adopts the to be employed in single phase TRL-PV system. An investigation is carried out to evaluate the effectiveness of employing 3L-ISI-NPCI in such system. In this thesis, the hysteresis current control is adopted as a current control technique to track the inductor current reference which has not been investigated before.

4.4 Constant and Variable Behaviour of a Three-level single-phase ISI-NPC Multilevel Inverter under HCC Controller with Grid.

This section investigates the effectiveness of using Hysteresis current control (HCC) on the performance of ISI-NPC inverter. Two operating conditions are investigated including constant and variable current controller. The system is modeled in MATLAB/SIMULINK for both constant and variable conditions as shown in Figures (4.39) and (4.40).

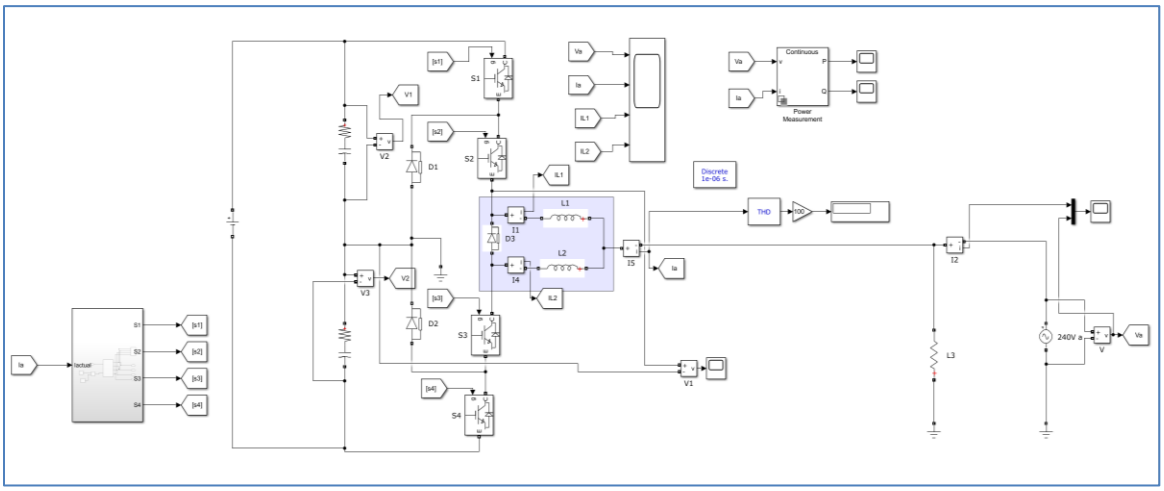

Figure (4.39) Simulink of 3 level ISI-NPC under HCC Controller

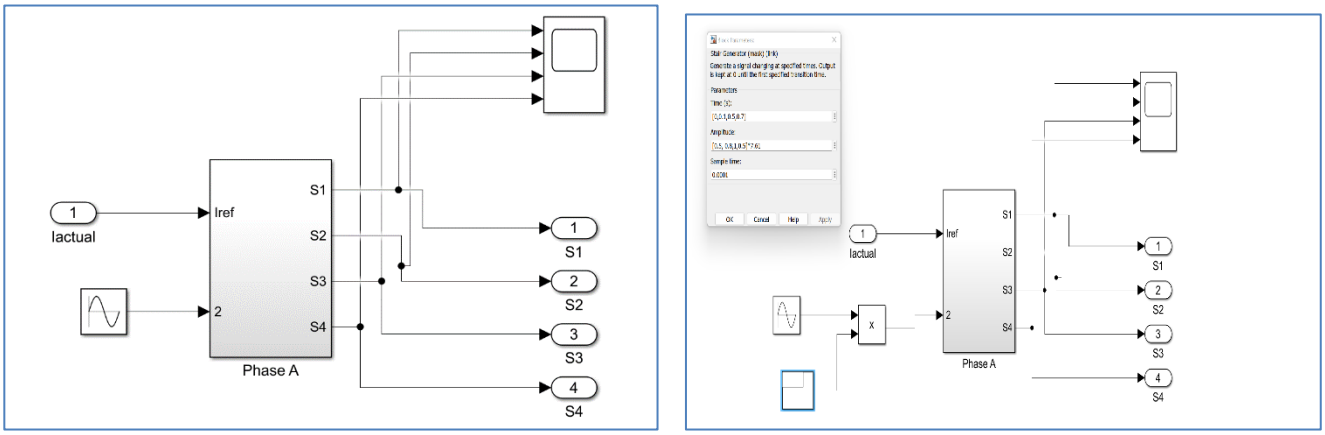

(a) (b)

Figure (4.40) Simulink of HCC Controller at (a) Constant HCC , (b)Variable HCC

The output voltage waveforms are stable with no overvoltage as shown in Figures (4.41) and (4.42).

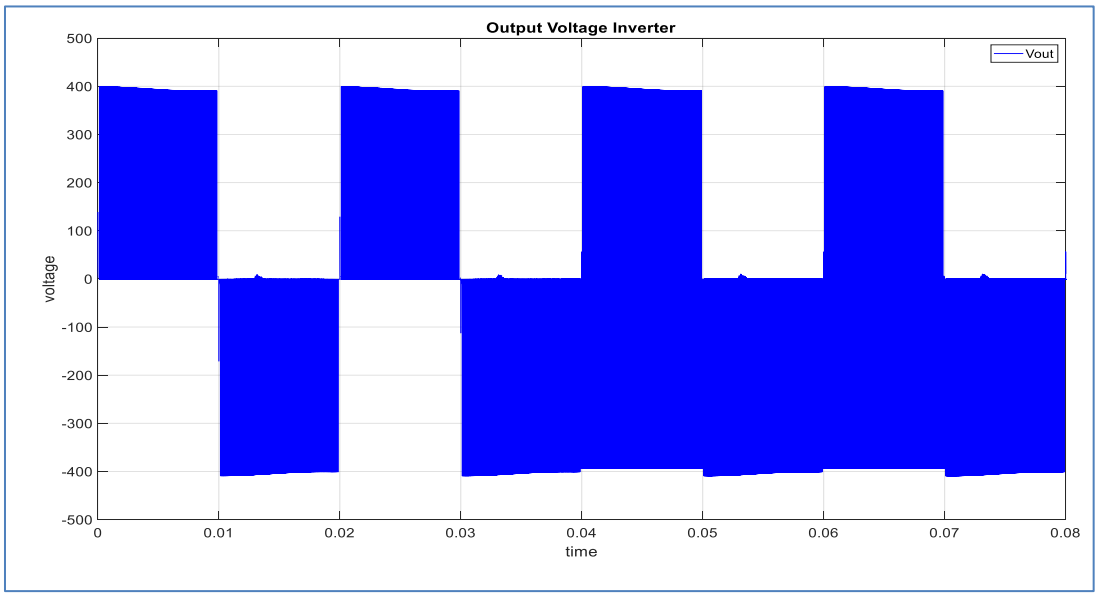

Figure (4.41) V_{out} of 3 level ISI-NPC Inverter under constant HCC

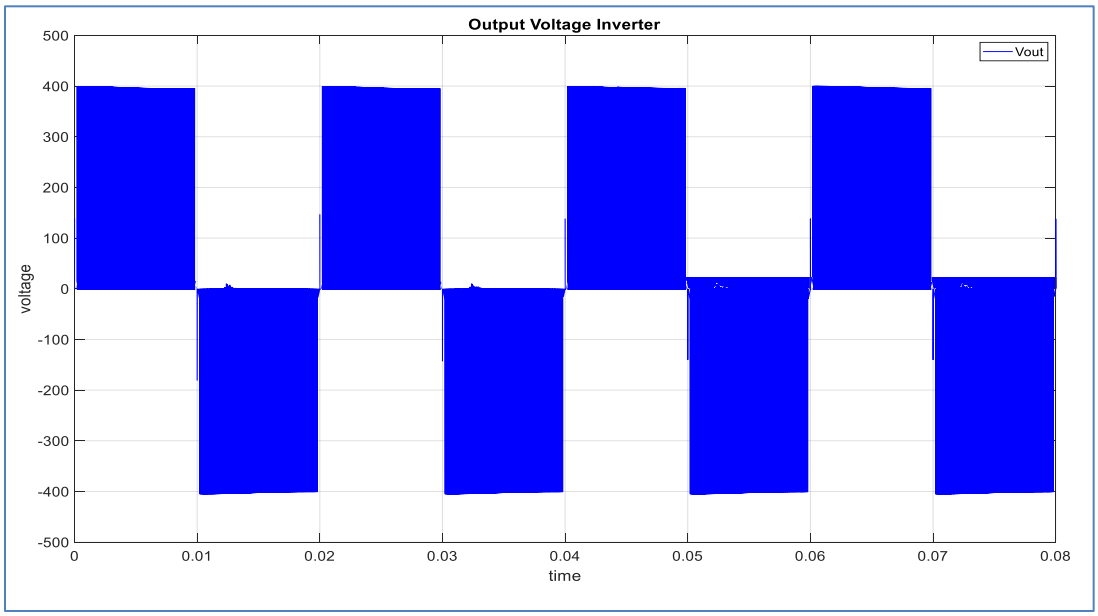

Figure (4.42) V_{out} of 3 level ISI-NPC Inverter under variable HCC

In terms of inductors and output currents, by applying constant HCC, the inductor currents can be as high as 7.61A, while the inductor currents do not exceed 4 A under variable HCC as shown in Figures.(4.43) & (4.44). The MLI output current is also higher under constant HCC.

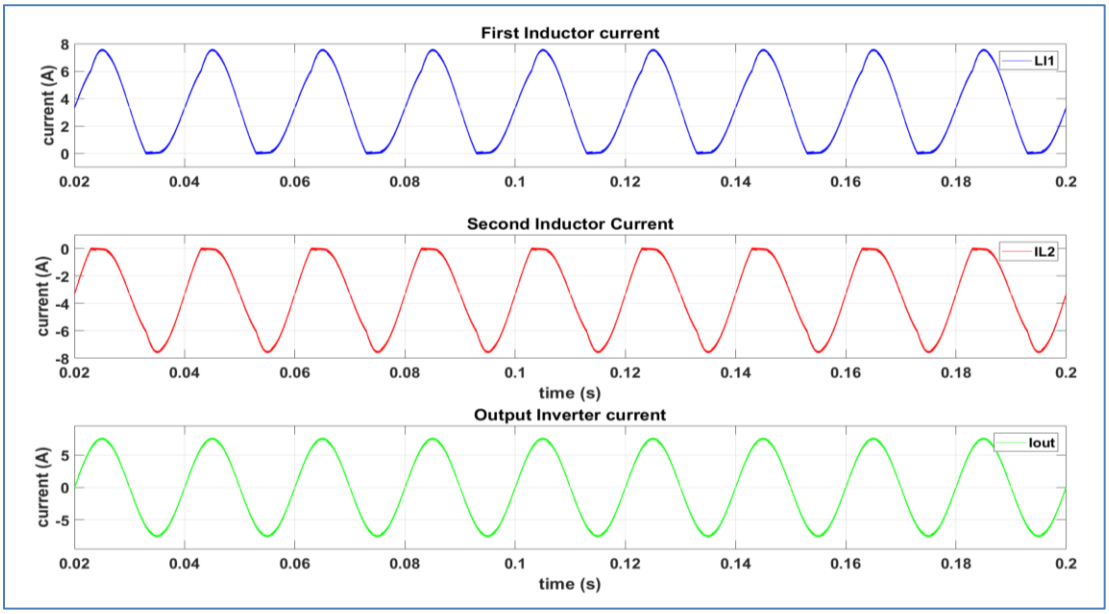

Figure (4.43) I_{L1}, I_{L2} and I_{out} of 3 level ISI-NPC Inverter under constant HCC

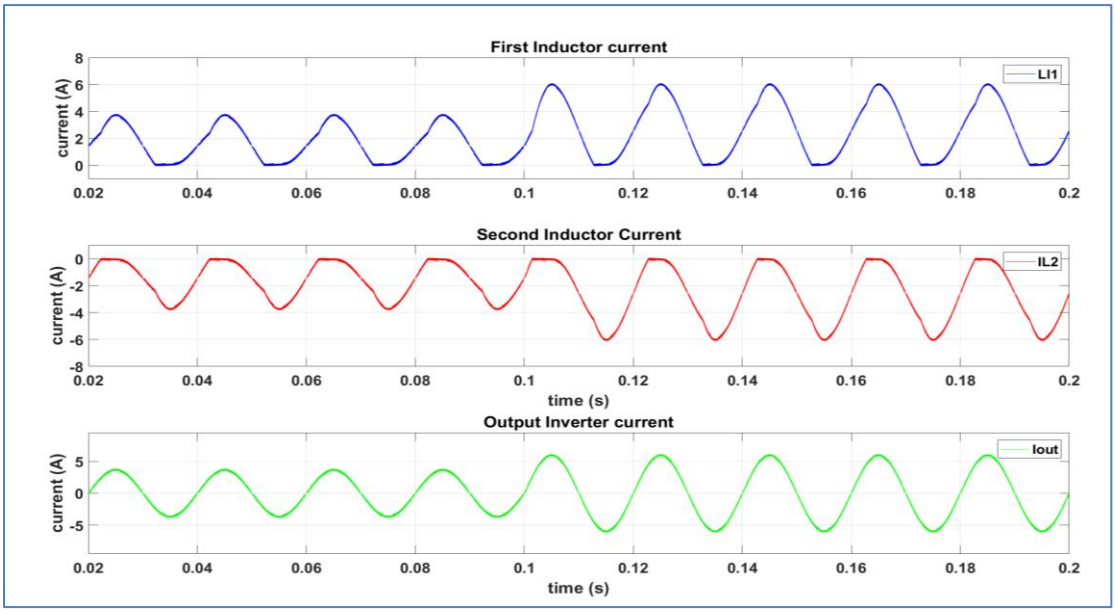

Figure (4.44) I_{L1}, I_{L2} and I_{out} of 3-level ISI-NPC Inverter under variable HCC

By using HCC controller, a voltage balancing of both capacitor can be achieved as shown in Figure (4.45) and (4.46). However, a higher voltages of VC1 and Vc2 are achieved with higher ripple values when applying a fixed value of inductor current (constant condition).

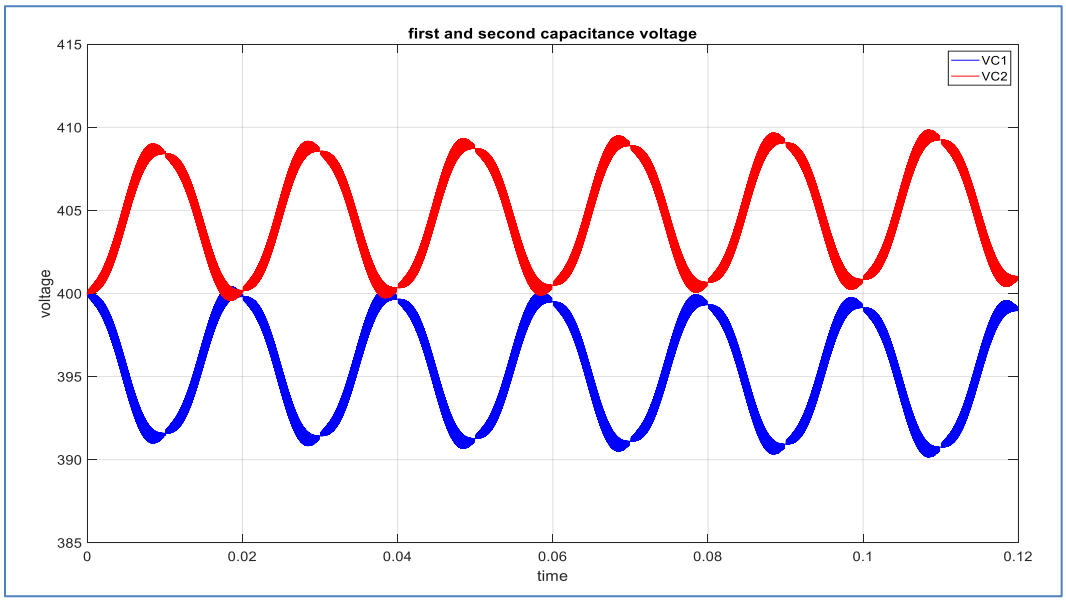

Figure (4.45) Vc_1 & Vc_2 of 3 level ISI-NPC Inverter under constant HCC

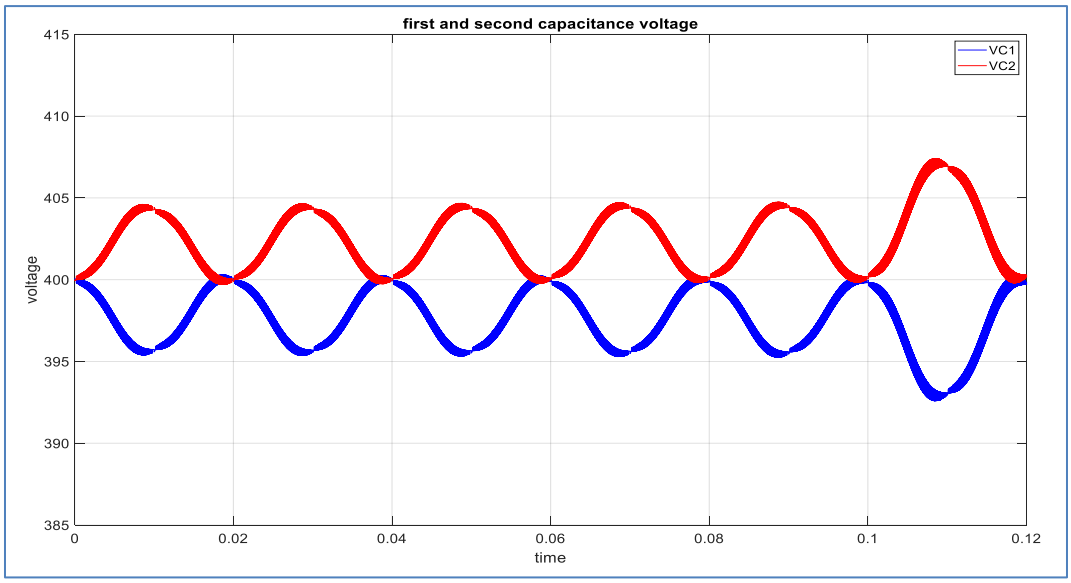

Figure (4.46) Vc_1 & Vc_2 of 3 level ISI-NPC Inverter under variable HCC

By comparing Figures (4.47) and (4.48), it can be observed that the currents in both capacitors C_1 and C_2 are much higher (almost double) with a value of 4 A when applying constant HCC .

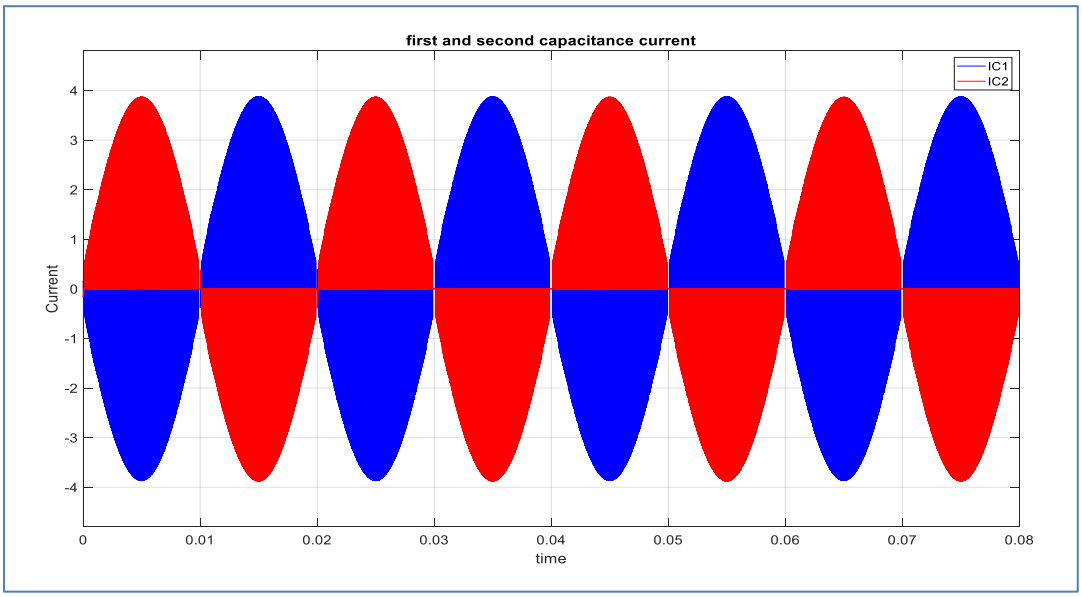

Figure (4.47) Ic_1 and Ic_2 of 3 level ISI-NPC Inverter under constant HCC

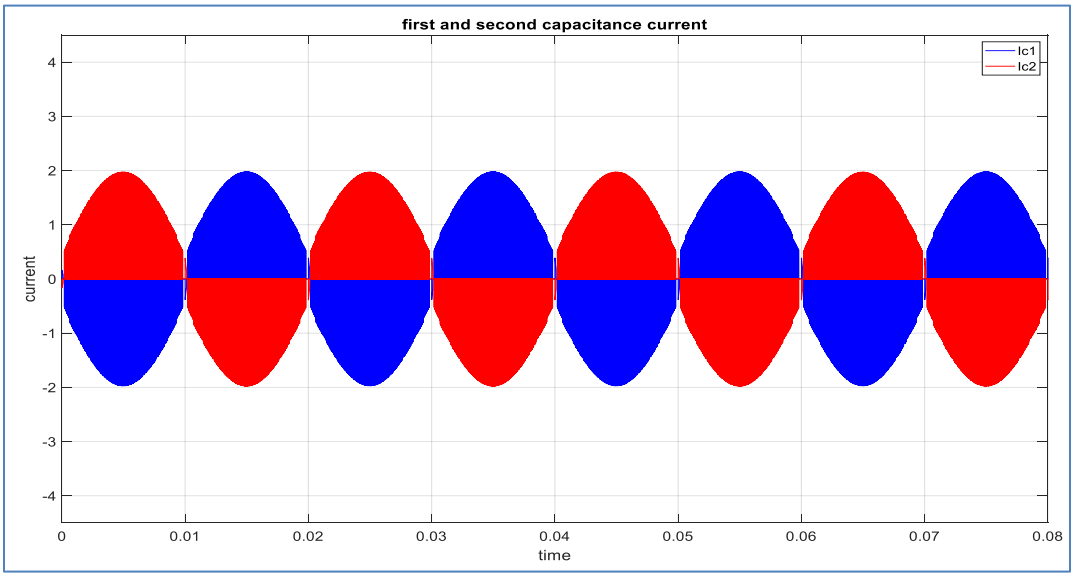

Figure (4.48) Ic_1 and Ic_2 ISI-NPC Inverter under variable HCC

Figures (4.49) and Figures (4.50), illustrate that adopting HCC controller is able to maintain a sinusoidal grid voltage. Both operating conditions of HCC controller are effective to keep the grid current sinusoidal.

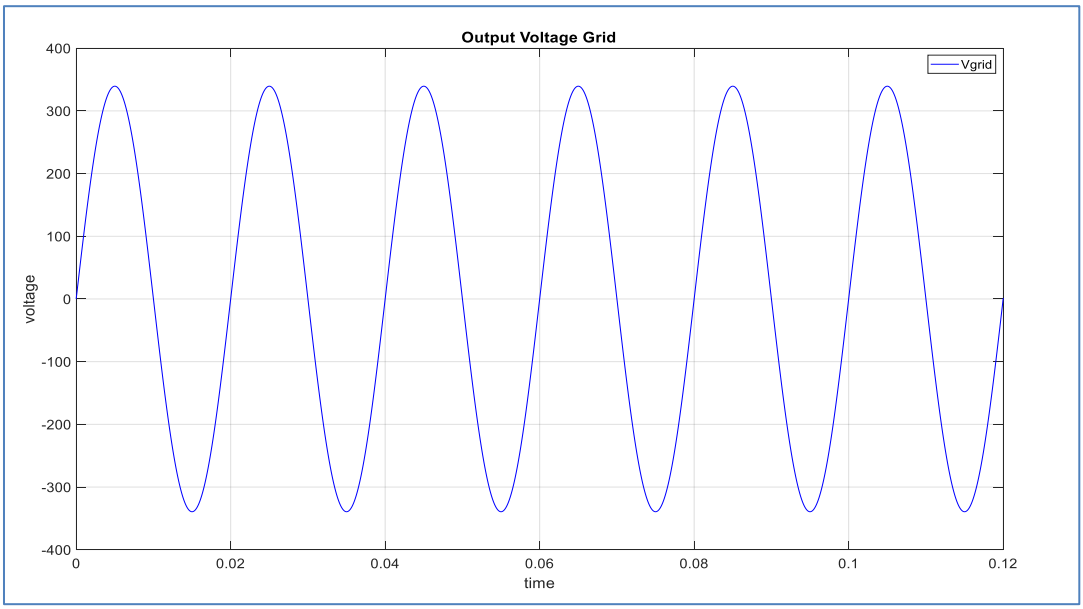

Figure (4.49) V_{grid} under constant HCC

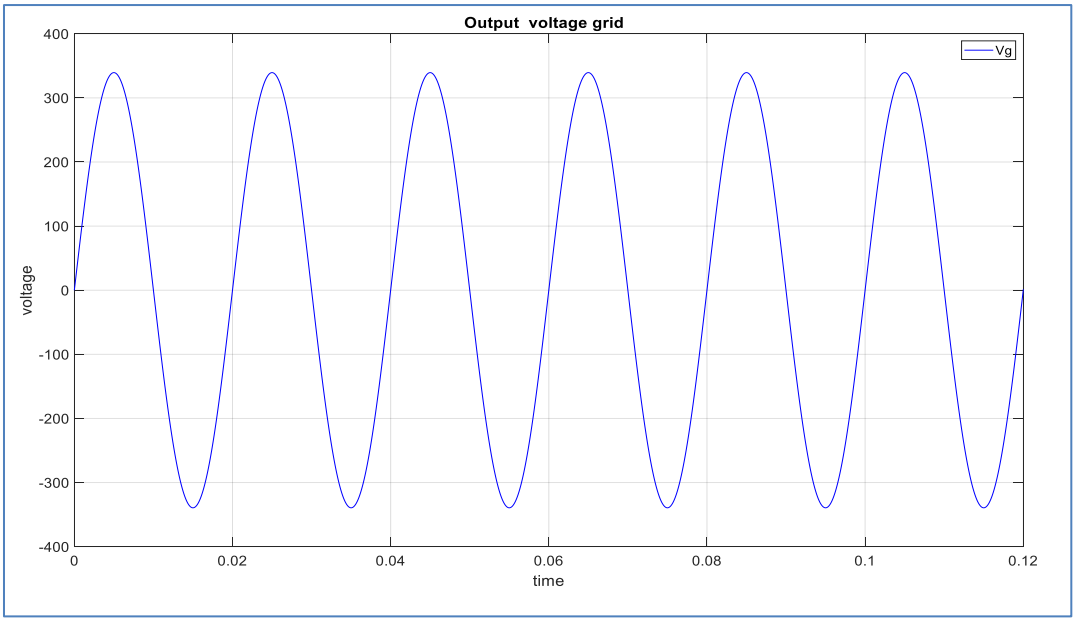

Figure (4.50) V_{grid} under variable HCC

Note the effect of the network current in the state of HCC , as it was shown from Figures (4.51), which represents the constant state, the current was greater than the current in the variable case, Figures (4.52) by about 4A, and the amount of ripple in the current was more in the variable state than in the constant state.

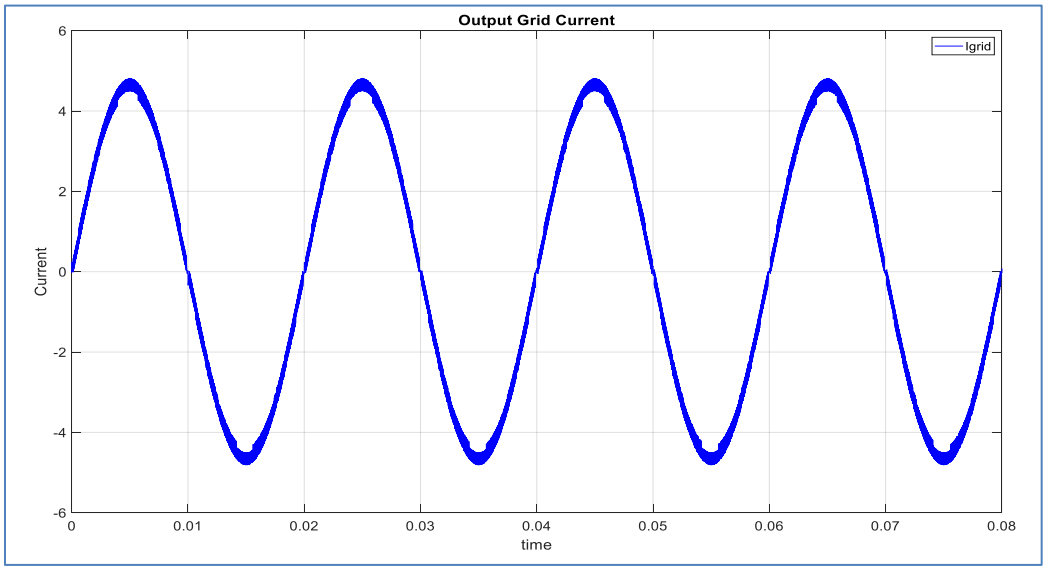

Figure (4.51) I_{grid} under constant HCC

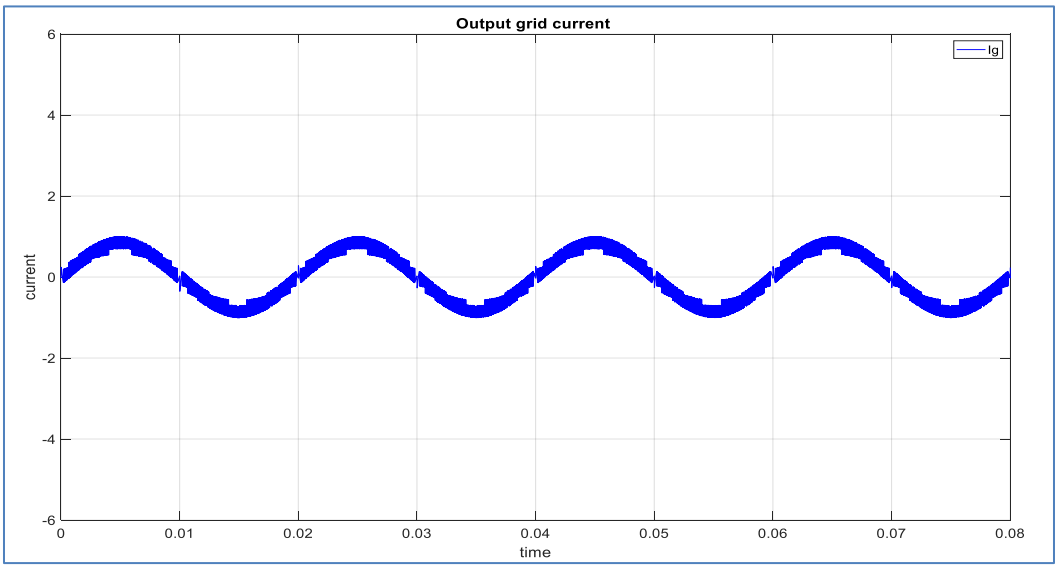

Figure (4.52) I_{grid} under variable HCC

Figures (4.54), which is the case of the constant HCC , where the power scales according to the current gradient when it was 0.5 of the total current, and then 0.8 of it also, until it reaches its stability at its original value of 7.61 A and then halves it again, but in the case of the constant Figures (4.53) ,where the amount of current is constant At its original value of 7.61A .

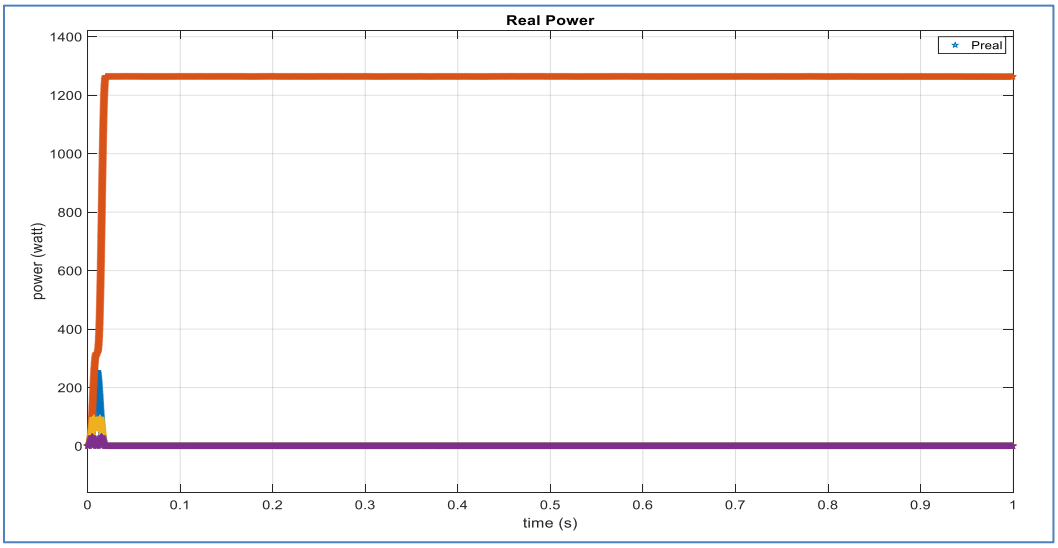

Figure (4.53) Real Power under constant HCC

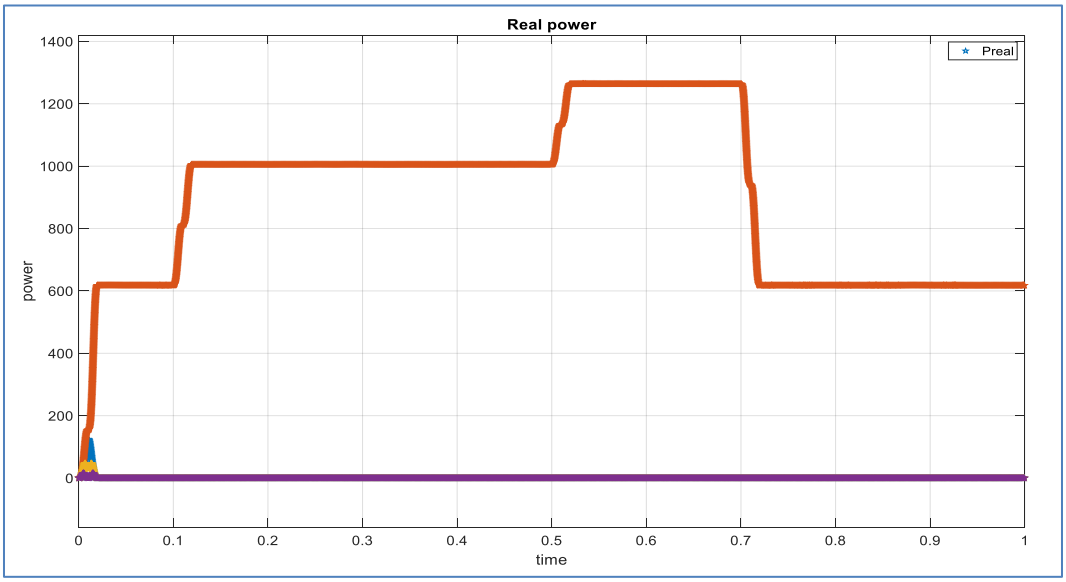

Figure (4.54) Real Power under variable HCC

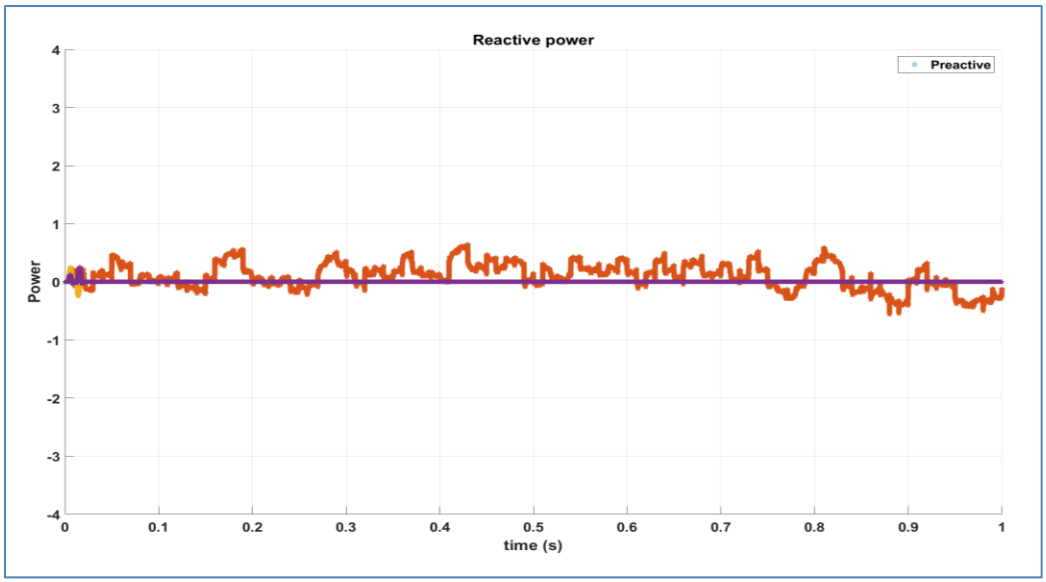

Figure (4.55) Reactive Power under constant HCC

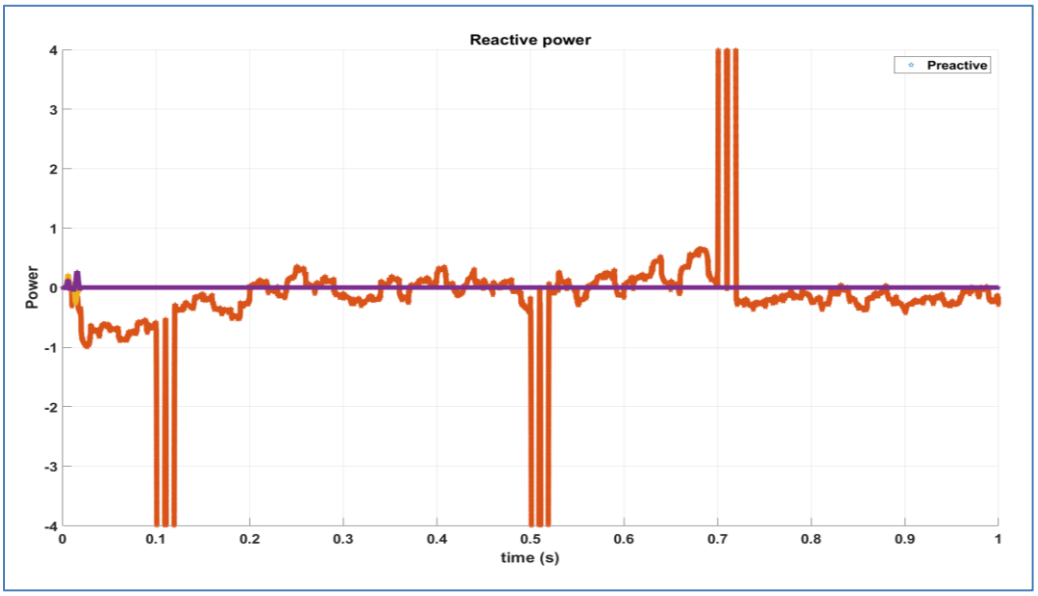

Figure (4.56) Reactive Power under variable HCC

The FFT window is the output current inverter in both cases, the constant and the variable HCC, and the THD current ratio, which represents the (total harmonic distortion) at 0 start time and 1 number of cycles, where the THD percentage in the case constant HCC was 0.49 % Figure (4.57), which is much less variable 3.34 % Figure (4.58)

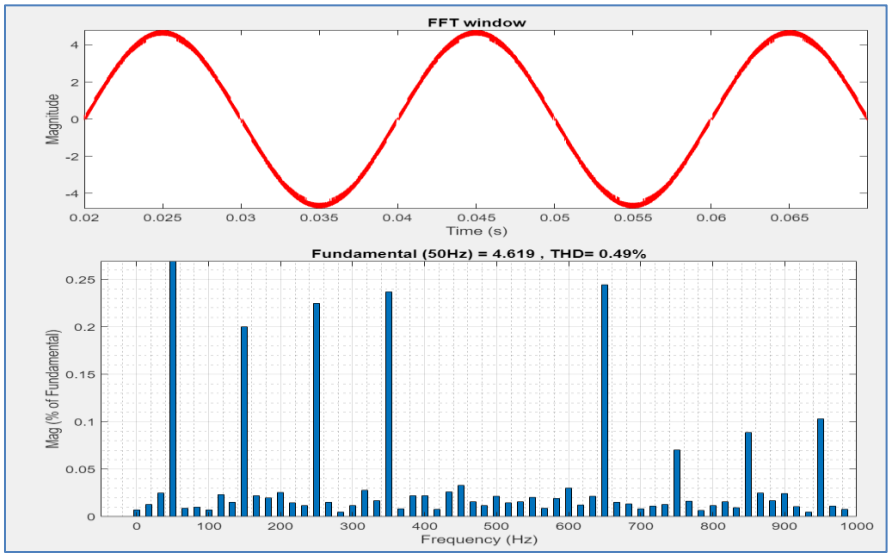

Figure (4.57) FFT analysis of current THD under constant HCC

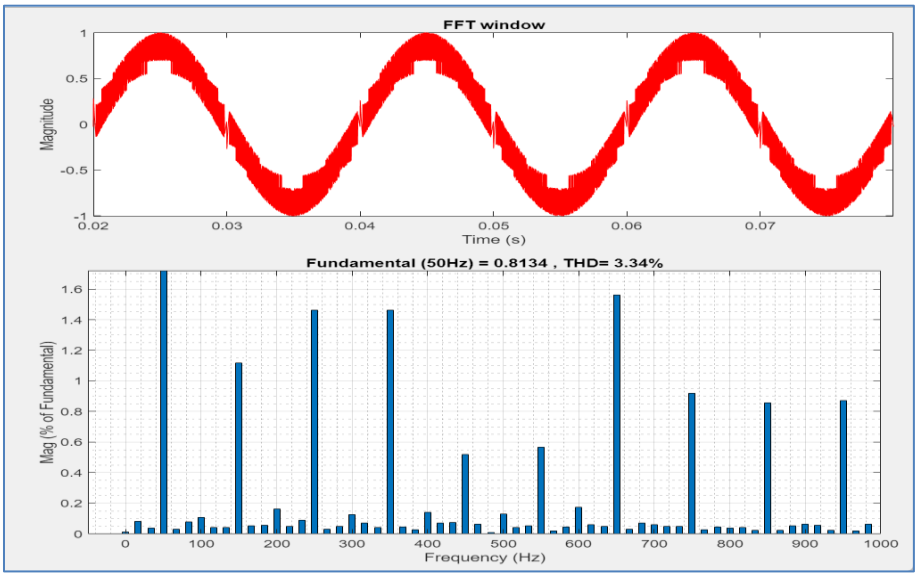

Figure (4.58) FFT analysis of current THD under variable HCC

Part Two: Multilevel Inverter With under PV system

4.5 Introduction

Nowadays, solar PV-based systems are mostly used in the sector of power generation due to environmental concerns. As a result, intensive research is being done to improve photovoltaic power plant efficiency and lower system losses and costs. To interface the PV system with a power grid, a power electronic inverter is needed. Transformer-less grid connected PV systems attracts many researchers for PV system generation due to its high efficiency, cost-effective, and lower THD. This thesis investigates for the effectiveness of employing ISI-NPC inverter in a transformer-less grid connected PV system with HCC current controller. In this chapter, the system is designed and modeled to examine the effectiveness HCC controller for grid connected 3L-ISI NPC inverter with a PV system instead of a DC source. For PV system operation, a maximum power point tracking is needed. Therefore, this chapter also investigate the effect of using the most common conventional MPPT (Peturb &Observe) and the common advent method (soft computing) Artificial Neural Network (ANN) with HCC controller This investigation has not been reported yet.

The system is divided into different stages. The first stage is focusing on the PV panel characteristics in terms of the effect of irradiance and temperature variations in addition to examining the impact of using conventional and modern MPPT approaches (P&O and ANN) on the power transfer to the utility grid.

The second stage is considering the behavior of the grid connected 3L-ISI inverter fed by PV model under HCC current controller.

4.6 Evaluation of single phase grid connected PV system operates with different MPPT approaches at constant irradiance and temperature Values

A conventional MPPT approach is used to track the maximum power point for extracting the PV maximum energy at all conditions Figure (4.59) . The Perturb & Observe and Artificial Neural Network technique are utilized in this work. Simulink models of the system utilizing the P&O algorithm are shown in Figure (4.60), and the ANN algorithm is shown in Figure (4.61).

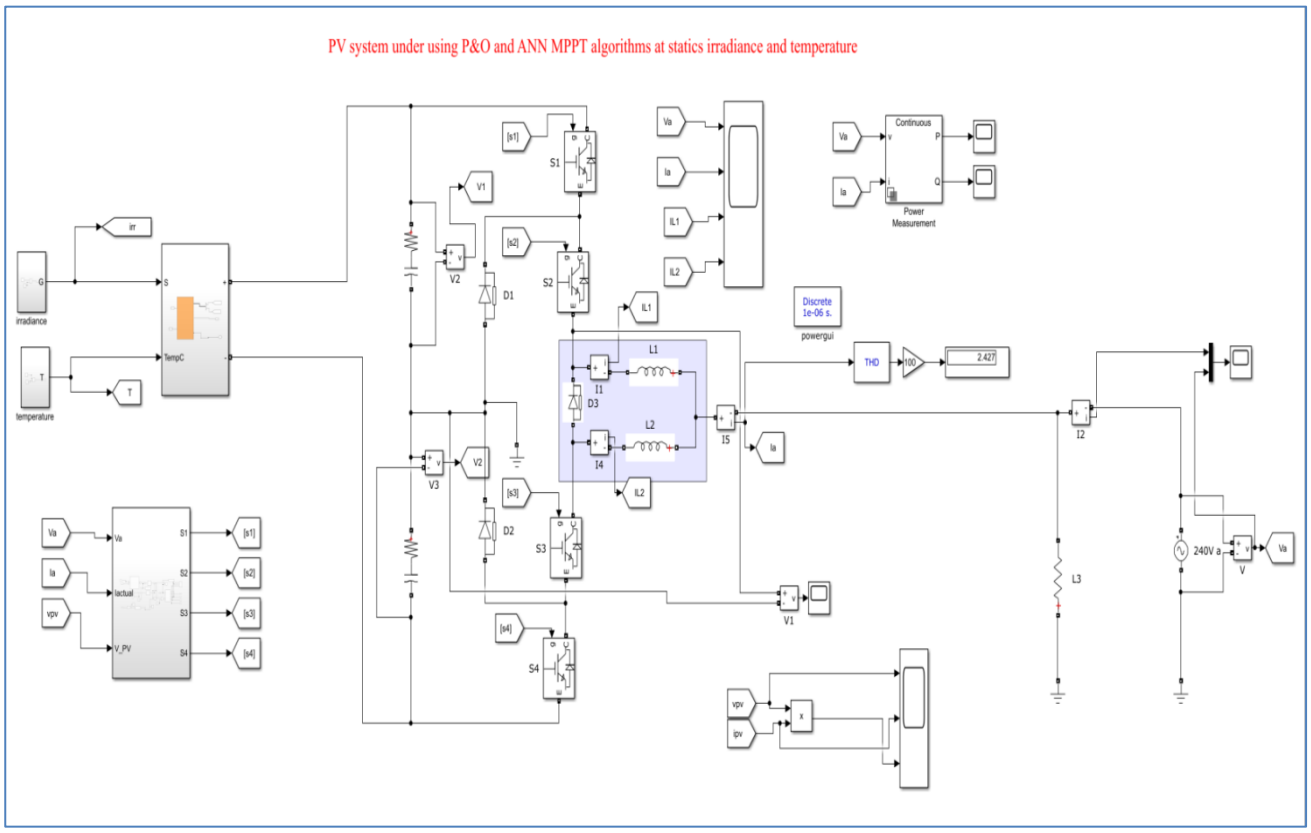

Figure (4.59) Simulink of PV system under P&O and ANN algorithms

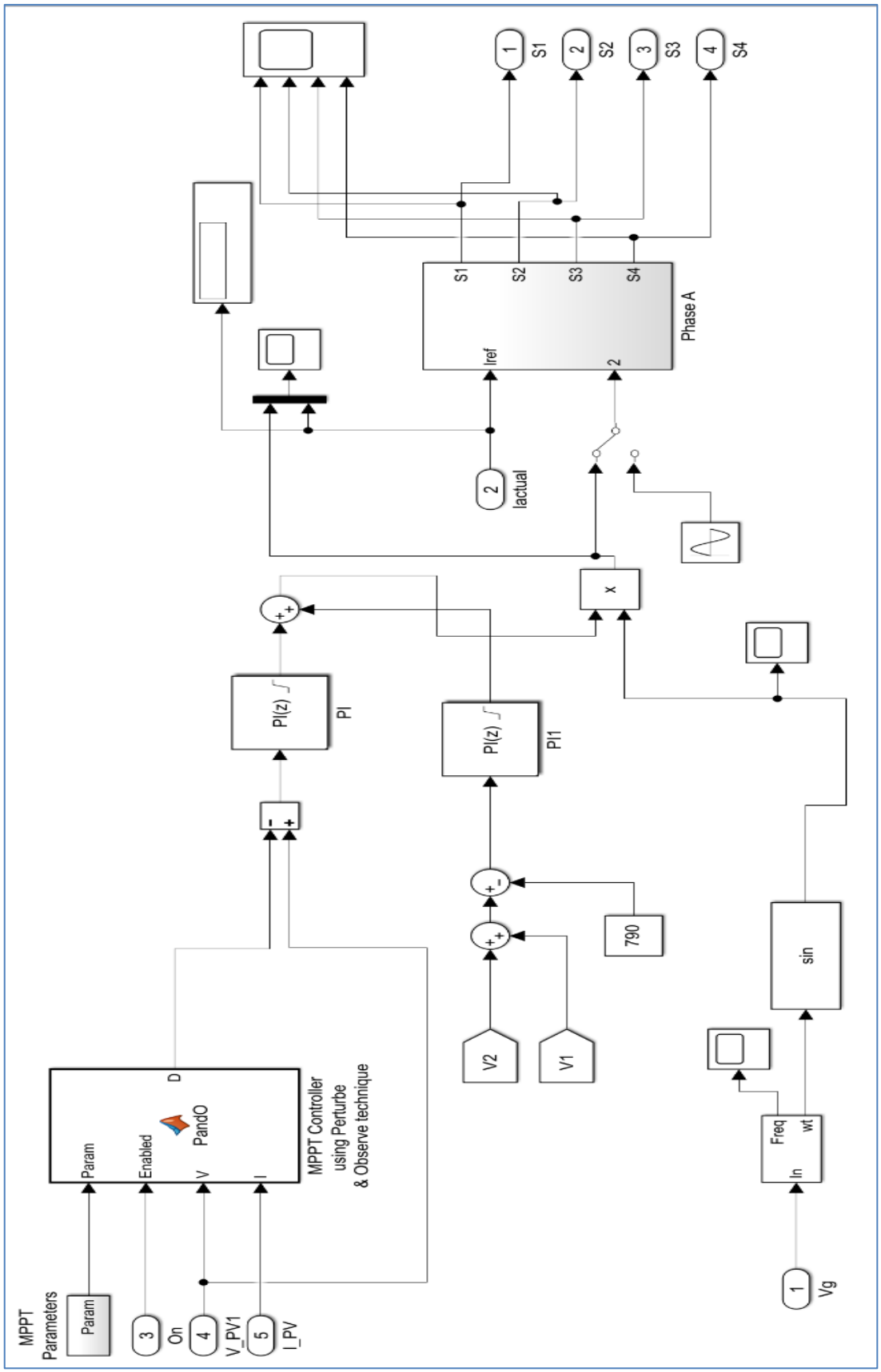

Figure (4.60) Simulink of controller with P&O algorithm

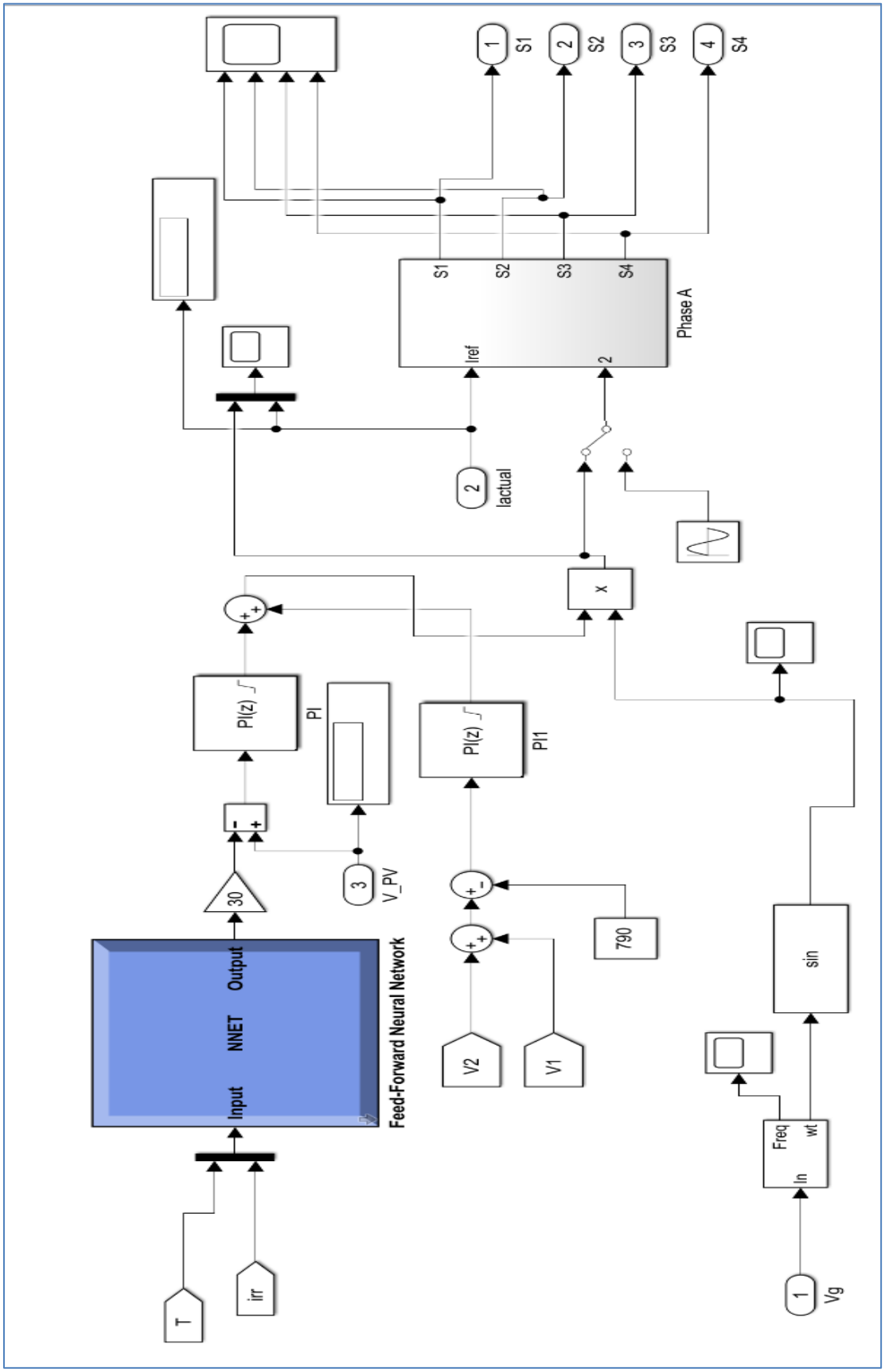

Figure (4.61) Simulink of controller with ANN algorithm

The constant of irradiance and temperature are stimulated as a step function with constant block in MATLAB/SIMULINK Figure (4.62) a and b illustrates this.

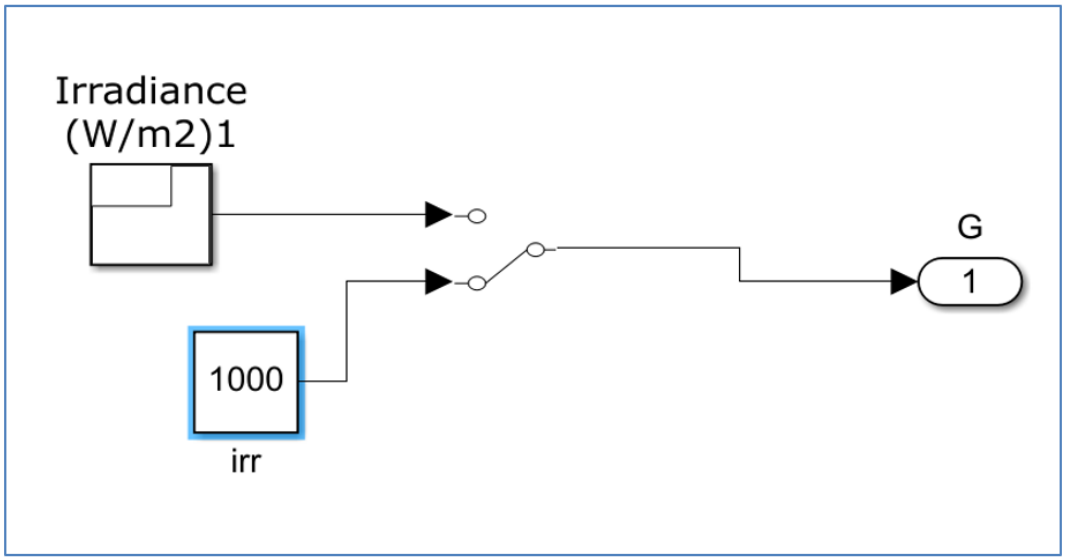

(a)

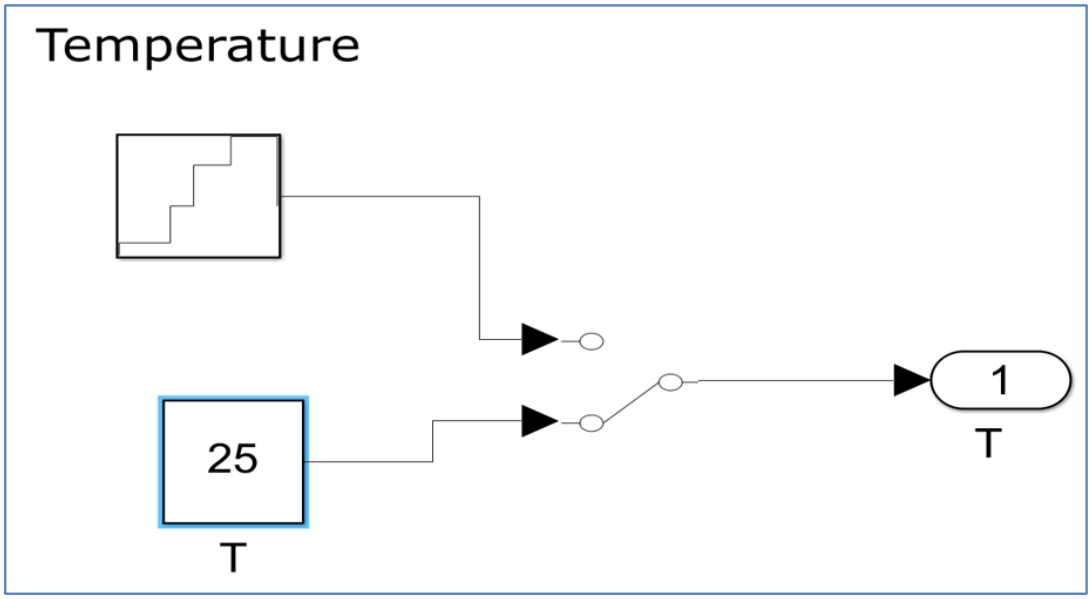

(b)

Figure (4.62) (a) Constant irradiance , (b) Constant temperature

After running the simulation, under fixed irradiance and temperature, this section compares the system's voltage and current waveforms by supplying the grid system from PV panel model. Both inductor currents I_{L1} and I_{L2} and $I_{L12.}$ By comparing Figure (4.63) and Figure (4.64), it is clear that a pure sinusoidal output current can be achieved using ANN approach.

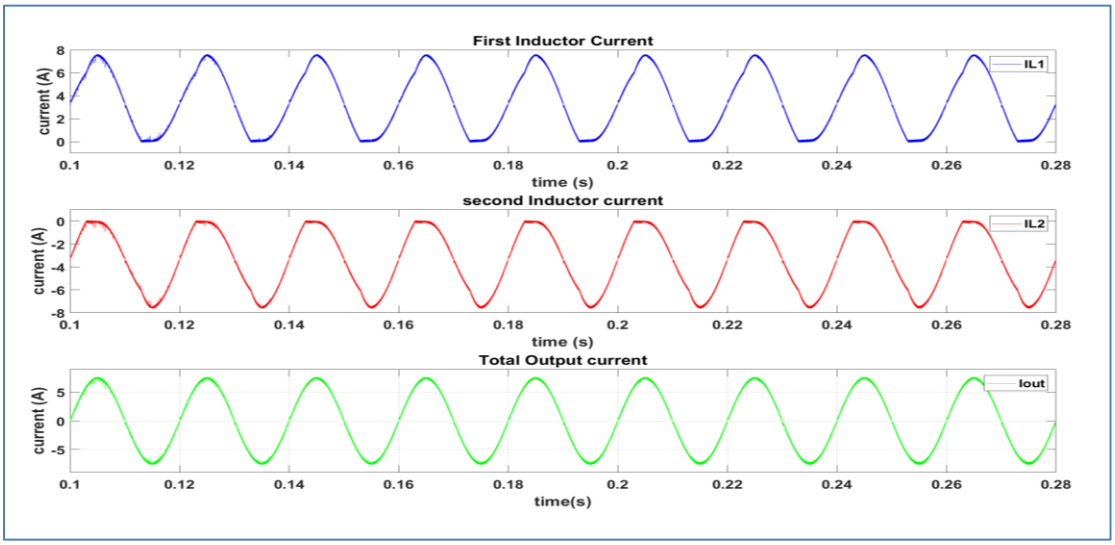

Figure (4.63) I_{L1} , I_{L2} and I_{out} of 3 level ISI-NPC inverter under P&O algorithm

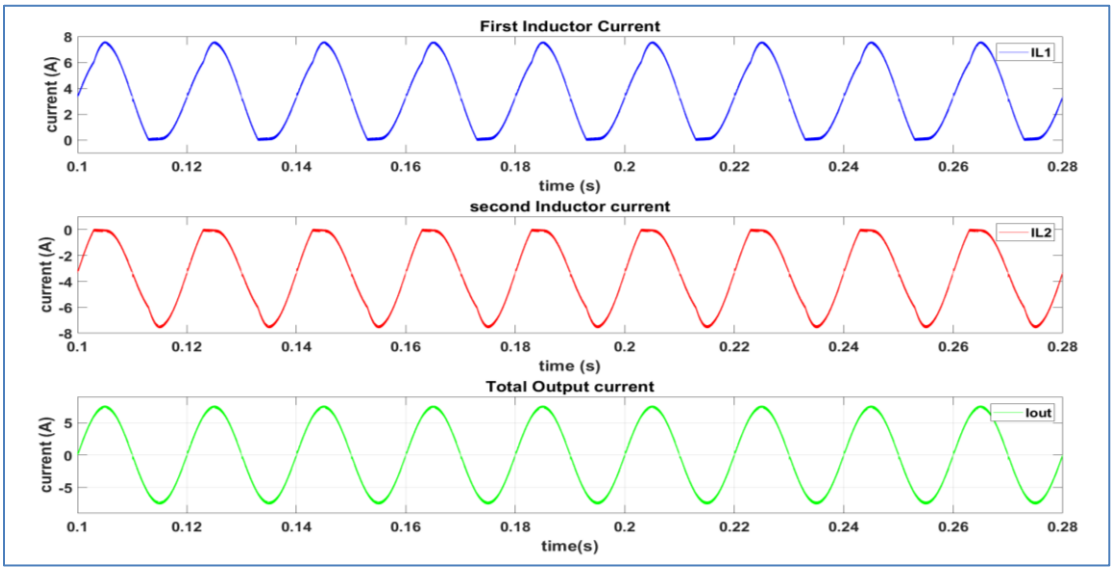

Figure (4.64) I_{L1} , I_{L2} and I_{out} of 3 level ISI-NPC inverter under ANN algorithm

As seen in Figures. (4.66) and (4.65), changing the MPPT methods at constant temperature and irradiance has a small impact on the output voltage. When utilising the P&O algorithm and the ANN MPPT, as shown in Figures (4.65) and (4.66), the ripple is incredibly minimal.

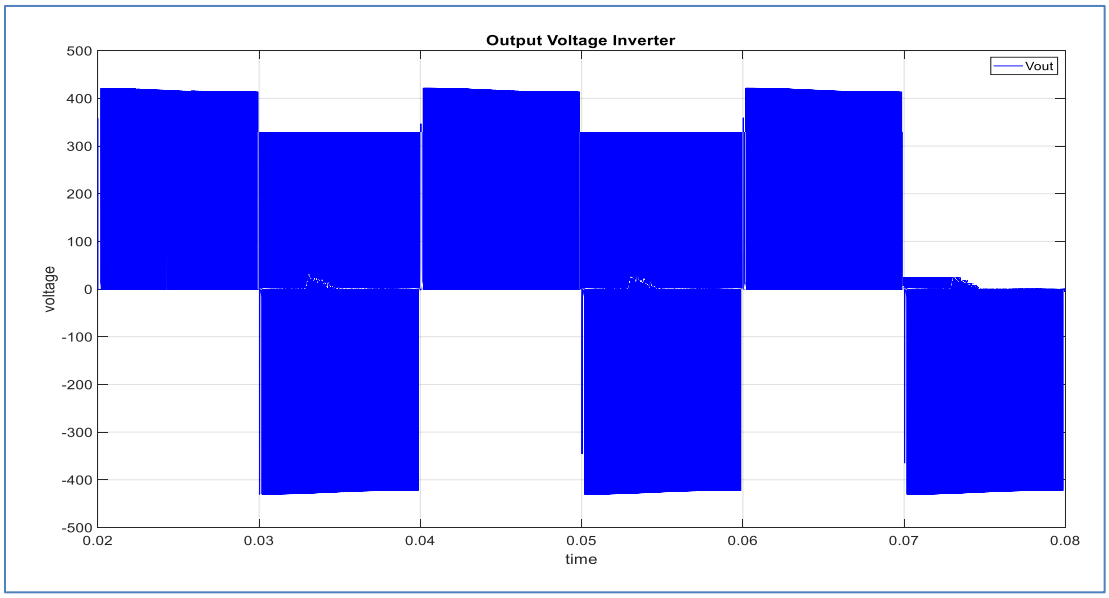

Figure (4.65) V_{out} of 3 level ISI-NPC inverter under P&O algorithm

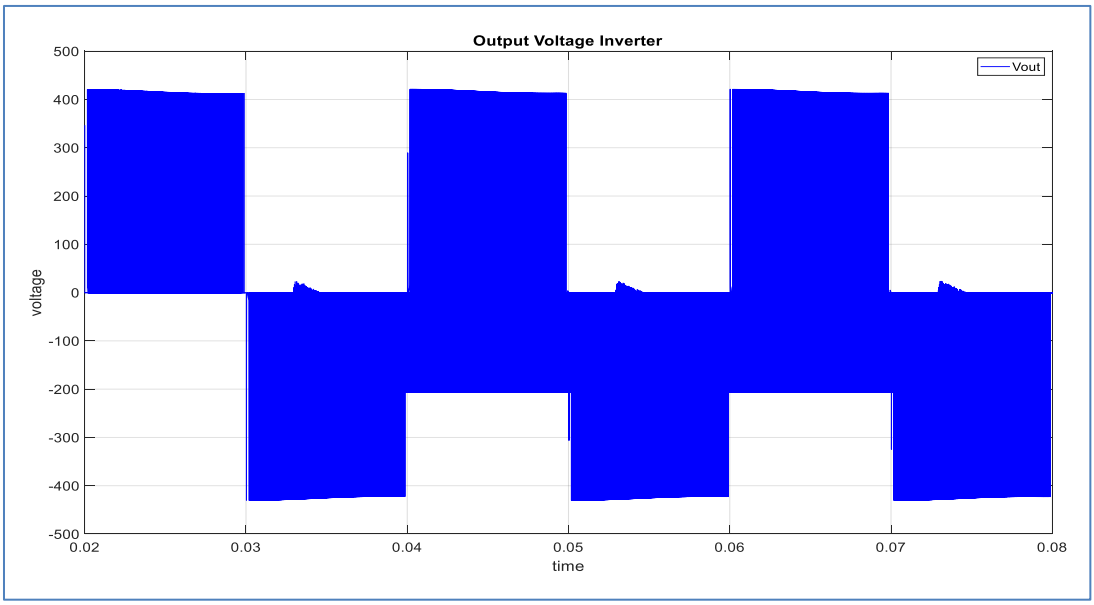

Figure (4.66) V_{out} of 3 level ISI-NPC inverter under ANN algorithm

All the PV panel output waveforms including the voltage V_{pv}, current I_{pv} and P_{pv} power are much smooth when using ANN approach. This is due to the fact that P&O produces oscillations around the MPP and periodic deviations from the maximum operating point under steady-state conditions, especially when the air of environment conditions are rapidly changing. Therefore, the ANN algorithm Figure (4.67), is much better than the P&O Figure (4.68) .

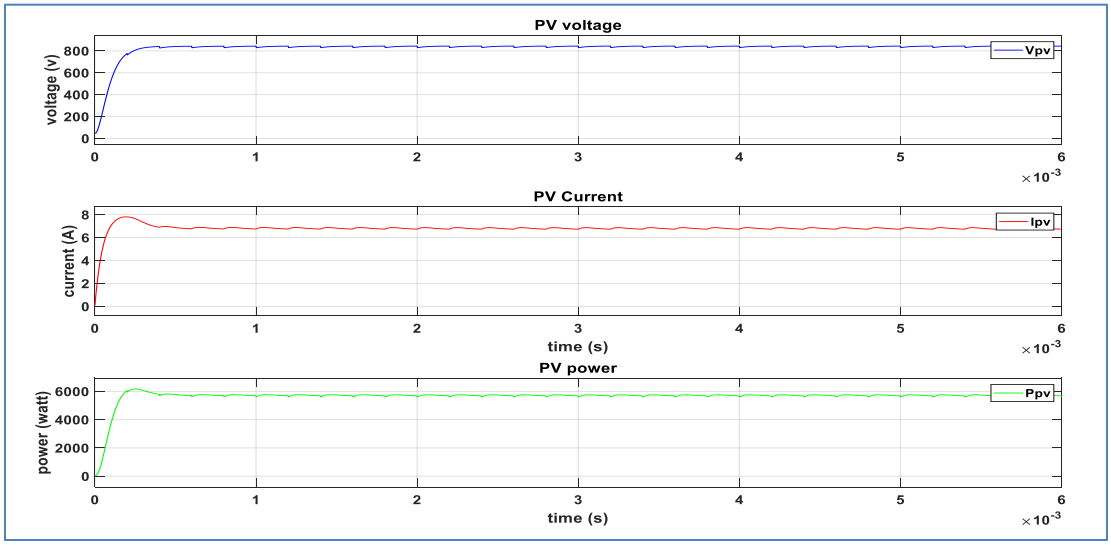

Figure (4.67) V_{PV}, I_{PV} and P_{PV} under P&O algorithm

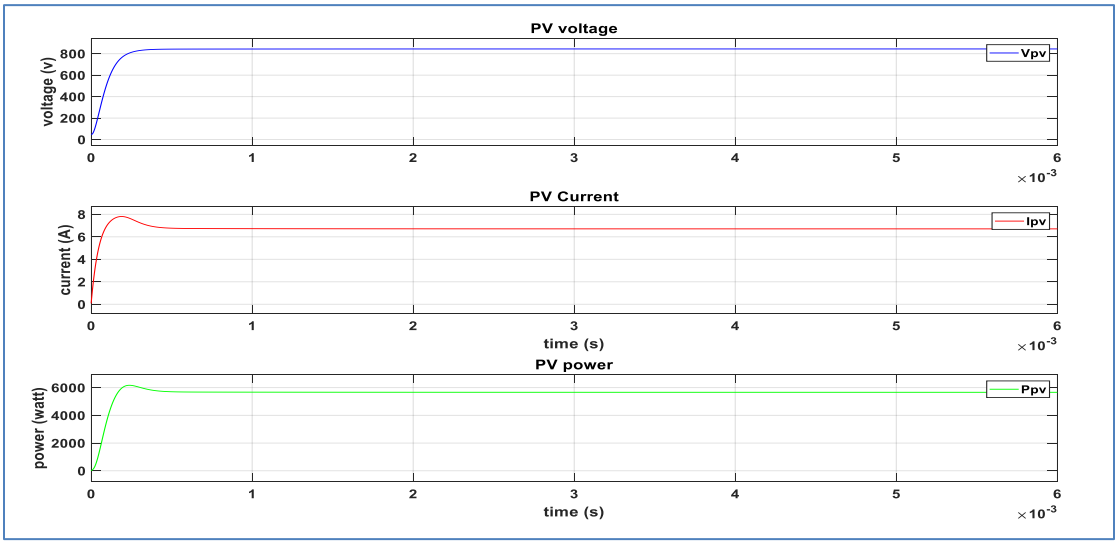

Figure (4.68) V_{PV}, I_{PV} and P_{PV} under ANN algorithm

The capacitor voltages have the same behavior with different MPPT with a voltage value of 420 V Both Figures (4.69) and (4.70) show this. The difference in the algorithm did not impact the voltage, which is approximately 430 volts Both Figures

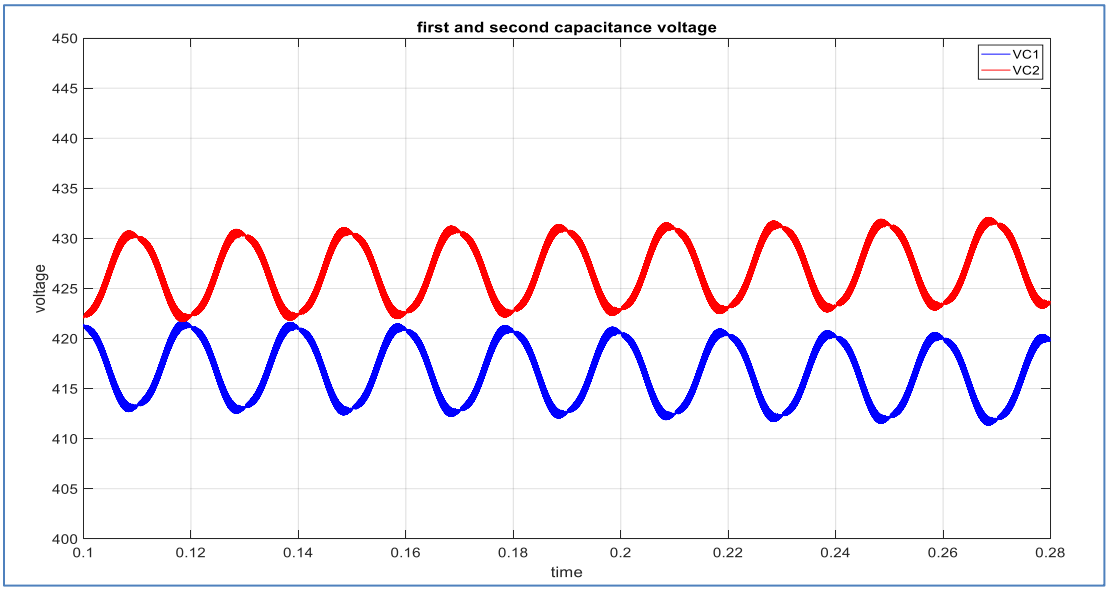

Figure. (4.69), V_{C1} and V_{C2} of 3level ISI-NPC inverter under P&O algorithm

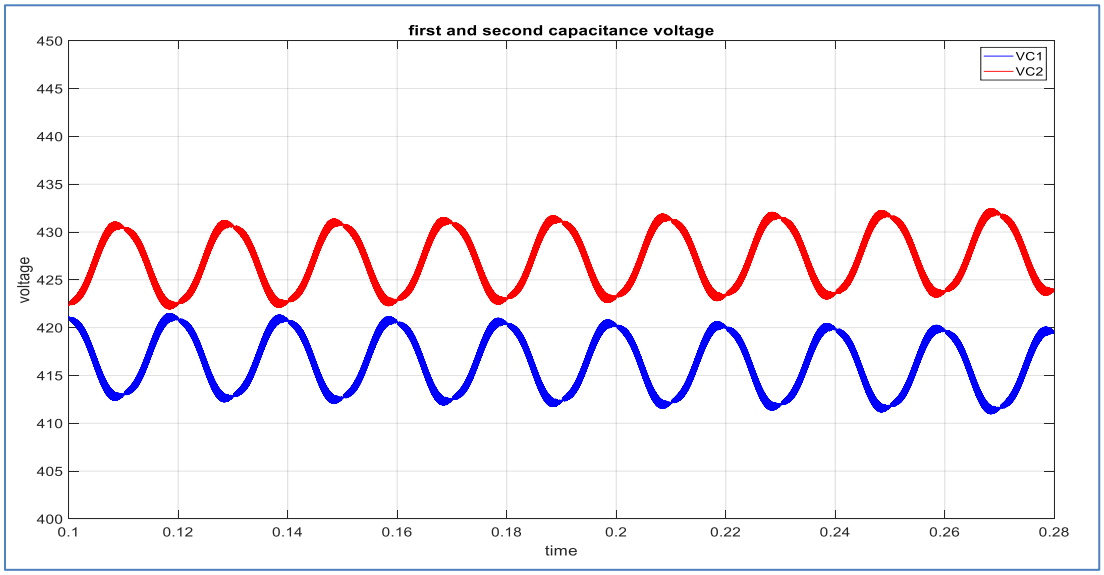

Figure (4.70) V_{C1} and V_{C2} of 3 level ISI-NPC inverter under ANN algorithm

Figure (4.71), shows the current of the first capacitor and the second capacitor when using the P&O algorithm and the second Figure (4.72), when using the ANN algorithm. The figures show that there is a quantity of ripple in Ic_1 and Ic_2 when using P&O, this leads to conclude that the ANN algorithm is more suitable to be used with grid connected 3L-ISI NPC PV system.

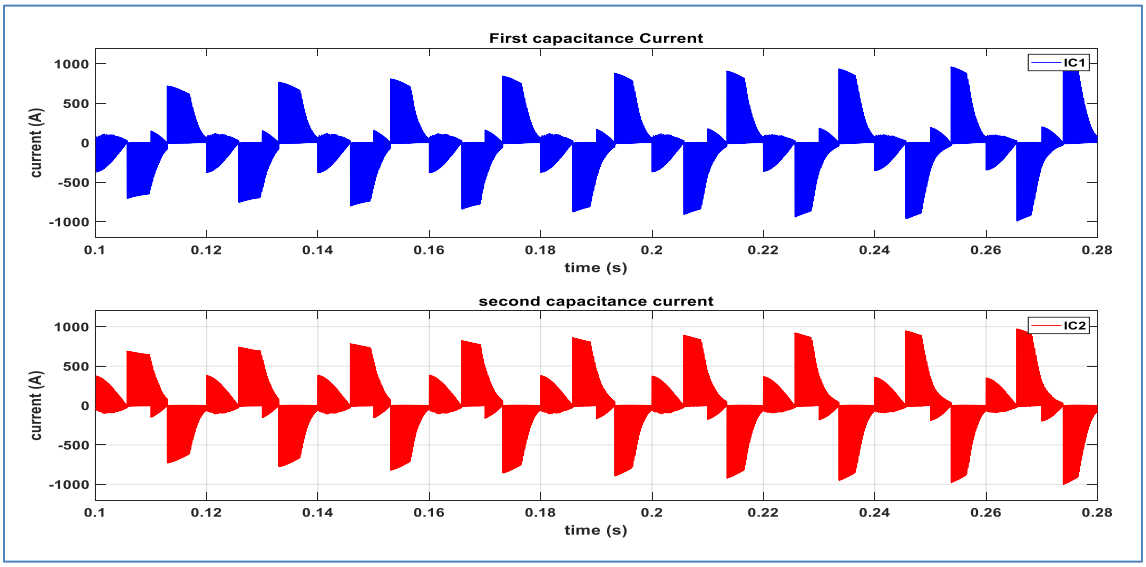

Figure (4.71) I_{C1} and I_{C2} of 3 level ISI-NPC inverter under P&O algorithm

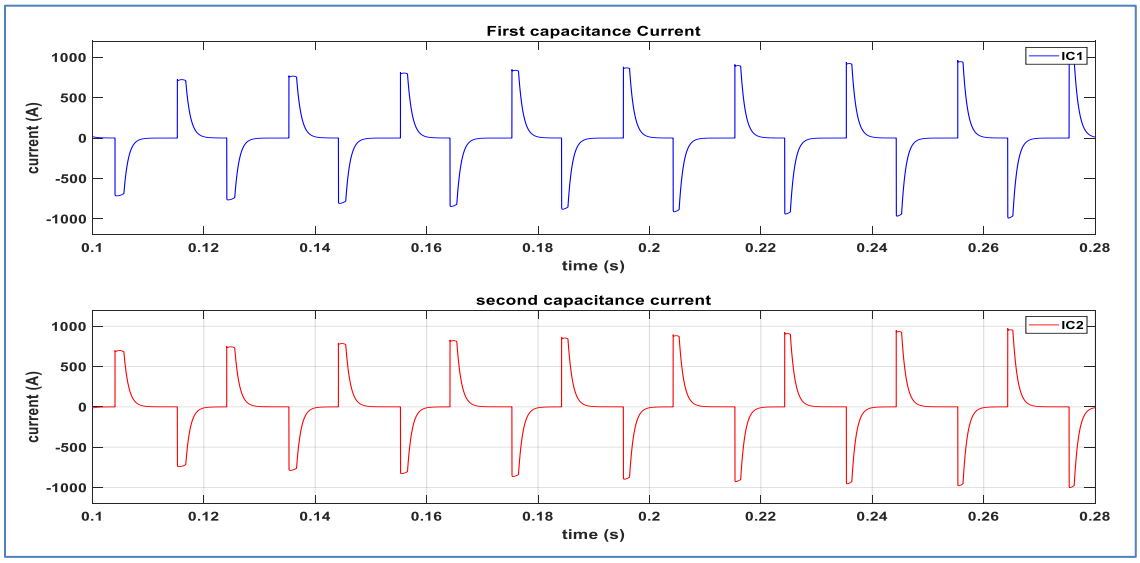

Figure (4.72) I_{C1} and I_{C2} of 3 level ISI-NPC inverter under ANN algorithm

Given that the temperature and irradiance were constant, as shown in Figures (4.73) and (4.74) under the impact of the P&O and ANN algorithms, respectively, the grid voltage was unaffected by the different MPPT algorithms, whether they were P&O or ANN.

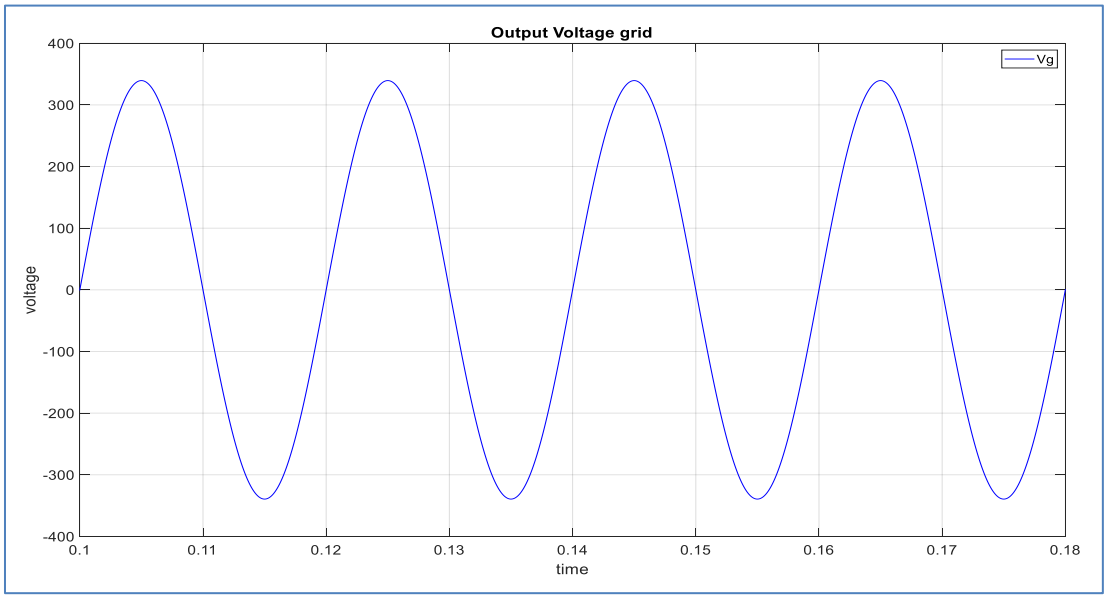

Figure (4.73) V_{grid} under P&O algorithm

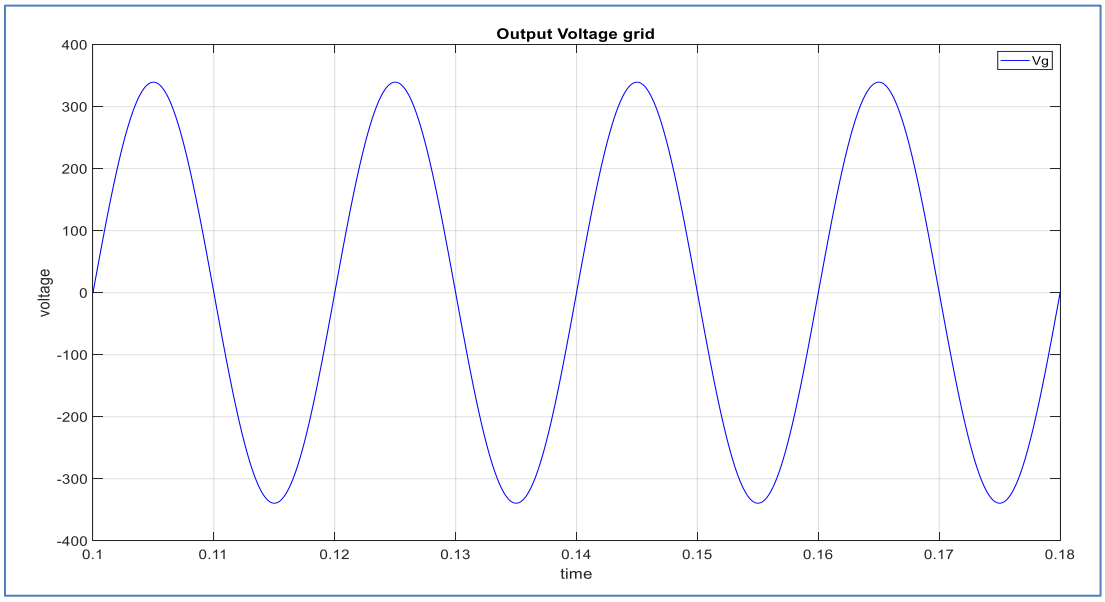

Figure (4.74) V_{grid} under ANN algorithm

The grid current when the perturb and observe algorithm is in use Figure (4.75) shows a high amount of ripple, in contrast to Figure (4.76), which is the grid current under the influence of the ANN algorithm where notice that the current is free of any distortion and this confirms that using the algorithm The ANN is better than the P&O algorithm at constant temperature and irradiance .

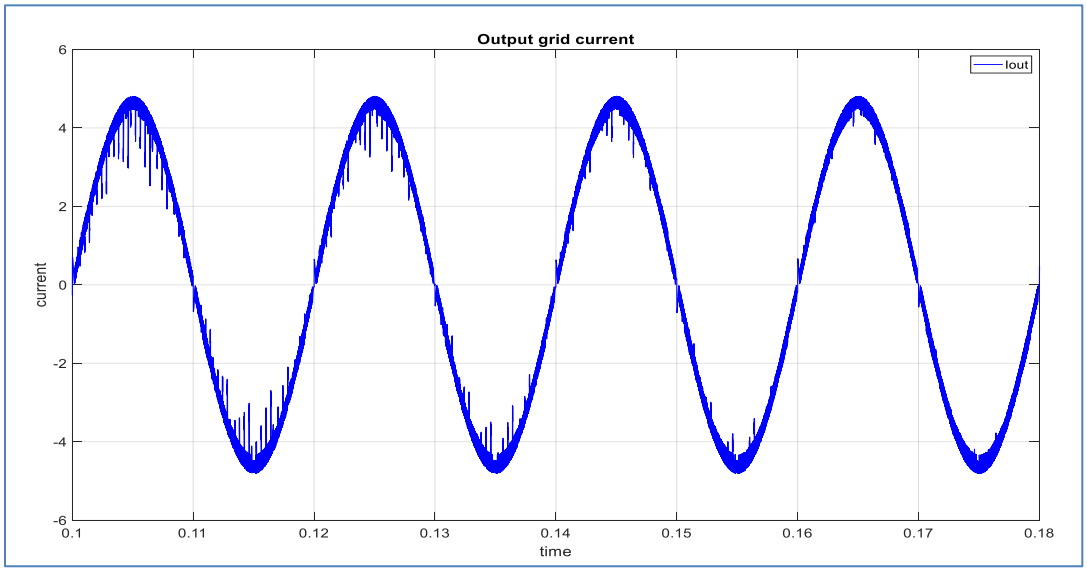

Figure (4.75) I_{grid} using the P&O algorithm

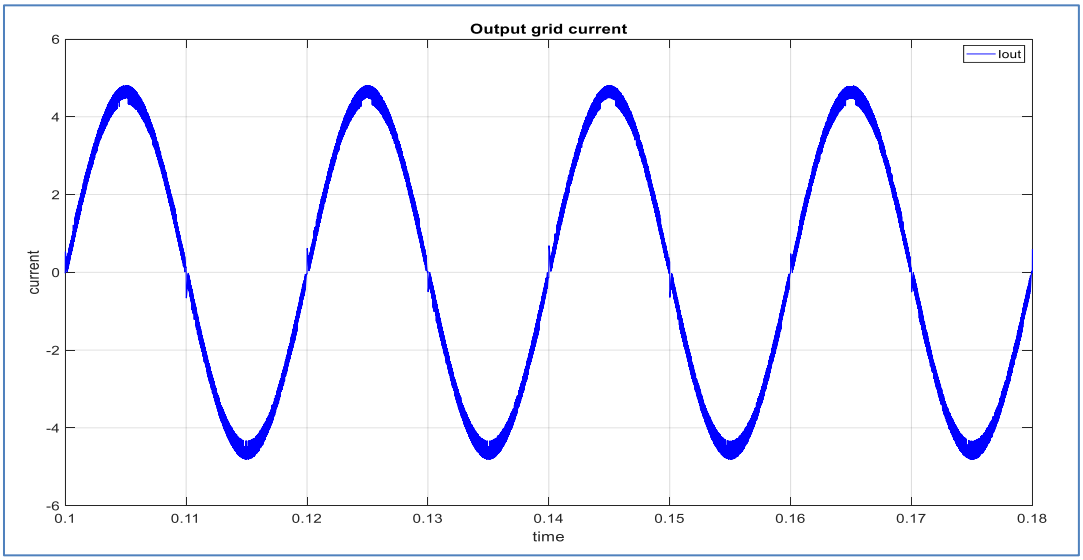

Figure (4.76) Igrid utilizing the ANN algorithm

The percentage of the current THD was calculated at 0.1 start time and at 3 number of cycle, where we note that the value of THD in the case of using P&O is much greater than using ANN algorithm, Both Figures (4.77) and (4.78) show this.

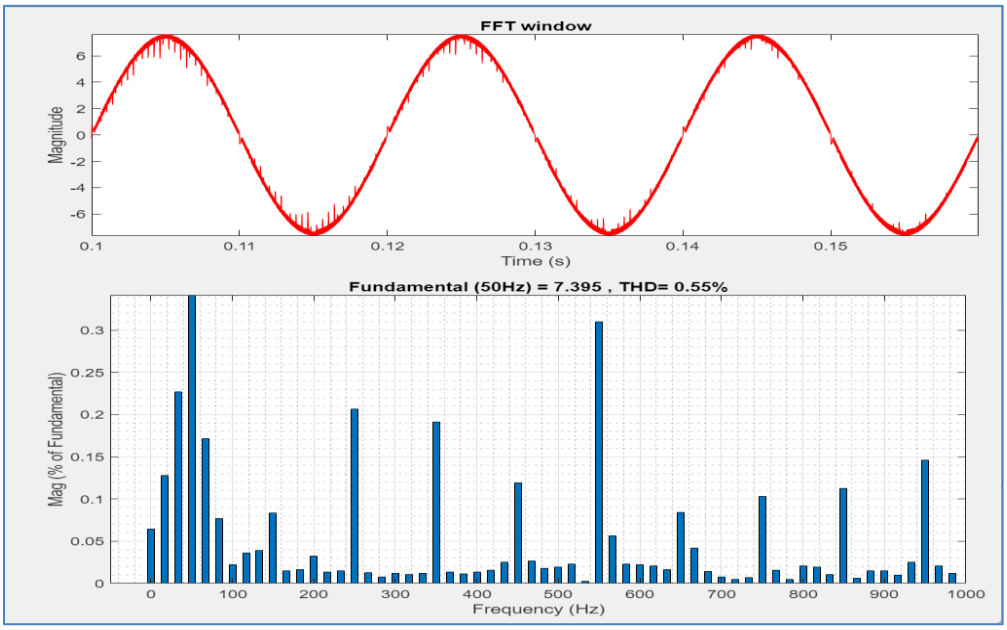

Figure (4.77) FFT analysis of current THD under P&O algorithm

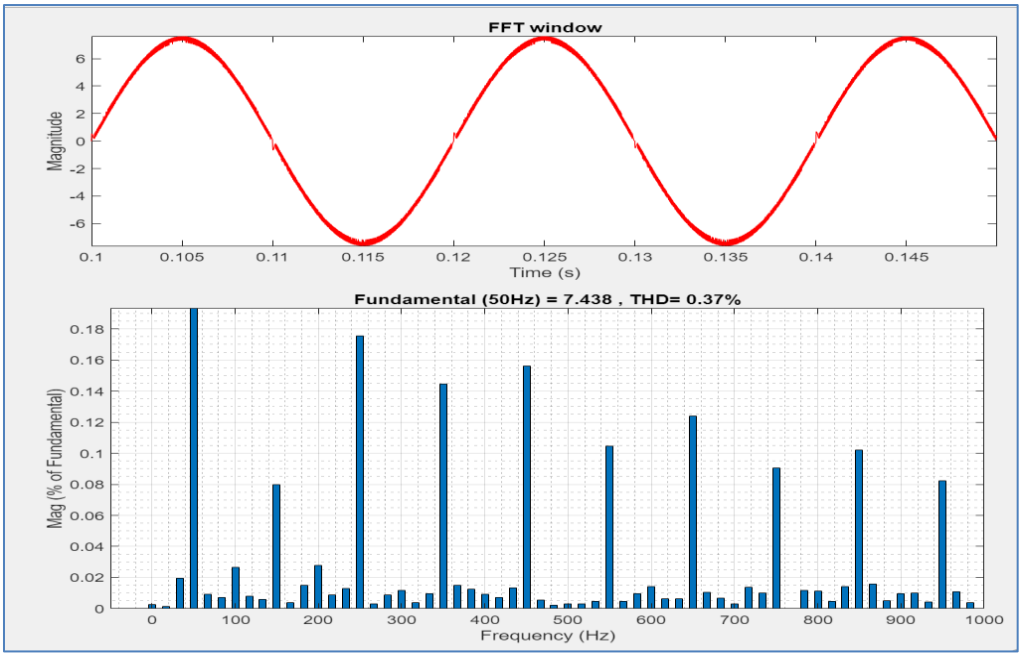

Figure (4.78) FFT analysis of current THD under ANN algorithm

4.7 PV system under using P&O and ANN algorithm at variable irradiance and temperature

One of the main influencing factors on the PV system is the temperature and radiation. They have an effect on voltage, current and capacity, where the current is directly proportional to the temperature, while the voltage is not affected by changing the temperature and radiation. Also, choosing the MPPT algorithm has an effect that will be explained later.

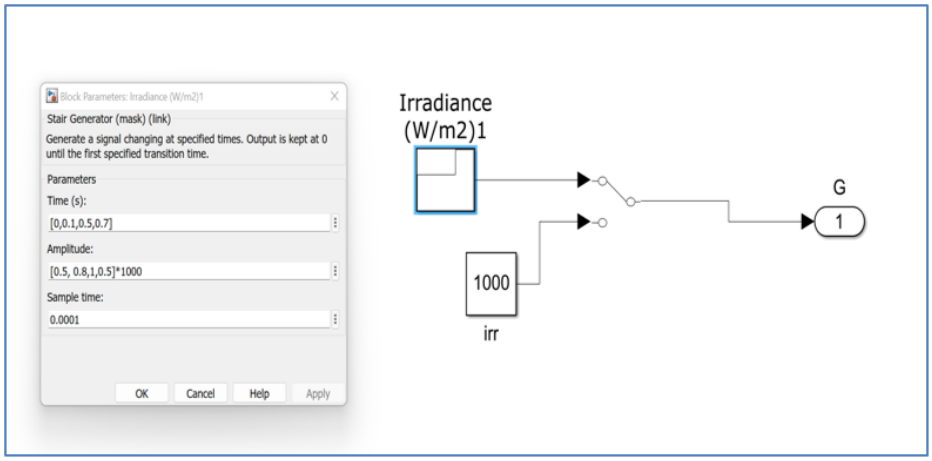

(a)

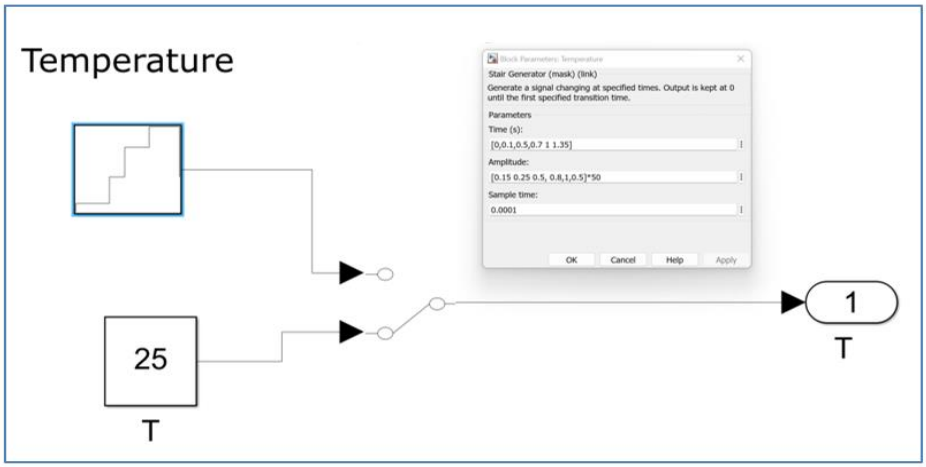

(b)

Figure (4.79) (a) Variable irradiance , (b) Variable temperature

The amount of ripple and distortion in the current of the first inductor and the second inductor and the output inverter current is evident in Figure (4.80), when using the P&O algorithm and at variable temperature and irradiance compared to Figure (4.81), shows results when using the ANN algorithm , which shows the output inverter current and the first and second inductors current are free of any ripple.

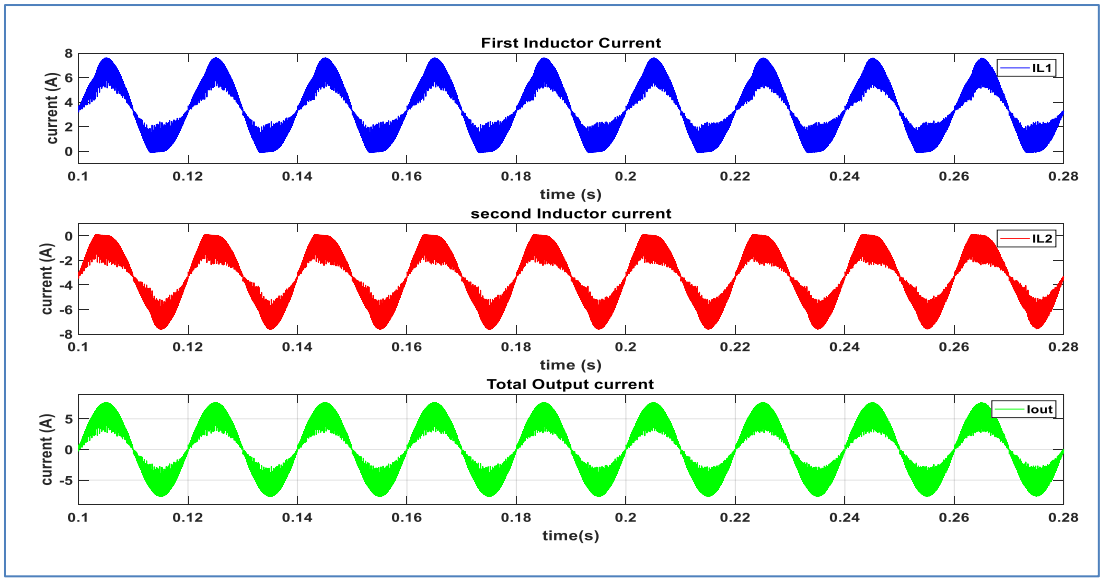

Figure (4.80) I_{L1} , I_{L2} and I_{out} of 3 level ISI-NPC inverter under P&O algorithm

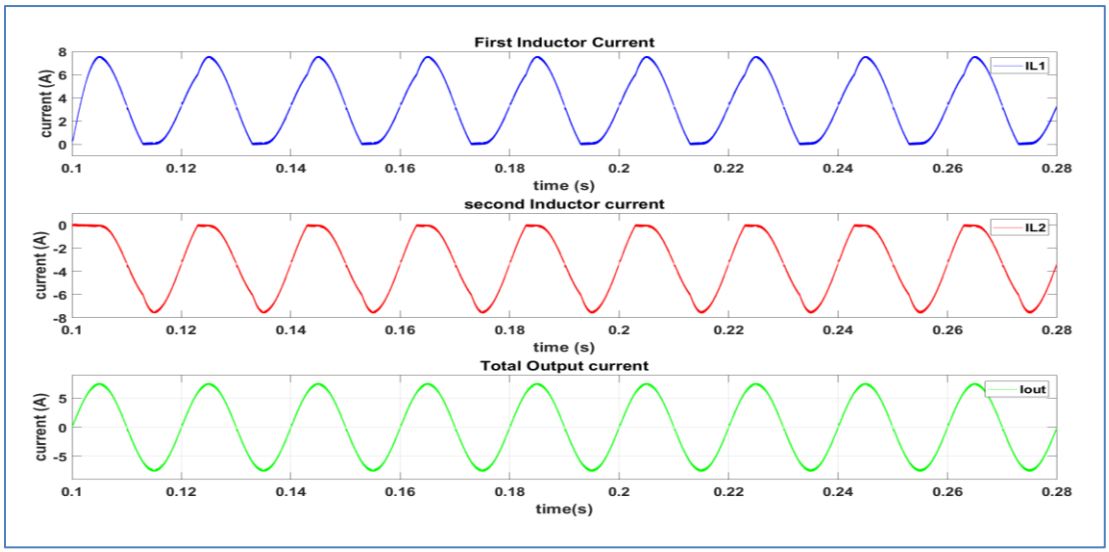

Figure (4.81) I_{L1} , I_{L2} and I_{out} of 3 level ISI-NPC inverter under ANN algorithm

According to the two figures above, varying the temperature and irradiance have no effect on the PV's voltage, because their relationship is direct, changing the irradiance has an impact on the current, which in turn has an impact on the power. also seen that a certain amount of oscillation manifests itself when the P&O method is applied, as illustrated in Figure (4.82).

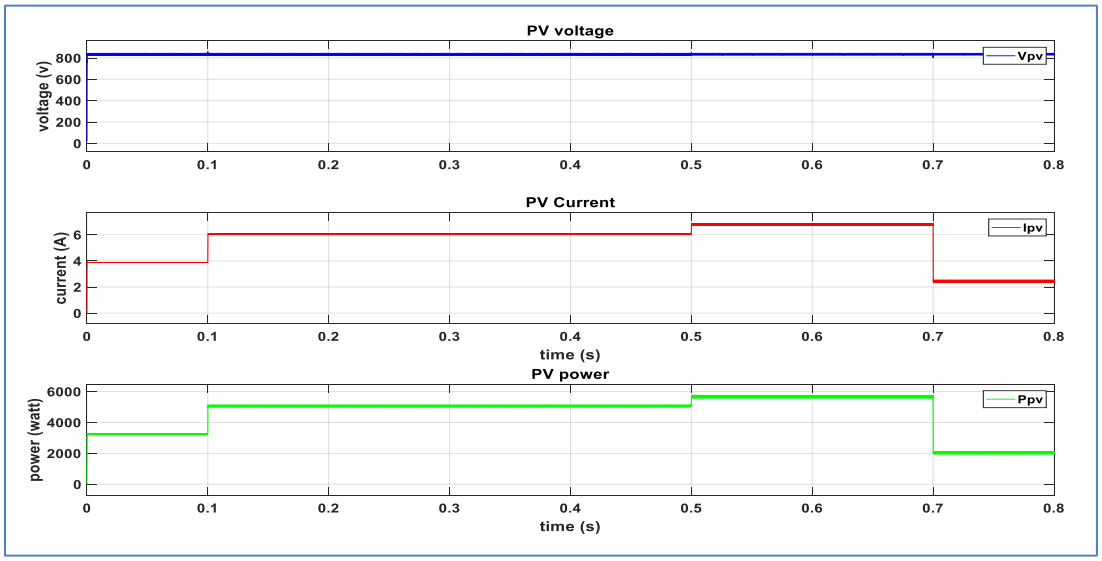

Figure (4.82) V_{PV}, I_{PV} and P_{PV} under P&O algorithm

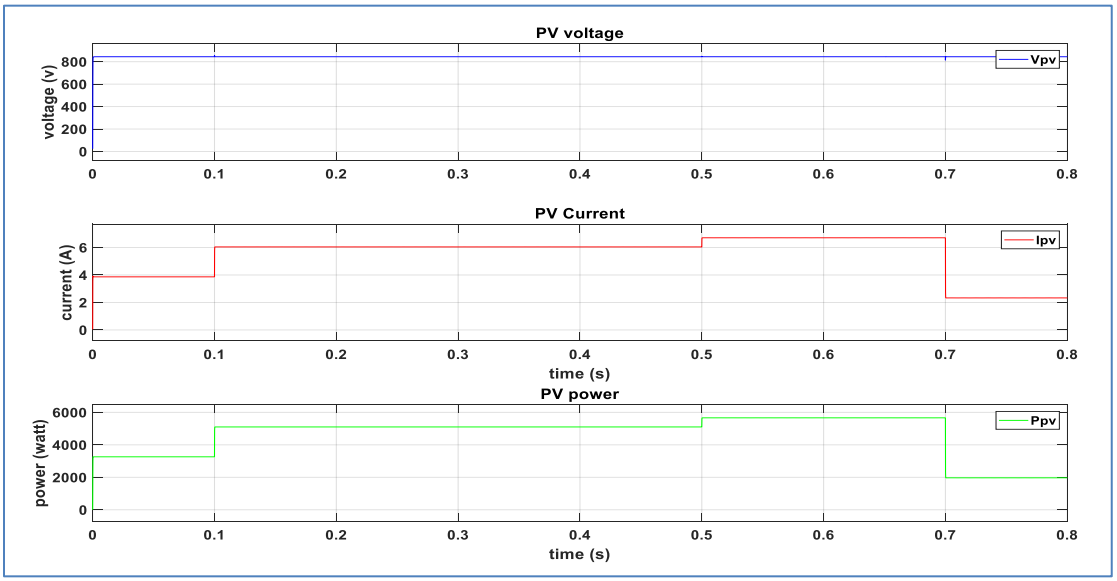

Figure (4.83) V_{PV}, I_{PV} and P_{PV} under ANN algorithm

The amount of the current THD percentage is clear through the FFT analysis in the case of changing irradiance and temperature when using the ANN algorithm, it was much less, almost non-existent, Figure (4.85), where the percentage is 0.27%, while when using the P&O Figure (4.84), where the percentage was 2.73% .

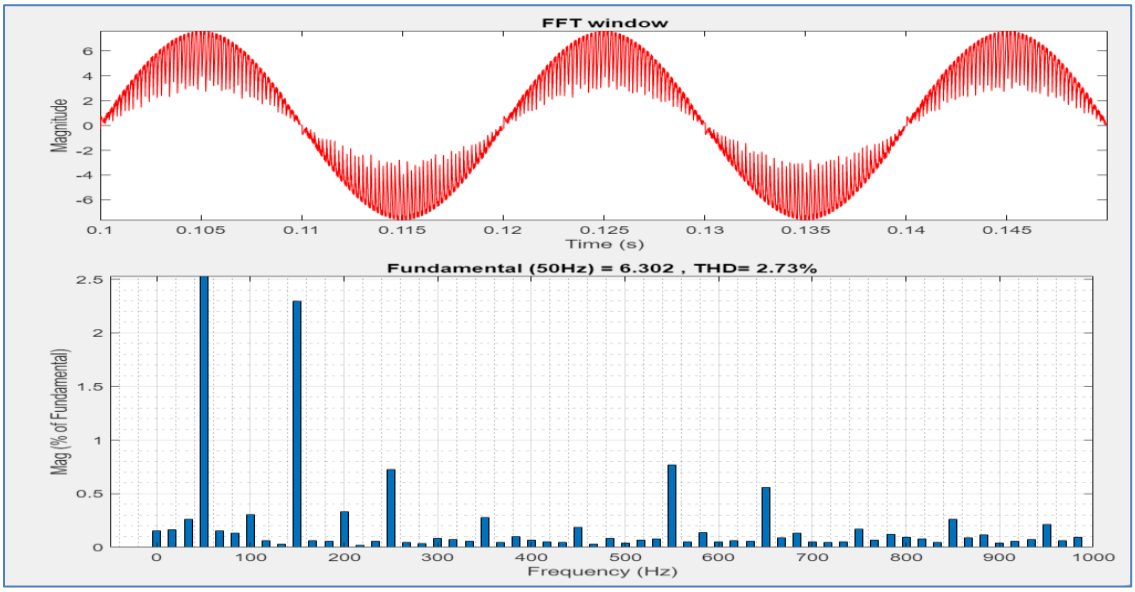

Figure (4.84) FFT analysis of current THD under P&O algorithm

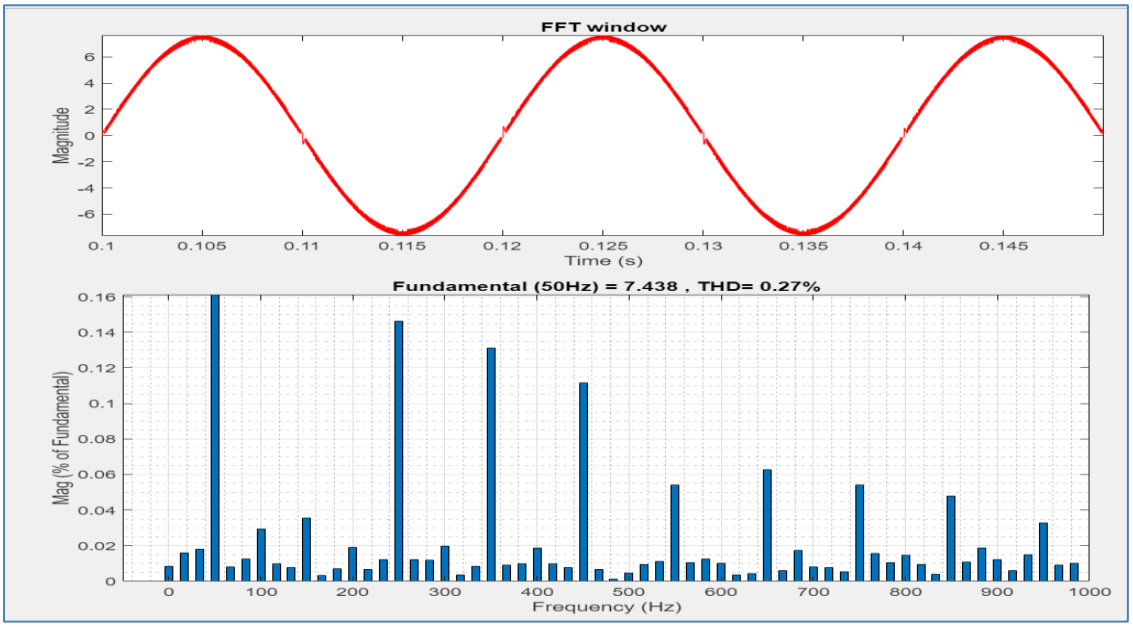

Figure (4.85) FFT analysis of current THD under ANN algorithm

CHAPTER FIVE

Conclusions and Future works

CHAPTER FIVE

Conclusions and Future works

5.1 Conclusions.

From the results presented in this research, the following points are concluded:

1. After a detailed comparison is carried out between NPC and SI-NPC in terms of output voltage and current waveforms, split inductors current waveforms, DC capacitors voltage waveforms, and the harmonics content in each topology. The SI-NPC topology has better performance with a current THD with a value of 2.32% under PD PWM and 5.43% under POD PWM in comparison with a THD value of 2.51% under PD PWM and 5.97% under POD PWM in NPC topology. However, SI-topology suffer from overvoltage and current on the semiconductor switches.
2. It is very important to introduce an efficient transformerless multilevel inverter in a single stage system as a replacement for the existing topology. Therefore, this thesis thoroughly investigates the performance of grid connected ISI-NPC to be employed in TRL system. Because it contains two inductors, L_1 and L_2. This adhesive topology gives it importance to cancel the shoot through problem, as well as the fact that it contains the midpoint to cancel the effect of the leakage current with a low %THD with a value of 0.67% under PD PWM and 1.16% under POD PWM, and no overvoltage upon the semiconductor switches.
3. To ensure high grid power quality. The systems were accomplished when using Hysteresis Current Controller (HCC) to track the inductor currents in two cases, one when the grid current (reference current) was constant at 7.61 A and the other when taking values for the current, for example (0.5 * 7.61),

(0.8 * 7.61), and so on. A better performance is achieved with a THD value of 3.34%.

4. To extract a maximum power from PV panel, the system behavior is examined to operate under different MPPT approaches (conventional and no-conventional approaches), the system two algorithms were used, one of which is P&O and the other is Neural network. It was also used in two cases, one when the irradiance and temperature are constant and the other when the irradiance and temperature change, where we note that the change in irradiance affects the current as they are directly proportional.
5. By evaluating the system behavior, it is clear that the single phase ISI-NPC can be considered as a better candidate to be employed in TRL PV system. It is also clear that, the use of the neural network algorithm is more efficient than the P&O algorithm as it is more suitable for use in terms of the amount of current ripples as well as the amount of power, and also the harmonic distortion ratio (THD) in the current is much less in the case of using Neural network, and this is considered a very important feature.
6. The use of two MPPT algorithms, namely the P&O and ANN, and the results proved that the use of the ANN algorithm was better than the use of the P&O algorithm, both in terms of currents and voltages, as well as the THD value of the output current inverter, and it also turned out that one of the disadvantages of the P&O algorithm is the amount of oscillation around the MPPT .

5.2 Future works

Enhancement of the single phase transformer-less PV system can be promoted by taking the following recommendations into account:

1. Design and implementation of a transformer-less grid-connected PV system by using different control system including predictive control system.
2. The proposed system can be modified using hybrid controller to improve system performance.
3. Developing a higher level topology used in the proposed system by increasing the number of levels (5- level ISI-NPC Inverter or more).
4. Adopting different modulation approach for ISI-NPC inverter.
5. Applying different grid synchronization approach to enhance the MLI behaviour.
6. Replacing the ISI-NPC with different developed NPC topology.

References:

[1] N. Kaushika, A. Mishra, A. K. Rai, N. Kaushika, A. Mishra, and A. K. Rai, "Introduction to solar photovoltaic power," *Solar Photovoltaics: Technology, System Design, Reliability and Viability*, pp. 1-14, 2018

[2] M. Boxwell, *The Solar Electricity Handbook-2017 Edition: A simple, practical guide to solar energy–designing and installing solar photovoltaic systems*. Greenstream Publishing, 2017.

[3] I. Pharne and Y. Bhosale, "A review on multilevel inverter topology," in *2013 International Conference on Power, Energy and Control (ICPEC)*, 2013: IEEE, pp. 700-703.

[4] W. Xiao, "*Photovoltaic Power System*." 2017. doi: 10.1002/9781119280408.

[5] S. Ozdemir, N. Altin, and I. Sefa, "Single stage three level grid interactive MPPT inverter for PV systems," *Energy Conversion and Management*, vol. 80, pp. 561-572, 2014.

[6] Z. Pan, F. Z. Peng, V. Stefanovic, and M. Leuthen, "A diode-clamped multilevel converter with reduced number of clamping diodes," in *Nineteenth Annual IEEE Applied Power Electronics Conference and Exposition, 2004. APEC'04.*, 2004, vol. 2: IEEE, pp. 820-824.

[7] F. Faraji, A. Hajirayat, A. A. M. Birjandi, and K. Al-Haddad, "Single-stage single-phase three-level neutral-point-clamped transformer-less grid-connected photovoltaic inverters: Topology review," *Renewable and Sustainable Energy Reviews*, vol. 80, pp. 197-214, 2017.

[8] S. Dhara, A. Hota, S. Jain, and V. Agarwal, "A novel single-phase t-type pv inverter with improved dc utilization," in *2018 IEEE International Conference on Power Electronics, Drives and Energy Systems (PEDES)*, 2018: IEEE, pp. 1-5.

[9] A. Sinha, K. C. Jana, and M. K. Das, "An inclusive review on different multi-level inverter topologies, their modulation and control strategies for a grid connected photo-voltaic system," *Solar Energy*, vol. 170, pp. 633-657, 2018.

[10] A. Kokila, "Comparison of SPWM and SVPWM control techniques for diode clamped multilevel inverter with photovoltaic system," in *2018 4th International Conference on Electrical Energy Systems (ICEES)*, 2018: IEEE, pp. 234-241.

[11] X. Guo, M. C. Cavalcanti, A. M. Farias, and J. M. Guerrero, "Single-carrier modulation for neutral-point-clamped inverters in three-phase transformer-less photovoltaic systems," *IEEE Transactions on power Electronics*, vol. 28, no. 6, pp. 2635-2637, 2012.

[12] F. B. Grigoletto, "Five-level transformerless inverter for single-phase solar photovoltaic applications," *IEEE Journal of Emerging and Selected Topics in Power Electronics*, vol. 8, no. 4, pp. 3411-3422, 2019.

[13] A. Zarein, A. Mosallanejad, and M. S. Ghazizadeh, “An improved transformerless grid-connected - Photovoltaic inverter with reduced leakage current and increasing number of output voltage level”, in *34th International Power System Conference, PSC 2019*, Dec. 2019, pp. 327–332. doi: 10.1109/PSC49016.2019.9081476.

[14] X. Jiang and M. L. Doumbia, "Comparative Study of Grid-Connected Multilevel Inverters for High Power Phtovoltaic Systems," in *2019 IEEE 7th International Conference on Smart Energy Grid Engineering (SEGE)*, 2019: IEEE, pp. 184-190.

[15] Y. Li, H. Tian, and Y. W. Li, "Generalized phase-shift PWM for active-neutral-point-clamped multilevel converter," *IEEE Transactions on Industrial Electronics*, vol. 67, no. 11, pp. 9048-9058, 2019.

[16] K. Chenchireddy, V. Jegathesan, and L. A. Kumar, "Design and Simulation of a Single Phase Four Level Neutral Point Clamped Inverter," *International Journal of Recent Technology and Engineering (IJRTE) ISSN*, pp. 2277-3878, 2019.

[17] B. Chokkalingam, M. S. Bhaskar, S. Padmanaban, V. K. Ramachandaramurthy, and A. Iqbal, "Investigations of multi-carrier pulse width modulation schemes for diode free neutral point clamped multilevel inverters," *Journal of Power Electronics*, vol. 19, no. 3, pp. 702-713, 2019.

[18] V. Muni, "A Novel Methodology for Single Phase Transformerless Inverter with Leakage Current Elimination for PV Systems Applications Power management system View project", 2019.

[19] J. Ferdous, S. Kabir, R. A. Siddique, and U. Salma, "Split inductor based neutral point clamped inverter using improved modulation technique to reduce common mode voltage," in *8th International Conference on Electrical and Computer Engineering*, 2014: IEEE, pp. 623-626.

[20] R. Palanisamy, P. Aravindh, and K. Vijayakumar, "Effectual svpwm for 3-level npc-mli with grid connected pv system," *International Journal of Electrical Engineering and Technology*, vol. 11, no. 3, 2020.

[21] A. Kumar, R. K. Mandal, R. Raushan, and P. Gauri, "Grid Connected Photovoltaic Systems with Multilevel Inverter", in *2020 International Conference on Emerging Frontiers in Electrical and Electronic Technologies, ICEFEET 2020*, Jul. 2020. doi: 10.1109/ICEFEET49149.2020.9187010.

[22] B. Karami *et al.*, "A New 5-level Grid-Connected Transformerless Inverter with Eliminating Leakage Current," in *2020 IEEE 9th International Power Electronics and Motion Control Conference (IPEMC2020-ECCE Asia)*, 2020: IEEE, pp. 454-459

[23] P. Madasamy *et al.*, "A simple multilevel space vector modulation technique and MATLAB system generator built FPGA implementation for three-level neutral-point clamped inverter," *Energies*, vol. 12, no. 22, p. 4332, 2019.

[24] H. S. Maaroof, H. Al-Badrani, and A. T. Younis, "Design and simulation of cascaded H-bridge 5-level inverter for grid connection system based on multi-carrier PWM technique," in *IOP Conference Series: Materials Science and Engineering*, 2021, vol. 1152, no. 1: IOP Publishing, p. 012034.

[25] A. El-Hefnawy, E. E. El-Kholy, G. El-Menofy, and D. S. Osheba, "A Proposed Five-level Neutral Point Clamped Inverter", *Electrical Eng*, vol. 44, no. 2, pp. 135–140, 2021.

[26] L. C. Breazeale and R. Ayyanar, "A photovoltaic array transformer-less inverter with film capacitors and silicon carbide transistors," *IEEE Transactions on Power Electronics*, vol. 30, no. 3, pp. 1297-1305, 2014.

[27] S. Kouro, J. I. Leon, D. Vinnikov, and L. G. Franquelo, "Grid-connected photovoltaic systems: An overview of recent research and emerging PV converter technology," *IEEE Industrial Electronics Magazine*, vol. 9, no. 1, pp. 47-61, 2015.

[28] A. Anzalchi and A. Sarwat, "Overview of technical specifications for grid-connected photovoltaic systems," *Energy conversion and management*, vol. 152, pp. 312-327, 2017.

[29] J. Siecker, K. Kusakana, and e. B. Numbi, "A review of solar photovoltaic systems cooling technologies," *Renewable and Sustainable Energy Reviews*, vol. 79, pp. 192-203, 2017.

[30] R. González, J. Lopez, P. Sanchis, and L. Marroyo, "Transformerless inverter for single-phase photovoltaic systems," *IEEE Transactions on Power Electronics*, vol. 22, no. 2, pp. 693-697, 2007.

[31] H. Xiao and X. Wang, *Transformerless Photovoltaic Grid-Connected Inverters*. Springer Nature, 2020.

[32] A. N. Deshmukh and V. K. Chandrakar, "Design and Performance Analysis of Grid-Connected Solar Photovoltaic System with Performance Forecasting Approach (PFA)," *Journal of The Institution of Engineers (India): Series B*, vol. 103, no. 5, pp. 1521-1532, 2022.

[33] L. Peng, Y. Sun, Z. Meng, Y. Wang, and Y. Xu, "A new method for determining the characteristics of solar cells," *Journal of power sources*, vol. 227, pp. 131-136, 2013.

[34] R. Prakash and S. Singh, "Designing and modelling of solar photovoltaic cell and array," *IOSR Journal of Electrical and Electronics Engineering (IOSR-JEEE)*, vol. 11, no. 2, pp. 35-40, 2016.

[38] M. Abdulkadir, A. Samosir, and A. Yatim, "Modeling and simulation of a solar photovoltaic system, its dynamic and transient characteristics in LABVIEW," *International Journal of Power Electronics and Drive Systems*, vol. 3, no. 2, p. 185, 2013.

[39] M. A. Enany, M. A. Farahat, and A. Nasr, “Modeling and evaluation of main maximum power point tracking algorithms for photovoltaics systems”, *Renewable*

and Sustainable Energy Reviews, vol. 58. Elsevier Ltd, pp. 1578–1586, May 01, 2016. doi: 10.1016/j.rser.2015.12.356.

[40] D. Kumar and K. Chatterjee, "A review of conventional and advanced MPPT algorithms for wind energy systems," *Renewable and sustainable energy reviews*, vol. 55, pp. 957-970, 2016.

[41] N. A. Kamarzaman and C. W. Tan, "A comprehensive review of maximum power point tracking algorithms for photovoltaic systems," *Renewable and Sustainable Energy Reviews*, vol. 37, pp. 585-598, 2014.

[42] N. Karami, N. Moubayed, and R. Outbib, "General review and classification of different MPPT Techniques," *Renewable and Sustainable Energy Reviews*, vol. 68, pp. 1-18, 2017.

[43] R. Ahmad, A. F. Murtaza, and H. A. Sher, "Power tracking techniques for efficient operation of photovoltaic array in solar applications–A review," *Renewable and Sustainable Energy Reviews*, vol. 101, pp. 82-102, 2019.

[44] G. S. Shehu, A. B. Kunya, I. H. Shanono, and T. Yalçınöz, "A review of multilevel inverter topology and control techniques," 2016.

[45] L. P. Suresh, "A brief review on multi level inverter topologies," in *2016 international conference on circuit, power and computing technologies (ICCPCT)*, 2016: IEEE, pp. 1-6.

[46] H.-P. Krug, T. Kume, and M. Swamy, "Neutral-point clamped three-level general purpose inverter-features, benefits and applications," in *2004 IEEE 35th Annual Power Electronics Specialists Conference (IEEE Cat. No. 04CH37551)*, 2004, vol. 1: IEEE, pp. 323-328.

[47] J. Rodriguez, S. Bernet, P. K. Steimer, and I. E. Lizama, "A survey on neutral-point-clamped inverters," *IEEE transactions on Industrial Electronics*, vol. 57, no. 7, pp. 2219-2230, 2009.

[48] R. Naderi and A. Rahmati, "Phase-shifted carrier PWM technique for general cascaded inverters," *IEEE Transactions on power electronics*, vol. 23, no. 3, pp. 1257-1269, 2008.

[49] N. Farah, "Cascaded Multilevel Inverter With PV System Self-tuning fuzzy logic of Induction motor View project An enhancement of fuzzy logic speed controller for high performance AC motor drive system: An Experimental Approach View project", 2015, doi: 10.13140/RG.2.1.1134.6002.

[50] B.-S. Jin, W.-K. Lee, T.-J. Kim, D.-W. Kang, and D.-S. Hyun, "A study on the multi-carrier PWM methods for voltage balancing of flying capacitor in the flying capacitor multi-level inverter," in *31st Annual Conference of IEEE Industrial Electronics Society, 2005. IECON 2005.*, 2005: IEEE, p. 6 pp.

[51] A. Dekka, A. Ramezani, S. Ouni, and M. Narimani, "A new five-level voltage source inverter: Modulation and control," *IEEE Transactions on Industry Applications*, vol. 56, no. 5, pp. 5553-5564, 2020.

[52] H. Shahane, S. Onkarkar, P. Khandekar, Z. Bhagat, R. Tondare "Review of Different PWM Techniques", 2018.

[53] J.-H. Kim and S.-K. Sul, "Carrier-based pulse width modulation for three-level inverters: neutral point potential and output voltage distortion," in *2006 CES/IEEE 5th International Power Electronics and Motion Control Conference*, 2006, vol. 1: IEEE, pp. 1-7.

[54] T. Erfidan, S. Urgun, Y. Karabag, and B. Cakir, "New software implementation of the space vector modulation," in *Proceedings of the 12th IEEE Mediterranean Electrotechnical Conference (IEEE Cat. No. 04CH37521)*, 2004, vol. 3: IEEE, pp. 1113-1115.

[55] B. Tolunay, "Space Vector Pulse Width Modulationfor Three-Level Converters: a LabVIEW Implementation," ed, 2012.

[56] B. V. Sumangala and Soumya S, "Application Of Space Vector Modulation Technique For Three Level Neutral Point Clamped Inverters" International Journal of Engineering Research & Technology (IJERT) ISSN: 2278-0181 www.ijert.org Vol. 2 Issue 6, June - 2013 .

[57] R. Rajaram, K. Palanisamy, S. Ramasamy, and P. Ramanathan, "Selective harmonic elimination in PWM inverter using fire fly and fireworks algorithm," *International Journal of Innovative Research in Advanced Engineering*, vol. 1, no. 8, pp. 55-62, 2014.

[58] C. G. Hu, S. S. Liu, Y. Yuan, and H. Z. Chen, "Selective Harmonic Elimination PWM Method Applied to Three-level Photovoltaic NPC Inverter," in *Advanced Materials Research*, 2013, vol. 614: Trans Tech Publ, pp. 1530-1533.

[59] M. Aspalli and A. Wamanrao, "Sinusoidal pulse width modulation (SPWM) with variable carrier synchronization for multilevel inverter controllers," in *2009 International Conference on Control, Automation, Communication and Energy Conservation*, 2009: IEEE, pp. 1-6.

[60] D. G. Holmes and T. A. Lipo, *Pulse width modulation for power converters: principles and practice*. John Wiley & Sons, 2003.

[61] T. D. Nguyen, D. Q. Phan, D. N. Dao, and H.-H. Lee, "Carrier phase-shift PWM to reduce common-mode voltage for three-level T-type NPC inverters," *Journal of Power Electronics,* vol. 14, no. 6, pp. 1197-1207, 2014.

[62] B. Chokkalingam, M. S. Bhaskar, S. Padmanaban, V. K. Ramachandaramurthy, and A. Iqbal, "Investigations of multi-carrier pulse width modulation schemes for diode free neutral point clamped multilevel inverters," *Journal of Power Electronics,* vol. 19, no. 3, pp. 702-713, 2019.

[63] M. Deepthi, "A Single-Phase Transformer less Inverter for Grid-Tied PV Applications by Using Hysteresis Controller", vol. 7.

[64] F. Faraji, A. A. M. Birjandi, S. M. Mousavi G, J. Zhang, B. Wang, and X. Guo, "An Improved Multilevel Inverter for Single-Phase Transformerless PV System", *IEEE Transactions on Energy Conversion*, vol. 36, no. 1, pp. 281–290, Mar. 2021, doi: 10.1109/TEC.2020.3006552.

[65] H. Xiao and S. Xie, "Transformerless split-inductor neutral point clamped three-level PV grid-connected inverter," *IEEE transactions on power electronics,* vol. 27, no. 4, pp. 1799-1808, 2011.

[66] M. YILMAZ and M. CORAPSİZ, "Artificial Neural Network based MPPT Algorithm with Boost Converter topology for Stand-Alone PV System," *Erzincan University Journal of Science and Technology,* vol. 15, no. 1, pp. 242-257.

الخلاصة

يعد نظام توليد الطاقة الشمسية الكهروضوئية أحد مصادر الطاقة المتجددة المفضلة القادرة على إنتاج طاقة كهربائية صديقة للبيئة بدون تلوث أو ضوضاء.

في النظام الكهروضوئي المتصل بالشبكة ، عادةً ما يتم استخدام محول التردد المنخفض لعزل العاكس جلفانيًا عن شبكة المرافق ولتصعيد جهد العاكس. يحتوي نظام المحولات الكهروضوئية على عيوب تتمثل في زيادة وزن النظام وحجمه وتكلفته وتقليل كفاءة النظام. للتغلب على هذه الجوانب السلبية ، يتم إدخال نظام PV متصل بالشبكة بدون محول مع عاكس متعدد المستويات (MLI). يتم استخدام MLI لدمج النظام الكهروضوئي مع شبكة المرافق. ومع ذلك ، فإن تيار التسرب بسبب عدم وجود عزل كلفاني هو أحد التحديات في مثل هذا النظام.

العاكس ذو الثلاثة مستويات المحايدة والمثبتة هو أحد طوبولوجيا الجاذبية المستخدمة في مثل هذه الأنظمة نظرًا لقدرته على التخلص من تيار التسرب مع توفر النقطة المحايدة. ومع ذلك ، فإنه يعاني من مشكلة إطلاق النار من خلال زيادة التشويه التوافقي الكلي.

تبحث هذه الرسالة في عاكس إلكتروني متعدد المستويات ذو طاقة واحدة على ثلاثة مستويات يعتمد على طوبولوجيا NPC ليتم استخدامه في نظام كهروضوئي متصل بشبكة بمرحلة واحدة ، والذي يتميز بعامل طاقة واحد وتشويه متناسق إجمالي منخفض التيار ، وضغط منخفض الجهد على مفتاح أشباه الموصلات ، لا تبادل لاطلاق النار من خلال المشكلة والموثوقية العالية والكفاءة.

يقارن هذا البحث بين أداء طوبولوجيتين للدائرة NPC-MLI (دائرة NPC الأساسية ودوائر NPC المنقسمة) تحت تقنيات تعديل عرض النبضة على مستوى الناقل المتغير (LSCB-PWM) ومدى ملاءمتها لاستخدامها في محول متصل بالشبكة- أقل من نظام الكهروضوئية.

تم تقديم تحقيق مفصل عن طوبولوجيا NPC المحسنة في هذا العمل ليتم استخدامها في النظام الكهروضوئي المتصل بالشبكة. من خلال فحص سلوك العاكس ISI-NPC في ظل مختلف (LSCB-PWM) ، تقترح الأطروحة العاكس ISI-NPC كمرشح فعال ليتم استخدامه في نظام PV بدون محول.

تم تصميم جهاز التحكم في تيار التباطؤ لتتبع تيار خرج العاكس وإجباره على أن يكون صفراً من أجل تحقيق طاقة شبكة عالية الجودة والحفاظ على عامل قدرة الوحدة.

يتم فحص خوارزميات تتبع الحد الأقصى من الطاقة التقليدية والمتقدمة بما في ذلك الاضطراب والمراقبة والشبكة العصبية الاصطناعية لضمان استخراج الطاقة القصوى من اللوحة الكهروضوئية. يتم تحقيق أداء أفضل في ظل نهج ANN.

تم تصميم النظام بأكمله واختباره في هذا العمل. تتحقق النتائج من قدرة العاكس ISI-NPC تحت سيطرة HCC والشبكة العصبية الاصطناعية على نقل الطاقة الكهروضوئية القصوى من خلال عامل قدرة 1 إلى شبكة المرافق ، وجودة طاقة عالية ، و THD تيار منخفض للغاية مع 0.37٪ أقل إجهاد تبديل أشباه الموصلات ، وبالتالي موثوقية عالية. لذلك ، تسلط الأطروحة الضوء على أن ISI-NPC تعتبر بمثابة MLI فعالة ليتم استخدامها في مثل هذا النظام.

وزارة التعليم العالي والبحث العلمي

جامعة بابل / كلية الهندسة

قسم الهندسة الكهربائية

عاكس احادي المرحله احادي الطورمتعدد المستويات بدون محول للتطبيقات الكهروضوئية

رسالة مقدمة الى قسم الهندسة الكهربائية - كلية الهندسة - جامعة بابل كجزء من متطلبات نيل درجة الماجستير في الهندسة الكهربائية – الالكترونيك الصناعي

من قبـــــل

أسراء حسين أمويشي حسون

بـــأشـراف

أ.م. د تهاني حمودي مزهر المهنا

1444هـ **2023م**